UNIVERSIDADE DE SÃO PAULO

FACULDADE DE ZOOTECNIA E ENGENHARIA DE ALIMENTOS

Departamento de Engenharia de Alimentos

DIANA ELIZABETH QUISPE ARPASI

Anaerobic treatment of post-hydrothermal liquefaction wastewater from Spirulina associated with microaeration and photocatalysis

Pirassununga

2021

DIANA ELIZABETH QUISPE ARPASI

Anaerobic treatment of post-hydrothermal liquefaction wastewater from Spirulina associated with microaeration and photocatalysis

"VERSÃO CORRIGIDA"

Tese apresentada à Faculdade de Zootecnia e Engenharia de Alimentos da Universidade de São Paulo, como parte dos requisitos para a obtenção do Título de Doutora em Ciências do programa de pós-graduação em Engenharia de Alimentos.

Área de Concentração: Biotecnologia Ambiental

Orientador: Profa. Dra. Giovana Tommaso

Pirassununga

2021

Ficha catalográfica elaborada pelo
Serviço de Biblioteca e Informação, FZEA/USP,
com os dados fornecidos pelo(a) autor (a)

Q8a

Quispe-Arpasi, Diana Elizabeth
Anaerobic treatment of post-hydrothermal liquefaction wastewater from Spirulina associated with microaeration and photocatalysis / Diana Elizabeth Quispe-Arpasi ; orientadora Giovana Tommaso. -- Pirassununga, 2021.
138 f.

Tese (Doutorado - Programa de Pós-Graduação em Engenharia de Alimentos) -- Faculdade de Zootecnia e Engenharia de Alimentos, Universidade de São Paulo.

1. hydrothermal liquefaction. 2. toxic wastewater. 3. anaerobic digestion. 4. intermittent aeration. 5. photocatalysis. I. Tommaso, Giovana, orient. II. Titulo.

DIANA ELIZABETH QUISPE ARPASI

Anaerobic treatment of post-hydrothermal liquefaction wastewater from Spirulina associated with microaeration and photocatalysis

Tese apresentada à Faculdade de Zootecnia e Engenharia de Alimentos da Universidade de São Paulo, como parte dos requisitos para a obtenção do Título de Doutora em Ciências do programa de pós-graduação em Engenharia de Alimentos.

Área de Concentração: Biotecnologia Ambiental

Data de aprovação: 20/12/2021

Banca examinadora:

Profa. Dra. Giovana Tommaso – Presidente da Banca examinadora
Faculdade de Zootecnia e Engenharia de Alimentos/USP – Orientadora

Prof. Dr. Marcelo Zaiat
Escola de Engenharia de São Carlos/USP

Profa. Dra. Márcia Helena Zamariolli Damianovic
Escola de Engenharia de São Carlos/USP

Prof. Dr. André Bezerra dos Santos
Universidade Federal do Ceará

Profa. Dra. Sávia Gavazza dos Santos
Universidade Federal de Pernambuco

Prof. Dr. Rogers Ribeiro
Faculdade de Zootecnia e Engenharia de Alimentos/USP

To Mom and Dad

For your immense love and support

ACKNOWLEDGMENTS

I am grateful to God for giving me opportunities that I would never imagine by myself and for putting the right people in front of me.

I am grateful to my family for always supporting me and believing in me.

I would like to express my deepest appreciation to my advisor, Professor Giovana Tommaso, for her guidance, patience, and understanding throughout all these years, especially during the pandemic.

Thanks to Professor Savia Gavazza and her research group for supporting and collaborating in this study.

Thanks to Professor Evaldo Espíndola for guiding me with the ecotoxicological analysis and allowing me to use their laboratory to conduct them.

Thanks to Professor Paulo Mazza Rodrigues for allowing me to use some facilities in his laboratory when I most needed them.

Thanks to Professors Eugenio Foresti, Marcia Damianovic, Marcelo Zaiat and Rogers Ribeiro their classes gave me a solid foundation to develop this study.

Thanks to my colleagues and friends: Bia, Tati, Danilo, Marco, Mariê, and everyone who worked in our research group for exchanging knowledge, and valuable experience.

Thanks to my Peruvian friends Lia, Victor, Gilda, Kyara, and Hubert for making me feel like I was at home even when we were homesick. I am really glad that I spent these years with you all.

Finally, I would like to thank the Coordination for the Improvement of Higher Education Personnel for the doctoral scholarship and the University of Sao Paulo for its fundamental contribution to my education as a researcher.

RESUMO

QUISPE-ARPASI, D. **Tratamento anaeróbio da fase aquosa da liquefação hidrotérmica de *Spirulina* associado a microaeração e fotocatálise.** 2021. 138 f. Tese (Doutorado) – Faculdade de Zootecnia e Engenharia de Alimentos, Universidade de São Paulo, Pirassununga, 2021.

A liquefação hidrotérmica é um processo termoquímico que vem sendo usado para a conversão de resíduos úmidos em óleo bruto. Durante a conversão hidrotérmica de microalgas, é gerada também uma água residuaria (em inglês: post-hydrothermal liquefaction wastewater, PHWW) com elevada concentração de matéria orgânica e de compostos aromáticos. Embora a digestão anaeróbia (AD) possa ser aplicada como uma etapa de recuperação de energia em forma de metano, a aplicação de outros métodos que possam otimizar o tratamento da PHWW é necessária. Em primeiro lugar, o tratamento anaeróbio da PHWW foi investigado em um processo em batelada sequencial, avaliando o efeito do incremento na concentração de matéria orgânica no afluente (1,6, 2,4, 3,2, 4 e 4,8 $g.L^{-1}$ de demanda química de oxigênio - DQO). Eficiências de remoção de matéria orgânica de DQO e produção de CH_4 foram 53%-49% e 180-158 $NmL.gDQOadd^{-1}$, respetivamente, para valores de concentração inicial de até 3.2 $gCOD.L^{-1}$. A aplicação de cargas orgânicas mais elevadas acarretou na queda da eficiência de remoção de DQO e produção de CH_4, propiciando a acumulação de ácidos graxos voláteis. Como relação a modelagem cinética, os dados experimentais foram ajustados ao modelo modificado de Haldane, observando uma inibição forte em concentrações maiores a 3,7 $gDQO.L^{-1}$. *Trichococcus*, *Aminobacteria* e *Methanosarcina* foram os microrganismos mais representativos após a aclimação da biomassa a PHWW. Em segundo lugar, o efeito da aeração intermitente na digestão anaeróbia da PHWW foi avaliado em dois processos em batelada sequenciais, o primeiro denominado R_1 totalmente anaeróbio e o segundo R_2 anaeróbio-aerado. Três concentrações de matéria orgânica foram investigadas (1,6, 3,2, e 4,8 $gDQO.L^{-1}$). Os resultados de R_2 apresentaram maiores eficiências de remoção para cada condição avaliada. Além disso, a acumulação de metabolitos observada em R_1 foi minimizada em R_2, enquanto que a remoção de compostos fenólicos também foi aprimorada com a introdução dos períodos de aeração intermitente. Por outro lado, a produção de CH_4 foi reduzida em 45% devido à disponibilidade de oxigênio. Microrganismos aeróbios capazes de degradar compostos aromáticos foram enriquecidos em R_2. Finalmente, a fotocatálise como pôs-tratamento da PHWW tratada anaerobiamente foi investigada. Eficiências de remoção atingiram 50% para

matéria orgânica (DQO), 83% para compostos fenólicos, e 95% para cor para as condições ótimas de pH (9,6) e adição de H_2O_2 (3,55 $g.L^{-1}$). Além disso, os ensaios de ecotoxicidade com *Daphnia similis* e *Eruca sativa* Mill mostraram que o processo de fotocatálise como pos-tratamento da digestão anaeróbia não trouxe maior toxicidade ao efluente.

Palavras-chave: liquefação hidrotérmica, efluente tóxico, digestão anaeróbia, aeração intermitente, fotocatálise

ABSTRACT

QUISPE-ARPASI, D. **Anaerobic treatment of post-hydrothermal liquefaction wastewater from *Spirulina* associated with microaeration and photocatalysis.** 2021. 138 p. PhD Thesis – Faculdade de Zootecnia e Engenharia de Alimentos, Universidade de São Paulo, Pirassununga, 2021.

Hydrothermal liquefaction is a thermochemical process that is being used for the conversion of wet feedstocks into bio-crude oil. During the hydrothermal conversion of microalgae, wastewater (PHWW) with an elevated organic and aromatic content is also produced. Although anaerobic digestion can be applied as a stage of energy recovery, the application of other methods that could enhance PHWW treatment is necessary. Firstly, the anaerobic treatment of PHWW was investigated in a sequencing batch process. The effect of increasing organic matter concentrations, measured as chemical oxygen demand (COD), was assessed (1.6, 2.4, 3.2, 4, and 4.8 $gCOD.L^{-1}$). COD removal efficiencies and CH_4 yields ranged from 53% to 49% and from 180 to 158 $NmL.gCODadd^{-1}$, respectively, for influent COD values up to 3.2 $g.L^{-1}$. Higher organic loads presented a drop in COD removal, CH_4 yield, and a volatile fatty acids accumulation. Regarding the kinetic evaluation, the experimental data were adjusted to the modified Haldane model, observing a strong inhibition at COD concentrations above 3.7 $gCOD.L^{-1}$. *Trichococcus, Aminobacteria,* and *Methanosarcina* were the most representative microorganisms after biomass acclimation to PHWW. In second place, the effect of intermittent aeration in the anaerobic digestion of PHWW was assessed in two sequencing batch processes, R_1 full anaerobic and R_2 anaerobic- aerated. Three increasing organic matter were investigated (1.6, 3.2, and 4.8 $gCOD.L^{-1}$). Results from R_2 presented higher COD removal efficiencies for each condition evaluated. Moreover, metabolites accumulation observed in R_1 was minimized in R_2, and phenolic removal was also improved. On the other hand, CH_4 production was reduced by 45% due to oxygen availability. Aerobic microorganisms capable of degrading aromatic compounds were enriched in R_2. Finally, photocatalysis as a post-treatment of anaerobically digested PHWW was investigated. Removal efficiencies reached 50% for COD, 83% for phenolic compounds, and 95% for color, under optimum conditions of pH (9.6) and H_2O_2 addition ($3.55g.L^{-1}$). Ecotoxicity assays with *Daphnia similis* and *Eruca sativa* Mill resulted in treated PHWW not negatively influenced by photocatalysis.

Keywords: hydrothermal liquefaction, toxic wastewater, anaerobic digestion, intermittent aeration, photocatalysis

LIST OF FIGURES

LIST OF TABLES

ABBREVIATIONS

AD-PHWW: Anaerobically digested – PHWW

ASBR: anaerobic sequencing batch reactor

AVOL: applied volumetric organic load

BTEX: Benzene, ethylbenzene, toluene, xylene

COD: chemical oxygen demand

CCD-FC: Central composite design-face centered

DO: dissolved oxygen

EC: Experimental condition

EC_{50}: Half-maximal effective concentration

GAE: Gallic acid equivalents

HAIB: Horizontal-flow anaerobic immobilized biomass reactor

HHV: Higher heating value

HTL: Hydrothermal liquefaction

HRT: Hydraulic retention time

IA/PA: Intermediate alkalintity/partial alkalinity

ORP: oxidation-reduction potential

PBR: Packed bed reactor

PHWW: Post-hydrothermal liquefaction wastewater

S/X: Substrate/ Biomass concentration

TKN: Total Kjeldahl nitrogen

TPh: Total phenolic compounds

TU_a : Acute Toxicological Units

TVS: Total volatile solids

UASB: Up-flow anaerobic sludge blanket

VFA: Volatile Fatty Acid

VSS: Volatile suspended solids

CONTENT

1. INTRODUCTION

With the increasing demand for energy, depletion of non-renewable energy, and high local and global pollution, the interest for biofuels production that are environmentally and economically sustainable has rapidly increased. Traditional biofuels generated from agricultural biomass, such as biodiesel and ethanol, have limitations associated with their requirements of arable land and clean water (SCHENK et al., 2008; DEMIRBAS, 2009). The use of microalgae for biofuels production has therefore been considered as an alternative approach that does not compete with agricultural crops. They also present high growth rates, can capture CO_2 and many species of microalgae have the ability to grow in wastewater conditions, efficiently reusing the nutrients (PITTMAN; DEAN; OSUNDEKO, 2011).

Hydrothermal liquefaction (HTL) is a thermochemical process that converts wet biomass, such as microalgae, into biocrude oil and by-products (aqueous phase, solid residue, and gaseous product) under conditions of moderate temperature (200-350 °C) and pressure (5-15 MPa). HTL process mimics the natural process believed to form petroleum crude oil where the organic material is reformed under intense heat and anoxic conditions. The generated biocrude has similar characteristics to crude oil and could be upgraded in existing fossil refineries (ROBERTS et al., 2013; ELLIOTT et al., 2014). The integration of biofuel production with microalgae cultivation for wastewater treatment has several advantages including a favorable return of energy, reduction of greenhouse gases emission, and diminution of the costs associated with nutrients and fresh water necessary for algae cultivation, thus becoming an economically viable alternative (PITTMAN; DEAN; OSUNDEKO, 2011).

One limitation identified in this proposal is the amount of carbon and toxic compounds (e.g. phenols, pyridines) released in the aqueous by-product, hereafter called post-HTL wastewater (PHWW) and classified as petrochemical wastewater. Recently, anaerobic digestion (AD) has

been studied as a way to convert PHWW high carbon content to produce biogas and detoxify the effluent before further applications. Although PHWW anaerobic digestion occurred at low concentrations and it is necessary to apply additional techniques capable of counteracting toxicants, anaerobes seem to have a higher tolerance to PHWW compared to microalgae strains (BUENO et al., 2020). Moreover, associating anaerobic digestion to the HTL process can increase the total energy recovered from microalgae (POSMANIK et al., 2017). In this way, the evaluation of methods that could enhance PHWW anaerobic digestion, and complete its stabilization is necessary to close the loop of biocrude oil production *via* hydrothermal liquefaction, and eventually scale-up the process.

The application of sequencing batch reactors and biofilm reactors under partial aerated conditions has been efficiently tested for the biological treatment of wastewaters with recalcitrant aromatic compounds, such as textile wastewater, where firstly, the azo bonds are cleaved under anaerobic conditions, followed by the biodegradation of aromatic amines under aerated conditions (ÇINAR et al., 2008; MENEZES et al., 2019). Such configuration could also improve the stabilization of PHWW, where its biodegradable organic matter can be converted into CH_4 and its remaining aromatic and organic content could be degraded under aerated conditions.

Other methods widely used for recalcitrant compounds conversion are advanced oxidation processes, among them, heterogeneous photocatalysis has shown promising results for the conversion of aromatic compounds remaining in PHWW after anaerobic digestion, such as benzene, toluene, cyclohexane (EINAGA; FUTAMURA; IBUSUKI, 2002); phenol derivatives (KHODJA et al., 2001), and N-heterocyclic compounds (KAUR; PAL, 2013). The integration of anaerobic digestion with photocatalysis could be an interesting approach, since anaerobic

digestion can degrade PHWW high organic content, and photocatalysis could complete its mineralization in terms of recalcitrant compounds and color (COSTA; ALVES, 2013).

1.1. Research hypothesis and objectives

In this way, this research aimed to study methods that can complete PHWW stabilization, associating anaerobic digestion with micro-aeration and photocatalysis. The primary hypothesis of the conducted study was “intermittent aeration and photocatalysis may enhance PHWW treatment by anaerobic digestion”. Three sub-hypotheses and specific objectives were considered and are presented below.

Sub-hypotheses:

- The sequential anaerobic treatment of PHWW would promote biomass acclimation to PHWW toxic characteristics
- The use of anaerobic-microaerophilic cultures would enhance PHWW biodegradation.
- The photocatalytic process would complete the stabilization of anaerobically digested PHWW.

Specific objectives:

- Evaluate the anaerobic degradation of PHWW in a sequential batch process
- Investigate the effect of intermittent aeration on the anaerobic digestion of PHWW.
- Determine the optimal conditions in the photocatalytic treatment of anaerobically digested PHWW (AD-PHWW).

2. LITERATURE REVIEW

2.1. Hydrothermal liquefaction of microalgae

The main routes to produce liquid biofuels from microalgae are transesterification, and thermochemical conversion *via* pyrolysis or hydrothermal liquefaction. Initial studies focused on the use of microalgae species with high lipid content to produce biodiesel through oil extraction followed by transesterification (SCHENK et al., 2008). Alternatively, thermochemical processes do not depend on the lipid content of the strains used, because it utilizes the whole algal biomass, converting most of the organic fractions (protein, lipids, and carbohydrates) (JENA; DAS, 2011; YU et al., 2011). In contrast to high-lipid species, low-lipid strains not suitable for lipid extraction have higher productivity and are more resistant to unfavorable conditions (e.g. wastewater systems). Thus, species with low-lipid content can achieve higher yields when converted through thermochemical processes (FRANK et al., 2013; KUMAR et al., 2016).

HTL consists of the direct liquefaction of wet feedstock such as algal biomass into biocrude oil at moderate temperatures and pressure. The resulting biocrude oil has similar properties to petroleum crude for ultimate analysis and energy content (Table 1), being a promising alternative to supply current energy demands (ROBERTS et al., 2013). Contrary to pyrolysis, the HTL process requires lower temperatures and is a preferred option for the conversion of wet feedstock (>80% moisture) such as microalgae biomass, because the intrinsic water acts as solvent and reaction medium at hydrothermal conditions, avoiding the energy expenditure related to the water volatilization (JENA; DAS, 2011; TOOR; ROSENDAHL; RUDOLF, 2011).

Besides biocrude oil, other co-products include aqueous phase, gaseous fractions, and solid residue. The distribution of the chemical compounds on the HTL products depends on the

feedstock characteristics and reaction conditions. Especially, the biocrude oil yield follows the conversion order of lipids > protein > carbohydrate (LEOW et al., 2015). On the other hand, according to Gai et al. (2014), reaction temperature and retention time are the operational factors that influence the oil yield and quality. A typical experimental HTL procedure of microalgae in a batch reactor is depicted in Figure 1.

Figure 1 - Experimental procedure of the hydrothermal conversion of microalgae in a batch reactor (a) reactor, (b) charging, (c) sealing, (d) heating, (e) cooling, (f) washing

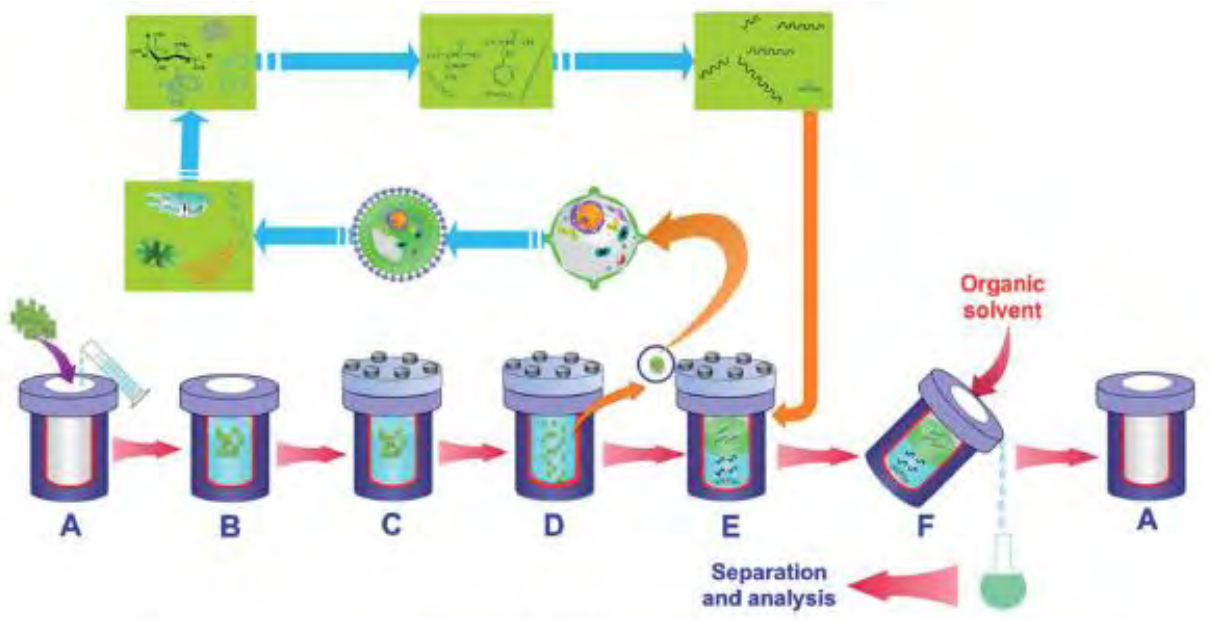

Source: Chen et al. (2015)

Table 1 summarizes the advances of low-lipid microalgae HTL. Key operation conditions included temperature between 200 and 375°C, retention time up to 120 min, and solids content varying from 5 to 35 wt.% for various strains. The biocrude oil from all the experiments presented a higher energy content (HHV) than the original feedstock, with maximum yields up to 65 wt.% obtained for the conversion of *Tetraselmis* sp. under 350°C, 5 min and 16 wt.% of solids. Further improvement in the biocrude yield and quality to remove its oxygen and nitrogen content can be achieved by applying a catalyst in the HTL process (TIAN et al., 2018).

Table 1 - Summary of the advances of low-lipid microalgae HTL

Specie	Algae HHV ($MJ.kg^{-1}$)	Algae lipid content (wt. %)	Operational conditions	Oil yield (wt. %)	HHV ($MJ.kg^{-1}$)	Energy Recovery (%)*	References
Porphyridium creuntum	23.3[a]	8	T=350°C, RT=60 min, SC= 10 wt.%	18	35.7[a]	51.6	Biller and Ross, (2011)
Spirulina sp.	24.6[a]	5	T=350°C, RT=60 min, SC= 10 wt.%	29	36.8[a]	50.7	Biller and Ross, (2011)
Spirulina platensis	20.5[b]	11.2	T=200-350°C, RT=0-120 min, SC= 10-30 wt.%	18 - 39.9	25.2 - 39.9[b]	22.1 - 77.7	Jena, Das and Kastner (2011)
Desmodesmus sp.	23.1[c]	10-14	T=175-375°C, RT=5-60 min, SC= 8 wt.%	8.6 - 49.4	30.1 - 36.2[c]	11 - 75	Alba et al. (2012)
Cholorogloepsis fritschii	22.6[a]	7	T=300°C, RT=60 min, SC= 10 wt.%	38.6	32[a]	54.6	Biller et al. (2012)
Spirulina platensis	23.8[a]	5	T=300°C, RT=60 min, SC= 10 wt.%	35.5	36.1[a]	53.7	Biller et al. (2012)
Scenedesmus dimorphus	23.7[a]	18	T=350°C, RT=60 min, SC= 10 wt.%	27.1	33.6[a]	38.5	Biller et al. (2012)
Tetraselmis sp.	19.2[d]	14	T=310-370°C, RT=5-60 min, SC= 16 wt.%	35 - 65	35[d]	38 - 87	Eboibi et al. (2014)
Chlorella pyrenoidosa	21.1[a]	N.A.	T=260-300°C, RT=30-90 min, SC= 15-35 wt.%	25.7 - 43.3	30.3 - 36.5[b]	36.9 - 69.6	Gai et al. (2014)
Petroleum crude	-	-	-	-	42.9[b]	-	Jena, Das e Kastner (2011)

HHV: Higher heating value; *Energy ratio of biocrude oil to feedstock; [a]Calculated according to Dulong's formula; [b]Measured using an oxygen bomb calorimeter; [c]Calculated according to Boie's formula; [d]Calculated according to Channiwala's formula; N.A.: Not available

Source: Own authorship

The reactions occurring during the HTL process from microalgae can be divided mainly into hydrolysis/decomposition and recombination. Firstly, the algal cell membrane is disrupted chemically due to the temperatures and pressure water, thus, intracellular components, lipids, proteins, and carbohydrates are decomposed into their corresponding monomers, such as fatty acids, amino acids, and sugars. As the temperature increases, monomers are decomposed too. Then, recombination reactions take place, such as cyclization involving alcohol, amino acids, and ammonia, generating phenols, cyclic amides, and other aromatics (e.g. N&O-heterocyclic compounds). Figure 2 depicts a representative scheme of how the feedstock macromolecules migrate to the reaction products during the HTL process (CHEN et al., 2014, 2015).

Figure 2 - Reaction pathway of algae macromolecules to the final HTL products

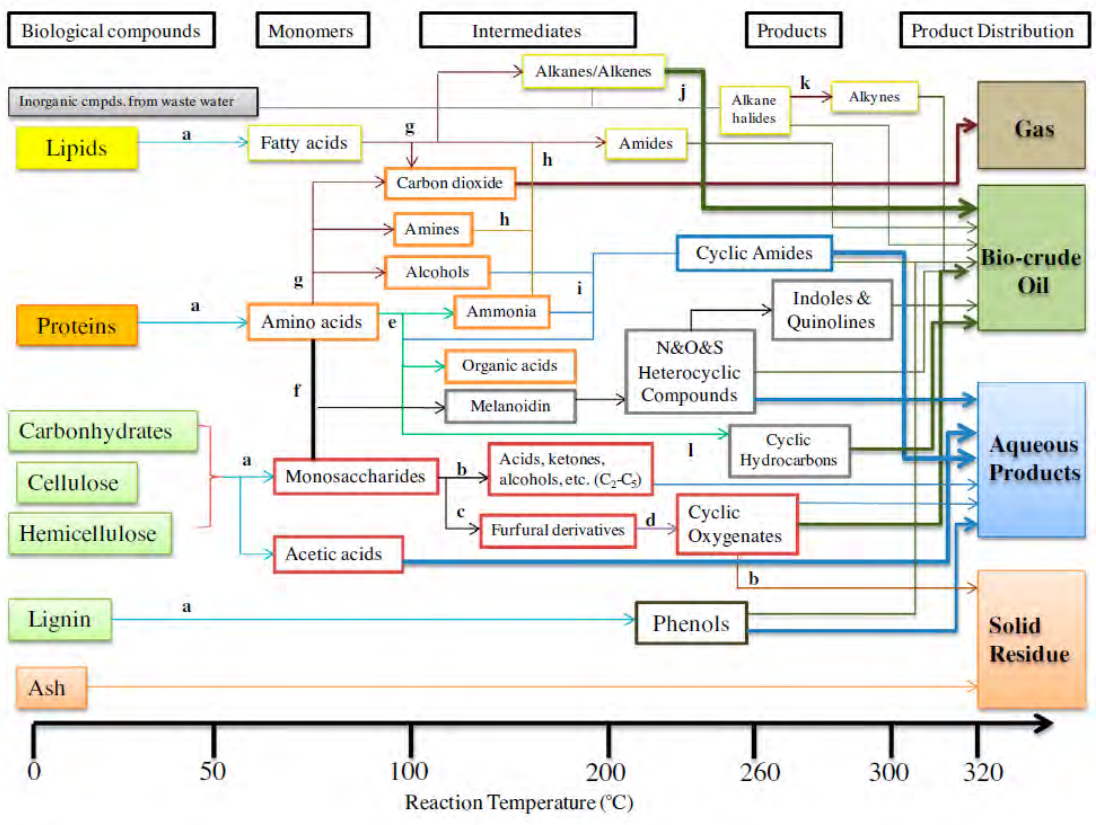

(a) hydrolysis; (b) decomposition; (c) dehydration; (d) polymerization; (e) deamination; (f) Maillard reaction; (g) decarboxylation; (h) aminolysis; (i) cyclization; (j) halogenations; (k) dehydrohalogenation; (l) condensation+pyrolysis. Source: Chen et al. (2014)

In general, the long-chain non-polar compounds form the biocrude oil, while the polar organic products, water-soluble salts, and aromatic compounds are dissolved into the aqueous phase. The gaseous products include mainly CO_2, and small amounts of H_2 and CH_4, whereas the solid residue includes inorganic compounds and bio-char (carbon-rich - charcoal) (CHEN et al., 2015).

2.2. Post-hydrothermal liquefaction wastewater (PHWW)

Along with the biocrude oil, the HTL process produces a large quantity of highly organic contaminated wastewater, known as post-HTL wastewater (PHWW), and classified as petrochemical refinery wastewater. PHWW from microalgae conversion can reach yields up to 45% at optimal HTL conditions (GAI et al., 2015a), accounting for approximately 40% and 75% of the carbon and nitrogen, respectively, that were originally present in the biomass (YU et al., 2011).

Major organic compounds identified in PHWW from microalgae through GC-MS were classified into five categories: fatty acid derivatives; ester, ketones, and alcohols; straight & branched amines; cyclic oxygenates (including phenols and derivatives); and N&O-heterocyclic compounds. The largest percentage of identified compounds belonged to N&O heterocyclic compounds (>30%) (GAI et al., 2015a), within them, the most reported compounds include pyridine, aniline, σ-valerolactam, ε-caprolactam, etc (PHAM et al., 2013; BUENO et al., 2021). Additionally, inorganic species such as Na, Mg, and K and some heavy metals (Ni, Cu, Co, and Zn) were also identified (MADDI et al., 2016; ZHENG et al., 2017).

Table 2 details the organic matter, nutrient content, and other major components found in PHWW from various low-lipid microalgae. As observed, the distribution of organic matter, nutrients, and other compounds depends highly on the feedstock characteristics and reaction

conditions. Gai et al. (2015a) reported that temperature and solid content were the operating variables that influence PHWW organic matter (chemical oxygen demand - COD) and nutrient concentration (nitrogen and phosphorus). For instance, the highest concentration of organics was reported for *Spirulina* conversion under 220°C, 60 min, and 25% of solids (RUIRUI et al., 2017), whereas the lowest concentration was found for *Cholorogloepsis fritschii* conversion under 300°C, 60 min and 10% of solids (BILLER et al., 2012). In general, aromatic compounds such as N&O-heterocycles, phenols, and benzene derivatives were identified as the most representative compounds in PHWW from algae conversion (TOMMASO et al., 2015).

Moreover, the toxic effects of PHWW were evaluated for some organisms. For instance, Pham et al. (2013) reported that *Spirulina*-derived PHWW was highly cytotoxic to mammalian cells, thus 7.5% of PHWW induced a 50% reduction in cell density during a chronic cytotoxicity assay. Moreover, Zheng et al. (2017), determined the potential toxicity of the same PHWW to anaerobes through an anaerobic toxic assay, which resulted in 50% inhibition when a PHWW concentration of 6% was utilized. These characteristics could cause serious problems of pollution if PHWW is not handled properly.

Since PHWW re-utilization is important to close the cycle of biocrude oil production various methods have been studied to treat PHWW, including direct recirculation, algae cultivation, and anaerobic digestion. Recirculating PHWW directly back into the HTL process avoids the use of fresh water in the process, as well as recovers carbon/energy in PHWW. Recycling PHWW increases the bio-crude yields with each recirculation. However, it also increments the content of water and oxygenated compounds on the biocrude. Additionally, the constant release of carbon and toxic compounds into the aqueous phase resulted in a PHWW more concentrated and recalcitrant to treatment (RAMOS-TERCERO; BERTUCCO; BRILMAN, 2015; BILLER et al., 2016; KLEMMER et al., 2016).

Table 2 - Organic matter and nutrients in post-hydrothermal wastewater (PHWW) from low-lipid microalgae

Microorganism	Operating parameters	COD (g/L)	TOC (g/L)	TN (g/L)	NH_4^+ (g/L)	TP (g/L)	C:N	Other components reported	Reference
Choloroglоepsis fritschii	T=300°C, RT=60 min, SC= 10 wt.%	-	9.06	5.64	4.748	0.280[b]	1.6	Acetate, nitrate, phenols, Ni	Biller et al. (2012)
Spirulina platensis	T=300°C, RT=60 min, SC= 10 wt.%	-	15.12	8.14	6.295	2.159[b]	1.9	Acetate, nitrate, phenols	Biller et al. (2012)
Scenedesmus dimorphus	T=350°C, RT=60 min, SC= 10 wt.%		11.12	3.14	5.28	1.47[b]	3.54	Acetate, nitrate, phenols, Ni	Biller et al. (2012)
Chlorella pyrenoidosa	T=260°C, RT=60 min, SC= 25 wt.%	97.6	-	19.8	-	8.16[b]	-	N&O-heterocycles, cyclic oxygenates, fatty acids	Gai et al. (2015b)
Spirulina sp.	T=250°C, RT=60 min, SC= 20 wt.%	-	26.72	10.15	-	-	2.63	Organic acids, N-aromatics, cyclic oxygenates	Madsen et al. (2017)
Chlorella vulgaris	T=250°C, RT=60 min, SC= 20 wt.%	-	24.79	6.85	-	-	3.62	Small organic acids, N-aromatics, fatty acids	Madsen et al. (2017)
Spirulina sp.	T=220°C, RT=60 min, SC= 25 wt.%	185.1	78.96	21.53	6.55	1.138	3.67	N-heterocycles, ketones, amino acids, amides, esters	Ruirui et al. (2017)
Spirulina sp.	T=300°C, RT=30 min, SC= 20 wt.%	89.04	55.15[c]	22.98	10.12	4.40	2.4	N&O-heterocycles, benzene derivatives, fatty acids	Zheng et al. (2017)
Spirulina sp.	T=300°C, RT=30 min, SC= 20 wt.%	143.8		21.3[a]	12.3	1.37[b]	-	N-heterocyclic compounds	Quispe-Arpasi et al. (2018)
Spirulina sp.	T=260°C, RT=60 min, SC= 20 wt.%	120		14.8[a]	7.8	0.33[b]	-	Volatile fatty acids, benzoate, aniline	Bueno et al. (2021)

COD: Chemical oxygen demand; TOC: Total organic carbon; TN; Total nitrogen; TP: Total phosphorus; C/N: Carbon/Nitrogen ratio; T: Temperature; RT: Retention time; SC: Solid content; [a]TKN; [b]Phosphate (PO_4^{-3}); [c]Calculated using given C/N ratio

Source: Own authorship

Recycling PHWW to support algal cultivation systems was also studied. This process takes advantage of their high content of nutrients (nitrogen and phosphorus) and other minerals (potassium, sodium, chlorides, etc.) that are essential for algae growth, avoiding the utilization of fresh nutrients. However, the use of high diluted concentrations (>100 times) is necessary to avoid growth inhibition due to the presence of inhibitory compounds such as phenols, fatty acids, and N-aromatic compounds. Thus, PHWW conversion by algal cultivation is limited and requires additional treatment (JENA et al., 2011; BILLER et al., 2012; GARCIA ALBA et al., 2013; LÓPEZ BARREIRO et al., 2015).

Anaerobic digestion has been considered a promising method to recover carbon from PHWW through biomethane production. Posmanik et al. (2017) studied the anaerobic degradation of PHWW from different mixtures of polysaccharides, proteins, and lipids through biochemical methane potential assays. They observed that the anaerobic biodegradability was mainly affected by the chemical composition of PHWW. Although no inhibition was observed for most of the samples, more studies are recommended to improve the process, focusing on reducing the toxic effect of PHWW.

In this sense, anaerobic digestion is a potential process that can complement the overall HTL process, being used as a step for PHWW treatment, and simultaneously as an energy/carbon recovery method to improve the process efficiency.

2.3. Anaerobic biodegradation of toxic compounds

Anaerobic digestion is one of the main processes used for the biological treatment of wastewaters. This process occurs in the absence of oxygen where the organic matter is degraded and converted into biogas (mainly CH_4 and CO_2) by several groups of microorganisms working in syntrophy (fermentative, acidogenic, acetogenic, and

methanogenic microorganisms), each carrying out specific reactions (RITTMAN; MCCARTY, 2010). Anaerobic digestion of wastewater integrates the production of renewable energy in the form of CH_4, with environmental vantages such as reduction of greenhouse emissions and controlled waste management (ANGELIDAKI et al., 2011)

In the anaerobic process, acidogenic bacteria deal with the fermentation of sugars, amino acids, and organic acids derived from the conversion of complex compounds of high molecular weight like carbohydrates, proteins, and lipids. Such compounds are fermented to organic acids (mainly acetic, propionic, and butyric acids), alcohols, ketones, CO_2, and H_2 in the absence of inorganic electron acceptors such as sulfate, nitrate, and oxygen. The acetogenic microorganisms transform the intermediate compounds into acetic acid, H_2, and CO_2 (PARKIN; OWEN, 1986; AQUINO; CHERNICHARO, 2005).

Syntrophic microorganisms such as H_2 producers and consumers have a very important role since CH_4 can be inhibited at H_2 partial pressures higher than 10^4 atm. Finally, methanogenic microorganisms are responsible for the last stage of anaerobic digestion. Approximately 70% of CH_4 is produced by acetoclastic methanogens by the conversion of the acetic acid. The remaining 30% is produced by hydrogenotrophic methanogens by the reduction of CO_2 using H_2 as the energy source. This last route is known as anaerobic respiration, due to it uses oxygen as an electron acceptor in the form of CO_2 (PARKIN; OWEN, 1986; AQUINO; CHERNICHARO, 2005).

Microorganisms in anaerobic systems differ in various aspects, such as physiology, nutritional needs, growth kinetics, and sensitivity to external conditions, a balance between the different groups of microorganisms involved is necessary to maintain the process stability. In the presence of stress factors, acidogenic, acetogenic, and methanogenic microorganisms do

not have balanced growth rates, which results in an accumulation of intermediate compounds (AQUINO; CHERNICHARO, 2005; CHEN; CHENG; CREAMER, 2008).

Toxic compounds are within the environmental factors that can disturb anaerobic systems. According to Speece (1996), a compound can be called a toxicant when it causes an adverse effect on microbial metabolism, slowing down the digestion rate (toxicity) or causing process failure (inhibition). The magnitude of this effect is related to chemical-related factors or environmental-related factors or a combination of both (KNAPP; BROMLEY-CHALLONER, 2003).

Concentration and nature are major chemical-related factors influencing the degradation of toxic compounds. According to Parkin and Owen (1986), several compounds that cause inhibition at high concentrations, are stimulants or can serve as a carbon source at lower concentrations. On the other hand, some organic compounds have certain chemical structures that are easier or resistant to biodegradation such as easily metabolizable units (such as ester and amide bonds); units that are difficult to metabolize (quaternary carbon structure in hydrocarbons); the presence of xenobiotic structural units (e.g. diazo linkage); degree of branching; and substituents nature, number, and position (KNAPP; BROMLEY-CHALLONER, 2003).

Within the environmental-specific factors affecting the degradation of toxic compounds, the main factor is the presence of appropriate microorganisms that have some ability to degrade the target substance. In some cases, unique environmental conditions or specific bacteria capable of degrading the recalcitrant compounds may be needed (RITTMAN; MCCARTY, 2010). Thus, determining the microbial community with the ability to degrade the target recalcitrant compound is critical.

Table 3 shows some toxic organic compounds found in both industrial wastewaters and PHWW (MADSEN et al., 2017; SI et al., 2018). Although compounds with structures such as substitutions, aldehydes, double bonds, and benzene rings exhibited toxicity to methanogenic cultures (CHOU et al., 1979), anaerobic degradation of toxic compounds can be achieved when appropriate precautions are provided to protect the biomass. For instance, anaerobic digestion has been utilized for the treatment of wastewaters containing aromatic compounds from the petrochemical industries (RAZO-FLORES et al., 2003; GARCIA et al., 2022). Due to the complex nature of these compounds, long hydraulic retention times (HRT) (up to 6 d) has been applied to obtain efficient anaerobic processes (VEERESH; KUMAR; MEHROTRA, 2005).

Table 3 - Toxic organic compounds found in industrial wastewaters

Type of wastewater	Organic compounds	Reference
Petroleum	Alkanes, alkenes, alkynes, benzene, toluene, ethylbenzene, xylenes	Doble and Kumar (2005)
Petrochemical	Alkanes, alkenes, aldehydes, benzenes, phenol, aniline, resorcinol, nitrobenzene	Chou et al. (1979)
Vinasse from sugarcane	Phenols, melanoidins	Moraes, Zaiat and Bonomi (2015)
PHWW	Phenols, N-heterocycles, benzenes, furfurals	Madsen et al. (2017)

Source: Own authorship

In this sense, the proposed pathway for monocyclic aromatic compounds, such as benzene, toluene, ethylbenzene, and phenol under methanogenic conditions is that subsequent reactions lead to benzoyl-CoA, a common intermediate for compounds with a benzene ring (Figure 3). Activated benzoyl-CoA then undergoes ring cleavage by the addition of water across a double bond next to the carboxyl group. The resulting straight chain is degraded *via* β-oxidation to acetyl-CoA (GHATTAS et al., 2017). According to Franchi et al. (2020), the dominant

bacterial classes associated with phenol degradation are *Bacteroidia*, *Clostridia*, and *Deltaproteobacteria.*

Figure 3 - Scheme of proposed activation mechanisms for aromatic hydrocarbon degradation

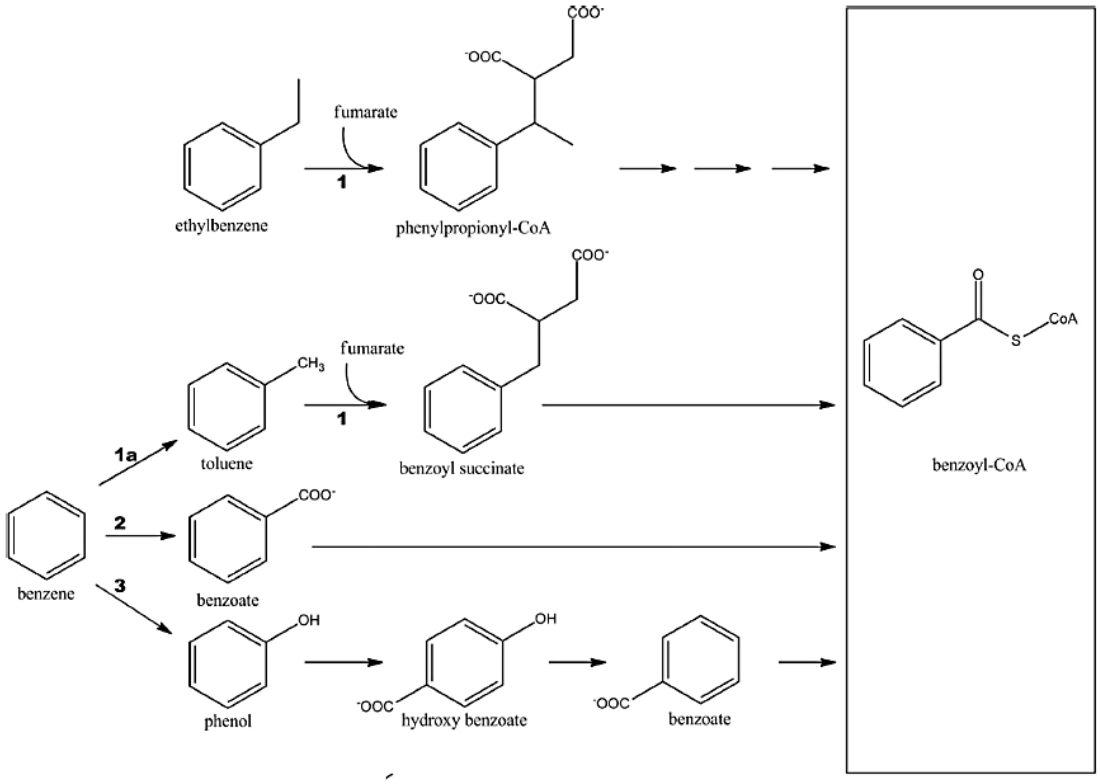

Source: GHATTAS et al. (2017)

2.4. Anaerobic digestion of PHWW

The application of anaerobic digestion for PHWW treatment has first studied in 2015. Initial studies have investigated the feasibility of the process under various PHWW concentrations through anaerobic biodegradability batch assays. Zhou et al. (2015) studied the anaerobic digestion of PHWW from the conversion of swine manure. PHWW concentrations were tested in a range from 3.3 to 66.7% v/v, obtaining positive results when the concentrations used were up to 6.7%. Higher concentrations showed strong inhibition effects in CH_4 production. Bueno et al. (2020) investigated the anaerobic degradation of PHWW from *Spirulina* biomass.

Although concentrations of organic matter above 10 $gCOD.L^{-1}$ inhibited the CH_4 production, maximum CH_4 values (306 $mLCH4.gCODadded^{-1}$) were reached at 7 $gCOD.L^{-1}$. Cyclic hydrocarbons and cyclic amine compounds were pointed at as the main responsible organics for the long lag phases and inhibition (TOMMASO et al., 2015).

Low values of CH_4 production and COD removal observed at high PHWW concentration are associated with two mechanisms, (a) a slower biodegradation rate by acidogenic/acetogenic microorganisms, and/or (b) an inhibition effect to methanogens or other microbes in the microbial community (POSMANIK et al., 2017). Tommaso et al. (2015) verified the first mechanism for the anaerobic degradation of PHWW from mixed-culture algae, where acetogenesis became the rate-limiting step. A more pronounced effect was reported by Si et al. (2019) for the anaerobic conversion of PHWW from swine manure, where even acetate accumulation was observed with the increase of PHWW concentration.

Studies assessing the continuous treatment of PHWW are scarce in the literature. Si et al. (2018) investigated the use of an up-flow anaerobic sludge blanket reactor (UASB) and a packed bed reactor (PBR) to treat PHWW from cornstalk. These high-rate anaerobic reactors reached COD removal efficiencies of 67.9% and 67.4%, respectively. An accumulation of lactate and butyrate was observed result of the partial degradation of phenols and N-heterocyclic compounds. Chen et al. (2020) studied the performance of two UASB reactors treating PHWW of cornstalk under mesophilic and thermophilic conditions. The mesophilic reactor presented higher COD removal efficiency and CH_4 yield, as observed in Table 4. On the other hand, an accumulation of formic, lactic, and acetic acids was found in the thermophilic reactor.

Table 4 summarizes advances in the anaerobic treatment of PHWW. Most studies reported a CH_4 yield higher than 200 mL/gCOD, with an average COD removal of 64%, indicating that

most of the organic matter in PHWW can be converted to methane. Biodegradability was highly influenced by feedstock characteristics, for instance, PHWW from agricultural residues needed less dilution to conduct anaerobic digestion effectively. Common compounds that were only partly degraded included derivatives of phenol, benzene, and pyridine (SI et al., 2018, 2019). Additionally, a lack of data about energy integration (biocrude oil + methane) was observed.

Based on sequencing analysis to identify microbial communities involved in PHWW degradation, the most-reported bacteria genus with the potential to degrade halogenated aromatic compounds was *Mesotoga* (BUENO et al., 2020). *Anaerolineaceae* genus also reported in various studies, was previously identified in a microbial community degrading high concentrations of phenol (ROSENKRANZ et al., 2013). The most-reported genera within the archaea were *Methanosaeta* (strict acetoclastic) and *Methanosarcina* (hydrogenotrophic and acetoclastic). *Methanobacteriaceae* genus, hydrogenotrophic methanogenic, was the most abundant in a UASB treating PHWW from cornstalk (SI et al., 2018).

Figure 4 shows the metabolism pathway proposed by Si et al. (2018) for the conversion of three toxic compounds commonly reported in PHWW (furfural, phenol, and pyridine). In this anaerobic degradation pathway, furfural is converted to furoic acid by *Desulfovibrio* sp. and then, methane can be produced by *Methanosaeta* sp. In the case of phenol degradation, this compound is firstly converted to benzoyl-CoA by *Geobacter* sp., and then β-oxidation reactions follows to produce acetate. On the other hand, pyridine degradation was proposed to be degraded aerobically by *Bacillus* sp. in the early stages of the process, due to oxygen being introduced in the system during the feeding.

Table 4 - Advances in the anaerobic treatment of PHWW

Feedstock	PHWW COD (g/L)	Configuration	Period/ Cycle/ HRT (d)	COD influent (g/L)	COD removal (%)	CH_4 yield (ml/gCOD)	Key microorganisms	Reference
Rice straw	16	ASBR	2	16	-	153	*Mesotoga, Methanosarcinales*	Chen et al. (2016)
Rice straw	28	BMP	30	0.75	-	253	*Alcaligenes, Methanosarcina*	Chen et al. (2017)
Cornstalk	76	UASB	1	8	68	-	*Anaerolineaceae, Methanobacteriaceae*	Si et al. (2018)
Cornstalk	76	PBR	1	8	67	-	*Thermotogaceae, Methanosaetaceae*	Si et al. (2018)
Swine manure	40	Batch/GAC	50	10	94	217	*Anaerolineaceae, Methanosarcinaceae*	Si et al. (2019)
Sewage sludge	60	ASBR	4	10	58	202	*Advenella, Methanosarcina,*	Usman et al. (2019)
Spirulina sp.	162	BMP	33	4	56	298	*Mesotoga Methanosaeta,*	Bueno et al. (2020)
Cornstalk	10	UASB Mesophilic	4	10	62	194	*Mesotoga, Methanosaeta*	Chen et al. (2020)
Cornstalk	10	UASB thermophilic	4	10	45	137	*Thermacetogenium, Methanothermobacter*	Chen et al. (2020)
Spirulina sp.	120	HAIB	1	1.6	58	87	*Anaerobaculum, Methanosaeta*	Bueno et al. (2021)

COD: Chemical oxygen demand, HRT: Hydraulic retention time; ASBR: Anaerobic sequencing batch reactor; BMP: Biomethane potential; UASB: Up-flow anaerobic sludge reactor; PBR: Packed bed reactor; GAC:Granular activated carbon; HAIB: Horizontal-Flow anaerobic immobilized reactor

Source: Own authorship

Figure 4 - Proposed metabolism pathway and involved microorganisms of anaerobic metabolism of dominant fermentation inhibitors (furfural, phenol, and pyridine) during anaerobic digestion of PHWW

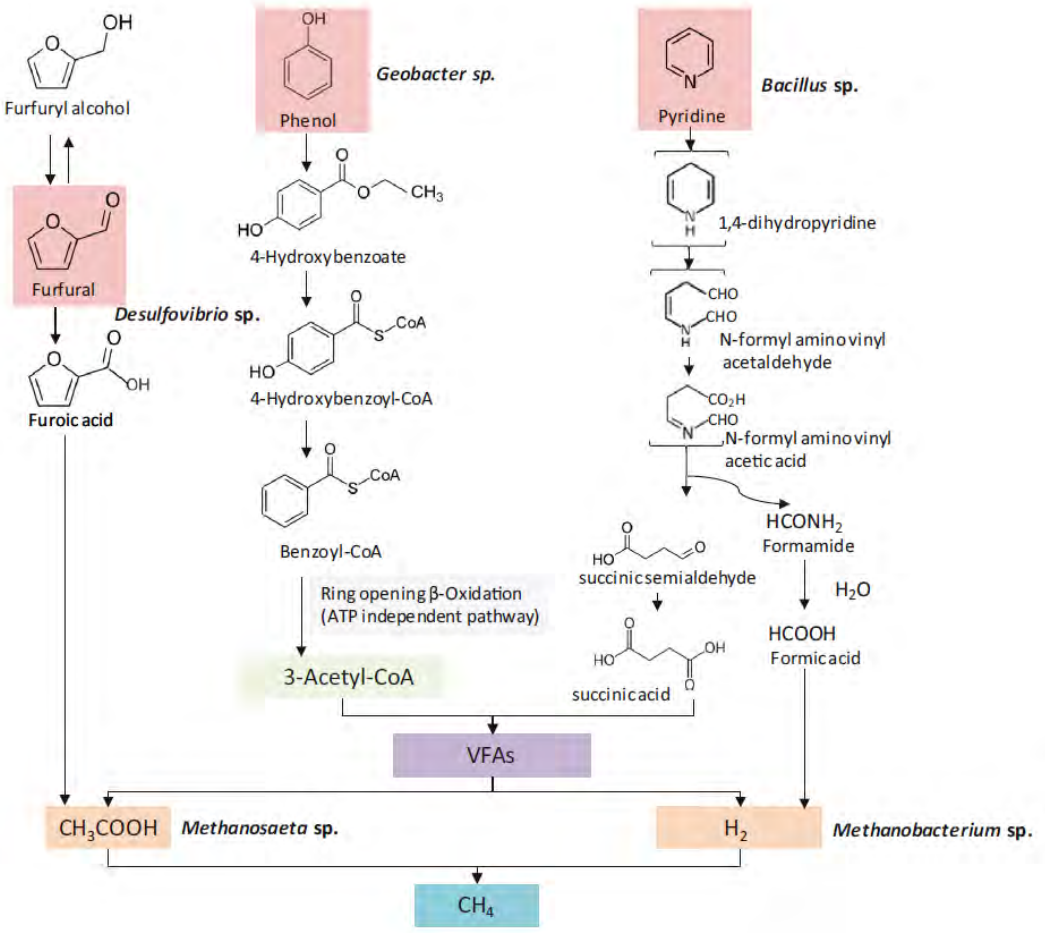

Source: Si et al. (2018)

From these studies, the feasibility of the anaerobic digestion for PHWW treatment is clear. Integrating HTL from algae biomass and anaerobic digestion can contribute to valorize PHWW and develop an algae bio-refinery approach with multiple product recovery. However, further optimization regarding PHWW aromatic content is necessary.

2.5. Strategies to enhance PHWW biodegradation

2.5.1. Biomass acclimation

Acclimation is a biological process in which a microbial population adapts to degrade a compound to which is exposed, generating additional enzymes and metabolic pathways. The toxicity of a compound could be reduced or eliminated if proper acclimation is conducted. Thus, acclimated biomass could resist toxic perturbations without disrupting the activity rate (SPEECE, 1996; MADIGOU et al., 2016).

The acclimation period can differ due to differences in substrate structure, source of inoculum, and environmental conditions. If the organism already has the potential to generate the required enzymes but needs the presence of the target compound to stimulate activity, the acclimation period can be short (minutes to hours). However, if only a few suitable organisms are present, having to grow to make an observable change in the target compound, the acclimation period can be longer (hours to weeks) (KNAPP; BROMLEY-CHALLONER, 2003).

Previous studies have investigated the acclimation of anaerobic biomass to aromatic compounds such as phenol, p-cresol, resorcinol, alkylphenols, and N-substituted compounds. Razo-Flores et al. (1996) studied the biodegradability of various N-substituted aromatic and alkylphenol compounds, using anaerobic biomass adapted to 2-nitrophenol and non-adapted biomass. The use of adapted biomass reduced lag phase duration and even became essential for some compounds degradation. Rosenkranz et al. (2013) evaluated the degradation of phenol in an ASBR, reporting that after the acclimation period (80 days), degradation rates steadily increased applying concentrations from 0.12 to 0.8 $g.L^{-1}$. Operation at higher concentrations (1.2 $g.L^{-1}$) resulted in a still efficient but slower process. Garcia et al. (2022) studied the degradation of p-cresol, resorcinol, and phenol. After treating these compounds simultaneously

in anaerobic membrane bioreactors, the half-maximal inhibitory concentrations for methanogenesis were determined and compared to non-adapted biomass, observing an increase for resorcinol from 0.25 to 3 $g.L^{-1}$ and for p-cresol from 0.60 to 0.73 $g.L^{-1}$.

In the case of PHWW, Zheng et al. (2017) studied the anaerobic biodegradability of PHWW from *Spirulina* sp. After exposing the microorganisms to a second feeding, the methane production was higher than the values obtained in the first feeding when compared to the corresponding control. Dias et al. (2021) investigated the anaerobic treatment of PHWW from spent coffee grounds under sequential batch conditions. Increasing concentrations of organic matter were applied sequentially, from 1 to 8 $gCOD.L^{-1}$, where the highest COD removal rate was found at 4 $gCOD.L^{-1}$. This approach verified the acclimation of anaerobic communities to higher concentrations of PHWW, reducing significantly the dilution ratio used at the beginning of the treatment.

2.5.2. Use of anaerobic-microaerophilic co-cultures

Sequential anaerobic-aerobic processes are usually used in the biological treatment of recalcitrant aromatic compounds. Where an anaerobic phase is required for aromatic pollutants degradation with nitro and azo substituents, and the reduced products persistent to anaerobic degradation (e.g. aromatic amines) are mineralized under aerobic conditions (DICKEL; HAUG; KNACKMUSS, 1993; AMARAL et al., 2017).

Although generally oxygen exposure is avoided in anaerobic systems, the combined activity of anaerobic and aerobic cultures can be achieved in a single reactor. Kato, Field, and Lettinga (1993) noted the simultaneous coexistence of methanogens and facultative bacteria in granular biomass under concentrations of dissolved oxygen (DO) up to 6 $mg.L^{-1}$. The tolerance to oxygen by strict anaerobes is associated with the rapid consumption of available oxygen by

facultative bacteria, normally present in the anaerobic communities. Moreover, anaerobic organisms often exist in structured communities such as floc, granules, and biofilms, where anaerobic niches can be created to protect methanogens from contact with oxygen. Thus, the facultative bacteria in the outer layers possibly act as both physical and biological shields against oxygen (KATO; FIELD; LETTINGA, 1997) (Figure 5).

The amount of oxygen supply must be controlled to not surpass the tolerant limits of methanogenic microorganisms. In this sense, limited aerated conditions must be met. Values of oxidation-reduction potential (ORP) between 0 to -300 mV indicate such conditions (NGUYEN; KHANAL, 2018).

Figure 5 - Anti-oxidative stress mechanism of the microbial community in micro-aerobic environments. Distribution of various microbial groups in bioflocs

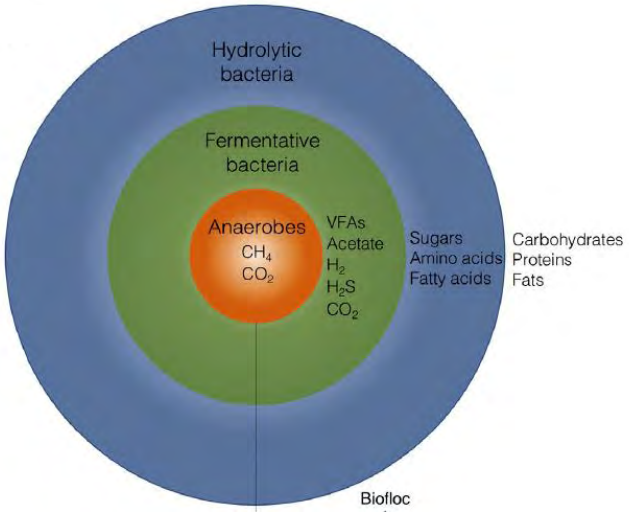

Source: Nguyen and Khanal (2018)

Azo dye degradation was achieved using mixed microbial cultures. Çinar et al. (2008) applied a sequential anaerobic/aerobic stage in a single reactor, where color removal reached up to 89% during the anaerobic stage and generated benzene-based aromatic amines were

removed in the aerobic phase (92%). Siqueira et al. (2018) assessed the biodegradation of benzene, ethylbenzene, toluene, and xylene (BTEX) in a UASB. Under micro-aerated conditions, removal efficiencies were above 83%. Carvalho et al. (2020) studied the feasibility of a micro aerated UASB to treat textile wastewater, comparing its effect with a conventional UASB. Two different redox zones were created in the partially micro aerated reactor. Although values of COD and color removal were not different from the conventional UASB values, the removal of aromatic amines was highly promoted in the micro aerated reactor, resulting in an effluent 16 times less toxic.

The unique micro aerated environment provides niches for both anaerobes and microaerophilic/facultative microorganisms. For instance, Carvalho et al. (2020) observed an enhancement in the growth of genera *Ornatilinea*, aromatic degrader, in a micro-aerated reactor, while coexisting with strict anaerobes such as *Methanobacterium* and *Methanosaeta*. Thus, the mechanism of enhancing biodegradation via limited oxygen supply is the increase of activity of facultative hydrolytic microorganisms that could degrade aromatic compounds under micro aerated conditions.

2.6. Anaerobic sequencing batch reactors

The application of adequate strategies that allow the maintenance of resistant microbial communities is the key to operating stable anaerobic systems despite the presence of toxic compounds. Ensuring high solid retention times also maximizes biomass acclimation to toxicity (PARKIN; OWEN, 1986; SPEECE, 1996).

The anaerobic sequencing batch reactor is a suspended growth reactor that operates in four continuous phases: feeding, reaction, settling, and liquid drawling. The high substrate content right after the feeding provides a high driving force for metabolic activity and increases substrate removal and biogas production rates. ASBR can provide adequate periods of

adaptation and robustness to the microbial consortium due to periodic exposure to target compounds (ZAIAT et al., 2001). In addition, ASBR decouples the reaction time and the solids retention time, favoring biomass retention by bio-granulation and floc formation (KHANAL et al., 2017). These characteristics made possible the application of anaerobic batch reactors as alternatives to continuous systems.

ASBR feasibility has been evaluated for the treatment of various types of effluents. Almeida et al. (2017) investigated the anaerobic treatment of vinasse from bioethanol production under mesophilic and thermophilic conditions, reporting increasing CH_4 production with an increment in organic load (1 to 10 $gCOD.L^{-1}$). Maximum values of CH_4 production were up to 302 $mL.gCOD^{-1}$ under mesophilic conditions. Silva et al. (2013) studied the anaerobic treatment of biodiesel production effluent in batch and fed-batch mode. Gradual increase in the organic load (1.23 – 2.52 $gCOD.L^{-1}.d^{-1}$) resulted in removal efficiencies up to 88%, even though stability could not be achieved at 3.77 $gCOD.L^{-1}.d^{-1}$. Rosenkranz et al. (2013) pointed out that ASBR allowed the specialization of the microbial community due to the reactor's strategic operation based on the progressive increase of organic matter.

In the case of PHWW (Table 4), Chen et al. (2016) studied the application of two ASBRs for the treatment of PHWW from rice straw. One reactor was fed with raw PHWW and the other with PHWW previously extracted with petroleum ether. The latter achieved higher CH_4 yields (218 $mL.gCOD^{-1}$). Usman et al. (2019) studied the anaerobic degradation of PHWW from sewage sludge in a sequencing batch process. CH_4 production and COD removal reached values of 202 $mL.gCOD^{-1}$ and 58%. Both studies reported minimal accumulation of volatile fatty acids.

Furthermore, the application of sequencing batch reactors using anaerobic-microaerophilic co-cultures was reported for azo dyes degradation. Menezes et al. (2019) compared three

reactors working with distinct cycles, the first was completely anaerobic (24 h) whereas the second and third included a micro-aerated stage (12 h) after an anaerobic stage (12). Micro-aeration was applied continuously to the second reactor and intermittently to the third reactor. Results indicated that both micro-aeration techniques improved the removal of aromatic amines and ecotoxicity. Overall performance of micro aerated reactors was equivalent; however, much lower oxygen consumption was reported by intermittent strategy.

2.7. Photocatalysis as a post-treatment of the anaerobic digestion

Advanced oxidation processes (AOPs) have been recognized as efficient treatments for recalcitrant wastewaters due to their ability to remove toxic and colored compounds from water that are not simply removed by the lone application of biological techniques. The total mineralization of the organics results in the formation of CO_2 and H_2O. The formation of salts can take place if there are nitrogen, sulfur, and chloride compounds in the medium (IOANNOU; PUMA; FATTA-KASSINOS, 2015).

Heterogeneous photocatalysis is an advanced oxidation process, which occurs by accelerating a photoreaction in the presence of a semiconductor catalyst (TiO_2, ZnO). This process is defined by the irradiation of a catalyst with sufficient energy to form a positive hole (h^+) in the valence band and an electron (e^-) in the conduction band (Eq. 1). The electron reduces the oxygen adsorbed on the catalyst (Eq. 2). The positive hole reacts with the organics absorbed on the surface of the catalyst (Eq. 3) or with water (Eq. 4), generating radicals that also degrade the organics in the solution (Eq. 5) (Figure 6) (AHMED et al., 2011; BRAME et al., 2015).

$$TiO_2 + hv\ (\lambda < 387\ nm) \rightarrow\ e^- + h^+ \quad (1)$$

$$e^- + O_2 \rightarrow O_2^{\cdot -} \quad (2)$$

Oxidative reaction:

$$h^+ + Organic \rightarrow \text{Intermediates} \rightarrow CO_2 + H_2O \quad (3)$$

$$h^+ + H_2O \rightarrow HO^{\cdot} + H^+ \quad (4)$$

Reductive reaction:

$$HO^{\cdot} + Organic \rightarrow \text{Intermediates} \rightarrow CO_2 + H_2O \quad (5)$$

Figure 6 - Schematic diagram illustrating the principle of UV photocatalysis

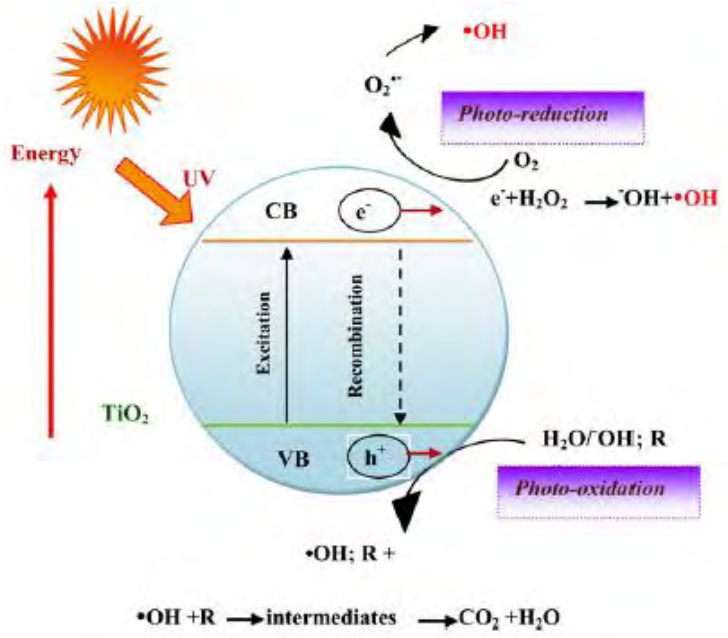

Source: Ahmed et al. (2011)

Several parameters may influence photocatalytic degradation including the initial concentration of organics (CHATZISYMEON; XEKOUKOULOTAKIS; MANTZAVINOS, 2009), type and concentration of the catalyst (PETERNEL et al., 2007), light intensity (GUPTA et al., 2012), pH (BIZANI et al., 2006), oxidants/electron acceptor such as H_2O_2 (NOGUEIRA et al., 2016) and aeration (PEKAKIS; XEKOUKOULOTAKIS; MANTZAVINOS, 2006). The type of substrate is the most important parameter since it influences all the parameters due to the complexity of the substrates that are normally destined to be treated by photocatalysis

(BRAME et al., 2015). One important factor to monitor during or after advanced oxidation processes is ecotoxicity, because the process itself may generate oxidation intermediates more toxic to biological systems than the original effluent in some cases (RIZZO, 2011).

The application of photocatalysis as post-treatment, where the highly biodegradable fraction was anaerobically removed, was investigated. Costa and Alves (2013) studied the photocatalysis of anaerobically treated olive oil mill wastewater from a lab-scale UASB. Removal efficiencies of COD, total phenolic content, and color reached 50%, 91%, and 79% after 4 hours of irradiation, for initial values of COD between 1.05 and 7.37 g/L.

Mabuza et al. (2017) studied the integration of anaerobic digestion under thermophilic conditions and photocatalytic degradation using a TiO2-ZnO hybrid catalyst for the treatment of molasses wastewater. The initial concentrations of COD and TOC were 6.6 g/L and 3.2 g/L, respectively. Efficiencies reached COD and TOC removal values of 90% and 80%, respectively, and photocatalysis achieved color removal of 92% after 30 min of irradiation.

Anaerobic digestion followed by photocatalysis could be beneficial, since the anaerobic process is highly indicated for wastewaters with high organic content, and photocatalysis is efficient in color and recalcitrant compounds removal. Therefore, the association of these processes is an interesting alternative for the treatment of PHWW and it is a more economically feasible option since AOPs are expensive techniques and the energy required for the photocatalysis can be provided by anaerobic treatment in an integrated system (APOLLO; ONYANGO; OCHIENG, 2014).

2.8. Final considerations

Nowadays, the production of bioenergy from sustainable sources such as the biocrude oil from the conversion of microalgae *via* the HTL process, is crucial, as well as the appropriate

management and treatment of resulting wastewaters. The integration of these technologies can be feasible when anaerobic digestion is used for PHWW treatment, recovering energy and carbon. However, to scale up this process is necessary to resolve the bottleneck associated with the aromatic content in PHWW. Therefore, this research is focused on studying techniques that could enhance the treatment of PHWW.

3. MATERIALS AND METHODS

3.1. Experimental design

The present research was focused on the investigation of methods that can complete PHWW stabilization. Therefore, three approaches were considered. The first approach studies the anaerobic treatment of PHWW in a sequencing batch process, evaluating the effect of the organic matter concentration in the influent, on biogas production and organics degradation. The second approach investigates the effect of intermittent aeration applied after an anaerobic phase on the degradation of PHWW in a sequencing batch process. The third approach studies the photocatalytic degradation of anaerobically digested - PHWW (AD-PHWW), determining the optimal conditions of photodegradation. The experimental design of this study can be found in Figure 7.

3.2. Methods

3.2.1. PHWW generation and characterization

Spirulina biomass (solids content of 95 wt.%) was obtained in dry-powder form from commercial sources. The HTL process was conducted in a 7.57 L stirred batch reactor (Parr Instrument Co., Moline, USA) (Figure 8). The feedstock was mixed with water and added to the reactor as a slurry with 20 wt% solid content. The reactor was then, purged with nitrogen gas to obtain an initial pressure of 0.65MPa. Hydrothermal conditions of 260°C and 1h retention time were applied according to Tian et al. (2018). After cooling down the reactor, the aqueous phase was separated from the raw oil and solid residue through vacuum filtration using a 0.45 μm pore size glass fiber filter. This research was focused on PHWW stabilization, so the gas, the biocrude oil, and solid residue were not further analyzed.

Figure 7 - Schematic diagram of the experimental design

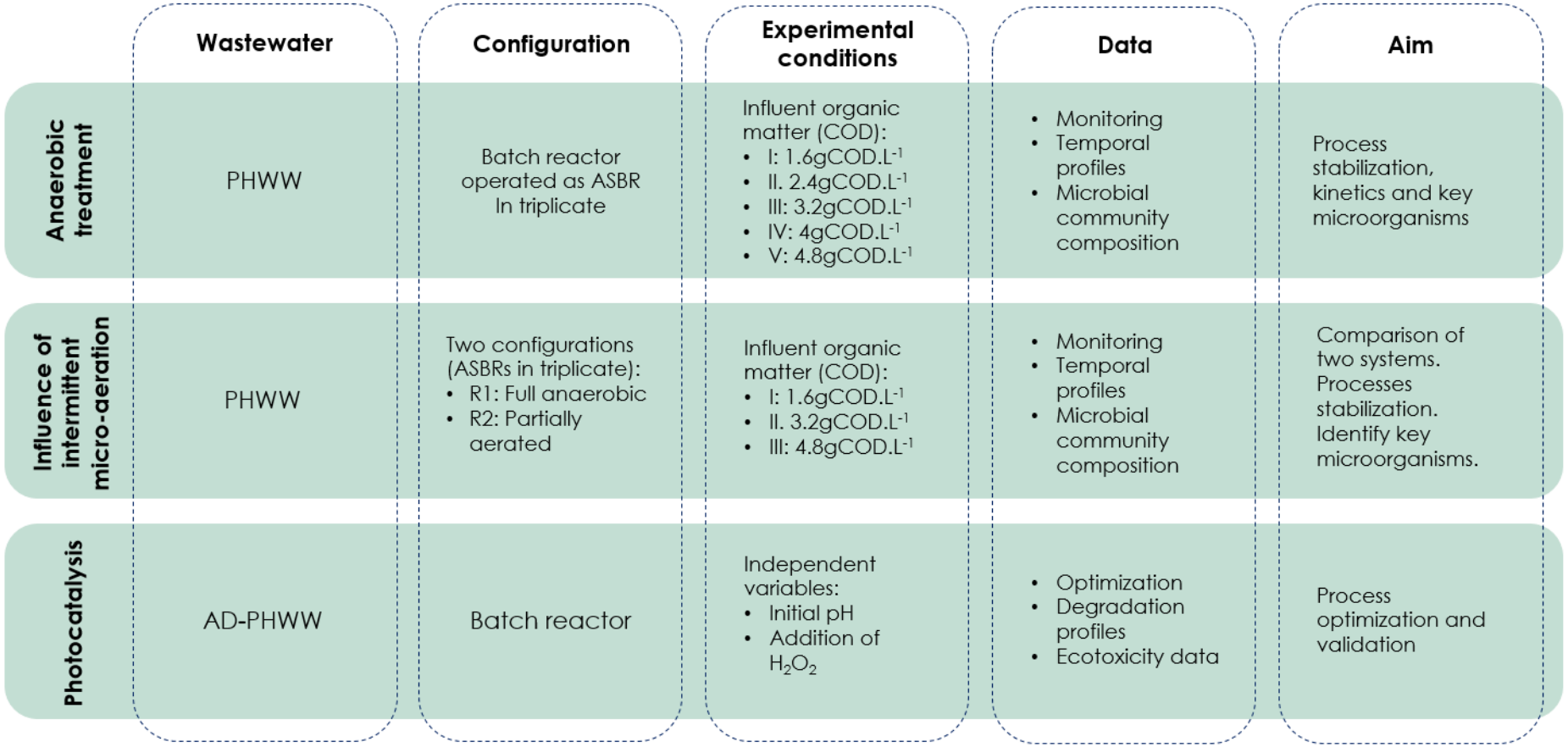

Source: Own authorship

Figure 8 - HTL set-up

Source: Own authorship

Filtered PHWW was used for the following analysis and experiments. PHWW was characterized in terms of pH, COD, total solids, electrical conductivity, total Kjeldahl nitrogen (TKN), ammonium nitrogen, phosphorus, total phenolic content, and volatile fatty acids. Ecotoxicity bioassays were also performed to assess the toxicity level of PHWW.

3.2.2. Anaerobic treatment of PHWW in a sequencing batch process

The anaerobic treatment of PHWW was studied in 1 L Duran® flasks (working volume of 600 mL) in triplicate. The reactors were operated in sequencing batch mode under mesophilic temperatures (37 ± 1°C) with a replacement volume of 75%. Sludge from an upflow anaerobic sludge blanket reactor treating waste from a poultry slaughterhouse (Dacar, SP, Brazil) was

used as inoculum with total volatile solids (TVS) of 63.4 $g.L^{-1}$ and added to the reactors as 5.6 $g.L^{-1}$ of volatile suspended solids (VSS) in the mixed liquor.

The feeding substrate consisted of PHWW diluted in tap water with nutrient media (ANGELIDAKI et al., 2009), prepared according to each experimental condition. External nitrogen supplementation was not included due to the low carbon/nitrogen ratio reported for PHWW. pH was adjusted in media to 7.3 ± 0.2 using HCl 6N. The reactors were flushed with nitrogen gas for 10 min after feeding and before sealing to provide anaerobic conditions for each cycle.

The reactors were subjected to subsequent experimental conditions, according to Table 5. Firstly, a pre-exposition period was applied to determine the sufficient time to degrade the organic matter, evaluating the COD degradation along the cycle during this period. The initial cycle time of 7 days was reduced to 3 days after observing a non-significant difference between the removal efficiencies. After this period, the cycle time was established as 72 h and five increasing organic loads were tested subsequently (from 0.4 to 1.2 $gCOD.L^{-1}.d^{-1}$), where the concentration of COD in the feeding substrate was incremented once the system reached an apparent steady rate regimen (from 1.6 to 4.8 $gCOD.L^{-1}$). This approach was used to stimulate the acclimation of the microbial community to PHWW complex nature. For each experimental condition, the applied volumetric organic load was calculated by Eq. (6):

$$\mathrm{AVOL}\ (\mathrm{gCOD.\,L^{-1}.\,d^{-1}}) = \frac{(V_F \times N) \times COD_0}{V_R} \times 100 \quad (6)$$

In which AVOL is the applied volumetric organic load ($gCOD.L^{-1}.d^{-1}$), V_F is the fed volume per cycle ($L.cycle^{-1}$), N is the number of cycles per day ($cycle.d^{-1}$), COD_0 is the initial concentration of organic matter ($gCOD.L^{-1}$) and V_R is the volume of liquid in the reactor (L).

Table 5 - Experimental conditions evaluated in the anaerobic treatment of PHWW

Parameters	Experimental conditions					
	Pre-exposition	I	II	III	IV	V
Influent COD ($g.L^{-1}$)	1.6	1.6	2.4	3.2	4	4.8
S/X ($gCOD.gVSS^{-1}$)	0.29	0.29	0.43	0.57	0.71	0.86
AVOL ($gCOD.L^{-1}.d^{-1}$)	-	0.4	0.6	0.8	1	1.2
Period (days)	28	48	54	45	39	39
Number of cycles	6	16	18	15	13	13

Source: Own authorship

To monitor the process performance, influent and effluent samples were collected and filtered (0.45 μm filters) for the following analyses: COD, pH, and alkalinity. Gas samples were also collected to quantify CH_4 content in the biogas. After reaching operational stability, temporal samples over the cycle time were taken to analyze COD, CH_4 production, VFA, and phenolic content. These analyses were performed according to Section 3.2.5. Operational stability (apparent steady-state) was considered achieved when a consistent alkalinity production was observed and the organic matter removal presented a relative standard deviation lower than 5%. VSS was also analyzed in the mixed liquor at the start and the end of the operational period. Samples of the inoculum and the sludge at the end of the reactors' operation were collected and submitted to molecular biology analysis according to Section 3.2.6 to analyze their microbial composition.

The efficiency of organic matter removal expressed as COD in filtered samples was calculated using Eq. (7):

$$COD\ removed\ (\%) = \frac{COD_0 - COD_f}{COD_0} \times 100 \quad (7)$$

Where COD_0 is the concentration of organic matter in the influent ($gCOD.L^{-1}$), and COD_F is the initial concentration of organic matter in the effluent ($gCOD.L^{-1}$).

CH_4 production values obtained from the temporal profiles of each experimental condition were adjusted using the modified Gompertz model (Eq. 8), as previously done by Tommaso et al. (2015):

$$P_{CH_4}(t) = P_{CH_4}\, exp\left\{-exp\left[\frac{k.e}{P_{CH_4}}(\lambda - t) + 1\right]\right\} \quad (8)$$

In this expression $P_{CH_4}(t)$ corresponds to the cumulative CH_4 production ($NmL.gVSS^{-1}$) at time *t*, P_{CH_4} is the CH_4 production potential ($NmL.gVSS^{-1}$), k is the maximum methane production rate ($NmL.gVSS^{-1}.h^{-1}$), λ is the duration of the lag phase (h), and *e* is Euler's number, the mathematical constant (2.71828). The maximum theoretical CH_4 potential was calculated considering that each gram of removed COD produced 0.350 L of CH_4 (SPEECE, 1996)$_S$. The methanogenesis percentage was calculated relating the CH_4 production (expressed in gCOD) and the mass of organic matter removed (expressed in gCOD) according to Eq. (9):

$$Methanogenesis\ (\%) = \frac{m_{CH_4}}{m_{COD_{rem}}} \quad (9)$$

A pseudo-first-order model considering a residual substrate concentration (Eq. 10) was adjusted to the COD and TPh degradation and profiles.

$$S(t) = S_R + (S_I - S_R).e^{-kt} \quad (10)$$

In which, $S(t)$ is the substrate (COD or TPh) at time *t*, S_R is the residual substrate at the end of the cycle time ($mg.L^{-1}$), S_I is the initial substrate ($mg.L^{-1}$), k is the first-order kinetic constant (h^{-1}).

Specific substrate utilization rates were calculated using the first-order kinetic constant obtained from the pseudo-first-order model (k) according to Eq. (11).

$$r_S = \frac{(S_I - S_R) \times k}{X} \quad (11)$$

Where r_S corresponds to the specific substrate utilization rate (mgCOD.gVSS^{-1}.h^{-1}), S_R is the residual COD at the end of the cycle time (mg.L^{-1}), S_I is the initial COD (mg.L^{-1}), k is the first-order kinetic constant (h^{-1}) and X is the biomass concentration (gVSS.L^{-1}).

To determine the maximum substrate utilization rate, a graph was constructed relating the initial substrate concentrations to the specific substrate utilization rates of each condition experimental tested. After observing a substrate inhibition, a modification of the Haldane model was fitted to the experimental data, as previously done by Dwyer et al. (1986) (Eq. 12) to determine kinetic parameters:

$$r_S = r_{max} \frac{S}{S + K_s + \left(\frac{S}{K_i}\right)^n} \quad (12)$$

Where r_S corresponds to the specific substrate utilization rate (mgCOD.gVSS^{-1}.h^{-1}), r_{max} is the maximum substrate utilization rate (mgCOD.gVSS^{-1}.h^{-1}), K_s is half-velocity constant (mgCOD.L^{-1}), K_i is the inhibition constant (mgCOD.L^{-1}), n is the inhibition response coefficient, and S is the substrate concentration (mgCOD.L^{-1}). All fittings were conducted using the Levemberg-Marquart algorithm (Origin 9.0 - OriginLab Corp, MA, USA).

3.2.3. Influence of micro aeration on PHWW biodegradation

The experimental set-up consisted of two independent sets of three reactors, assembled in 1 L Duran® glass bottles (useful volume of 600 mL). R_1 was completely anaerobic (operated as a control) and R_2 was partially aerated. Each cycle lasted 72 h, where R_2 combined three stages, a 48 h anaerobic stage, followed by a 12 h partially aerated stage with intermittent air supply

(30 min every 2 h), and lastly an 11.5 h anaerobic stage. Figure 9 shows a scheme of the system used for R_2. The reactors were operated in sequence batch mode with a volume exchange ratio of 75% at mesophilic temperatures (37 ± 1 ◦C).

Figure 9 – Partially aerated set-up (R_2)

Source: Own authorship

The dispersion of fine bubbles of air was accomplished using circular aerators (Resun Air Curtain) of microperforated rubber placed at the bottom of the reactors and supplied by aquarium pumps. The airflow rate was 0.5 ± 0.05 $mL.min^{-1}$ controlled by valves and monitored periodically by a rotameter. Electronic programmers were used to control the air pump's energy supply.

The inoculum sludge used was previously detailed in Section 3.2.2. A gradual increase of the organic load was applied (0.4, 0.8, and 1.2 $gCOD.L^{-1}.d^{-1}$) to promote biomass acclimation, according to Table 6. Influent and effluent collected samples were filtered and monitored in terms of COD, pH, alkalinity, NTK, and NH_4. Temporal concentration profiles were analyzed after the system reached operational stability over the cycle time. Analyzed parameters included COD, CH_4 production, VFA, phenolic content, oxidation-reduction potential (ORP),

and dissolved oxygen (DO). These analyses were performed according to Section 3.2.5. Temporal profiles of COD, TPh, and CH_4 were adjusted to a first-order model with residual concentration (Eq. 10) and a Gompertz model (Eq. 8), respectively, as conducted in Section 3.2.3. Sludge samples of the reactors were taken at the end of the operational period of both configurations and submitted to microbial diversity analysis according to Section 3.2.6.

Table 6 - Experimental conditions evaluated in the anaerobic and partially aerated treatment of PHWW

Parameters	Experimental conditions		
	I	III	V
Influent COD ($g.L^{-1}$)	1.6	3.2	4.8
AVOL ($gCOD.L^{-1}.d^{-1}$)	0.4	0.8	1.2
Period (days)	60	72	75
Number of cycles	20	24	25

Source: Own authorship

3.2.4. Photocatalysis as a post-treatment

PHWW used in this experiment was anaerobically pre-treated in a 2 L lab-scale HAIB reactor for 200 days. AD-PHWW was collected when the HAIB reactor was operating with an organic load rate of 1.6 g $COD.L^{-1}.d^{-1}$, HRT of 24 h and has reached apparent steady-state condition with an average COD removal efficiency of 58%. Table 7 presents AD-PHWW characterization, which evidences that although the anaerobic reactor managed to remove a significant part of the organic matter in PHWW, a subsequent treatment for its aromatic content is needed. Further details about the operation of the HAIB reactor were reported in the study of Bueno et al. (2021).

Photocatalytic experiments were assembled using an irradiation system constituted of a shaker incubator, UV lamp, a 250 mL jacketed cylindrical glass reactor, and a thermostatic bath (Figure 10). The internal walls of the shaker incubator were covered with aluminum foils to prevent light entrance from the exterior of the system. UV irradiation was provided by a low-pressure mercury lamp (Osram, HNS, G13, 15W) emitting nearly monochromatic light at 254 nm. The lamp was placed 15 cm above the sample's surface.

Table 7 - Main characteristics of post-hydrothermal liquefaction wastewater after the anaerobic treatment in the HAIB reactor

Parameter (Unit)	HAIB effluent (mean ± SD)
pH	8.05
COD ($mg.L^{-1}$)	605 ± 7
TKN ($mg.L^{-1}$)	154 ± 6
NH_4^+ ($mg.L^{-1}$)	136 ± 15
Volatile acidity ($mgCH_3COOH.L^{-1}$)	0.55
Total phenolic compounds ($mgGAE.L^{-1}$)	29.8 ± 0.13
Conductivity ($\mu S.cm^{-1}$)	883
VIS_{340}[a] (cm^{-1})	0.273 ± 0.015
UV_{278}[a] (cm^{-1})	0.7 ± 0.013
UV_{254}[a] (cm^{-1})	0.685 ± 0.009

[a]Dilution factor 1:5

Source: Own authorship

The mixture to be treated included 50 mL of AD-PHWW, 2 $g.L^{-1}$ of TiO_2 (anatase, 21 nm particle size), and oxidant (H_2O_2 as 35% v/v solution) according to each experimental condition. Initial pH was adjusted using either HCl 1 $mol.L^{-1}$ or NaOH 1 $mol.L^{-1}$ when

necessary. UV irradiation was carried out for 4 h at 27 ± 2 °C, under magnetic stirring of 120 rpm. Samples collected were filtered using 0.45 µm glass fiber filters to remove catalyst particles. Residual H_2O_2 in samples was removed using catalase solution ($1 g.L^{-1}$), prepared with catalase from bovine liver (2000 – 5000 $units.mg^{-1}$).

Central composite design – Face centered (CCD-FC) was used to investigate the photodegradation of AD-PHWW regarding the initial pH [x_1], and addition of H_2O_2 [x_2]. Table 8 shows the CCD-FC matrix which includes 8 experiments plus central point replications elaborated using the software Statistica.

Table 8 - FC-CCD matrix of independent variables

Run	Initial pH [x_1]	Addition of H_2O_2 ($g.L^{-1}$) [x_2]
1	7	2
2	7	4
3	12	2
4	12	4
5	9	2
6	9	4
7	7	3
8	12	3
9	9	3
10	9	3
11	9	3

Source: Own authorship

The following quadratic regression was used to fit the response surface models generated from experimental results (Eq. 13):

$$y = \beta_0 + \sum_{i=1}^{k} \beta_i x_i + \sum_{i=1}^{k} \beta_{ii} x_i^2 + \sum_{i=1}^{k-1} \sum_{j=i+1}^{k} \beta_{ij} x_i x_j + \varepsilon \quad (13)$$

In which y is the response variable, β_0 is the constant coefficient of intercept, β_i is the linear effect coefficient of the quadratic model, β_{ii} is the quadratic effect coefficient, β_{ij} is the linear model coefficient of the interaction between independent variables i and j; ε is the error term, x_1 and x_2, are the independent variables.

The response variables were COD, phenolic content, and color removal. These analyses were performed according to Section 3.2.5. COD reduction (%) was calculated using Eq. (7). The extent of color removal was assessed by absorbance decrease at 340 nm.

Experiments were carried out at optimum conditions of initial pH and addition of H_2O_2, obtained after optimization to validate the models. Samples taken at pre-defined times (0, 0.5, 1, 2, 3, and 4 h) were analyzed in terms of COD, phenolic content, and color removal. Data obtained was adjusted to the pseudo-first-order Langmuir-Hinshelwood model (Eq. 14), used to describe the reaction occurring on the solid-liquid surface under irradiation (KUMAR; PORKODI; ROCHA, 2008).

$$-ln\left(\frac{C}{C_0}\right) = k.t \quad (14)$$

Where C is the final compound concentration, C_0 is the initial compound concentration, t is the irradiation time, and k is the first-order rate constant determined from the slope of the straight line.

3.2.5. Analytical methods

COD, solids, total Kjeldahl nitrogen (TKN), and ammoniacal nitrogen (NH_4^+) analyses were performed according to the Standard Methods for Examination of Water and Wastewater (APHA, 1998). The total phenolic content was expressed in terms of gallic acid equivalents (GAE) (SINGLETON; ORTHOFER; LAMUELA-RAVENTÓS, 1999). pH and was measured with a calibrated potentiometer. ORP was monitored with an ORP electrode. DO was measured by a dissolved oxygen meter. Electrical conductivity was measured with a calibrated conductivimeter. Sample absorbance was scanned on a UV-vis spectrophotometer, and the maximum absorbance was used to assess the extent of color removal that occurred during the photocatalytic treatment (PEKAKIS; XEKOUKOULOTAKIS; MANTZAVINOS, 2006). Alkalinity analyses were determined according to Ripley, Boyle, and Converse (1986).

Biogas production was measured using a pressure transducer (model GN200, Data Logger). CH_4 quantification was analyzed according to the methodology proposed by Kaminski et al. (2003) on a gas chromatograph equipped with a flame ionization detector (GC-FID) (Trace 1300, Thermo Fisher Scientific®) in a controlled temperature environment (25°C). VFA quantification (acetic, propionic, butyric, valeric, and caproic acids) was carried out following the methodology developed by Adorno, Hirasawa, and Varesche (2014). Samples for VFA analysis were first extracted using ethyl ether as a solvent and then injected into GC-FID. Separation was achieved using a HP INNOWAX column (30 m x 0.25mm x 0.25 µm).

3.2.6. Analysis of microbial diversity

Samples of collected sludge were subjected to DNA extraction and quantification according to Carvalho et al. (2020). The microbial diversity analysis was conducted using amplicon sequencing in the V3/V4 region of the 16S rRNA gene via Illumina MiSeq. The

libraries were prepared following the manufacturer's guidelines (Neoprospecta Microbiome Technologies, Brasil). Primers 341F (CCTACGGGRSGCAGCAG) (WANG; QIAN, 2009) and 806R (GGACTACHVGGGTWTCTAAT) (CAPORASO et al., 2012) were used. The libraries were sequenced using MiSeq Sequencing System (Illumina Inc, USA). Paired-end reads were merged using Pandaseq v.2.11 software, the sequences were clustered and the chimeras were removed. Final operational taxonomic units were identified using Blastn v.2.6.0+ against a curated database derived from RDII and NCBI platforms.

3.2.7. Ecotoxicological assessment

The ecotoxicological bioassays aimed not only to evaluate the toxicity of PHWW but also, to study the effects of the treatments applied on PHWW toxicity. Aquatic organism *Daphnia similis* (zooplankton) commonly called water flea, and plant seed *Eruca sativa* Mill (arugula) were chosen as test-organism. Zooplankton was cultivated at the Ecotoxicology and Ecophysiology of Aquatic Organismsms Laboratory at the Center for Water Resources and Applied Ecology of the University of Sao Paulo and was kept at controlled conditions of temperature (20 ± 2), light period (16:8 h light/dark) and culture media in accordance with ABNT (2016).

Acute toxicity with *D. similis* was performed to determine the effective concentration of a PHWW sample that could immobilize 50% of the organisms within 48 h (EC_{50}). Bioassays were conducted following the guidelines issued by ABNT (2016). Samples concentrations were assessed, being diluted using dechlorinated tap water with conductivity 160 of µS/cm, pH 7 - 7.6, and hardness of 40 - 48 mg $CaCO_3.L^{-1}$. 10 mL of the test solutions and five organisms (<24 h old) to non-toxic plastic vessels with four replicates per concentration. The control consisted of an equal number of organisms exposed only to culture media. Immobile organisms were checked after 48 h of exposure. The same controlled conditions (temperature and light

period) used in the cultivation of these organisms were followed. Test media was monitored for pH, conductivity, and dissolved oxygen at the start and end of all the toxicity tests. Results were expressed in EC_{50} and acute toxicological units (Eq. 15).

$$TU_a = 100/EC_{50} \quad (15)$$

Phytotoxic bioassays with *Eruca sativa* Mill seeds were performed to verify the acute toxicity of PHWW in terms of germination inhibition (EC_{50}) and other effects (germination ratio and germination index). Bioassays were conducted following US EPA procedures (1996) using seven concentrations of PHWW (0.1, 0.5, 1, 2.5, 5, 7.5, and 10%). Tests were conducted using 49 x 13 mm disposable plastic Petri dishes and filter paper. Ten undamaged and similar-size seeds were laid on the filter paper in each dish with 1 mL of test concentration. A control test with distilled water was carried out. Three replicates were carried out per concentration and control. The germination test took place at 20 ± 2°C in the dark for four days of exposure. Germinated seeds were counted to calculate the EC_{50} and germination ratio (Eq. 16). Root elongation and shot length were also measured to determine the germination index (Eq. 17) (PRIAC; BADOT; CRINI, 2017).

$$GR\ (\%) = \frac{GSS}{GSC} \times 100 \quad (16)$$

$$GI\ (\%) = \frac{RLS \times GSS}{RLC \times GSC} \times 100 \quad (17)$$

Where RLS is the average root elongation in the sample, RLC is the average root elongation in control, GSS is the number of germinated seeds in the sample, GSC is the number of germinated seeds in the control. EC_{50} values were determined from the concentration-response curves obtained for each condition using Origin 9.0 (OriginLab Corp, MA, USA).

3.2.8. Statistical analysis

Kolmogorov-Smirnov and Levine's tests were conducted to verify the data's normal distribution and the homogeneity of variance of each experiment statistically evaluated, respectively. The analysis of variance (ANOVA) was performed to assess the significant effect of the influent organic matter on PHWW anaerobic treatment (COD removal efficiency and CH_4 yield). Tukey's multiple comparison test was used to compare the means (95% confidence interval). The significant difference between R_1 and R_2 during the micro-aeration experiments was analyzed using Student's t-test at a 95% confidence level. These analyses were conducted using the software Minitab 18 (Minitab Inc, PA, USA).

The statistical adequacy of models obtained from the CCD-FC experiments was determined using the regression coefficient analysis (R^2 and $\text{Adj.}\,R^2$) and analysis of variance with the lack of fit test. The overlay contour plot methodology was used to find a common optimal region when considering all three dependent variables simultaneously. These analyses were performed using the software Statistica 12 software (Statsoft Inc, OK, USA).

.

4. RESULTS AND DISCUSSION

4.1. PHWW characterization

Table 9 shows the main characteristics of PHWW generated from the conversion of *Spirulina* biomass. The wastewater contained a high concentration of organic compounds, similar to the values observed for the same feedstock (QUISPE-ARPASI et al., 2018; BUENO et al., 2021). Within the major organic compounds previously found in PHWW from microalgae, organic acids and aromatic compounds represented the highest percentage (GAI et al., 2015a; ZHENG et al., 2017). In the present study, VFA concentration (acetic, propionic, butyric, and valeric acids) accounted for 4.3% of the total COD in PHWW. Whereas, the phenolic content reached 3.9 $gGAE.L^{-1}$ (3.45 $gCOD.L^{-1}$) in agreement with Bueno et al., (2021) (4.9 $gGAE.L^{-1}$). Aromatic compounds, such as phenol derivatives and N&O heterocyclics are generated from the thermal degradation of carbohydrates and proteins during HTL (GAI et al., 2015a; MADDI et al., 2016). Furthermore, nitrogen content (TKN and NH_4^+) was similar to values reported by Biller et al. (2012).

PHWW from *Spirulina* also exhibited ecotoxic and phytotoxic properties. EC_{50} values obtained from the concentration vs response curves were 0.49 ± 0.02% for *D. similis* (48 h) and 5.2 ± 0.97% for *E. sativa* Mill (96 h) (Figure 10), where the lower the EC_{50} value the higher the toxicity. Thus, TU_a values reached 205 ± 8 and 19 ± 4, respectively. Differences in sensibility between test organisms can occur due to their heterogeneous nature. For instance, Pham et al. (2013) conducted a cell chronic cytotoxic assay and reported that PHWW from *Spirulina* sp. was highly cytotoxic to mammalian cells, where 7.5% of PHWW induced a 50% reduction in cell density. Alimorardi et al. (2020) determined the concentration of PHWW from *Chlorella kessleri* that produced a 50% reduction in the maximum growth rate of *Pseudomonas putida*. Results indicated that EC_{50} was in the range from 1 to 6.8% for various HTL temperatures (270–345 °C).

Table 9 - Characteristics of post-hydrothermal liquefaction wastewater

Parameter (Unit)	Value
pH	8.7
COD ($g.L^{-1}$)	131.6 ± 1.6
TKN ($g.L^{-1}$)	11.7 ± 0.1
NH_4^+ ($g.L^{-1}$)	6.7 ± 0.1
Total phosphorus ($g.L^{-1}$)	1.2 ± 0.1
Total phenolic compounds ($gGAE.L^{-1}$)	3.9 ± 0.2
Conductivity ($mS.cm^{-1}$)	42.35
TS ($g.L^{-1}$)	57 ± 0.6
TVS ($g.L^{-1}$)	49 ± 0.2
Acetic acid ($g.L^{-1}$)	1.8 ± 0.03
Propionic acid ($g.L^{-1}$)	0.96 ± 0.01
Isobutyric acid ($g.L^{-1}$)	0.15 ± 0.02
Butyric acid ($g.L^{-1}$)	0.47 ± 0.03
Isovaleric acid ($g.L^{-1}$)	0.61 ± 0.04

Source: Own authorship

On the other hand, *D.similis* was used to evaluate vinasse toxicity in the work described by Ferreria et al. (2011), obtaining EC_{50} values of 2.2% (TU_a = 45). Which indicates that PHWW was more toxic to *D.similis* than vinasse. According to the authors, the low EC_{50} obtained was caused mainly by the elevated organic matter and the high molecular weight compounds found in vinasse. Moreover, Pelegrini, Pelegrini, Paterniani (2006) reported that 1 $g.L^{-1}$ of phenol inhibited 80% of *E. sativa* seeds germination. Pham et al. (2013) found a synergistic cytotoxicity effect among specific aromatic compounds reported in PHWW when in a mixture.

Therefore, it could be inferred that PHWW toxicity level is related to its complex and high aromatic content.

Figure 10 - Concentration vs. response curves for *D. similis* (a) and *E. sativa* Mill (b)

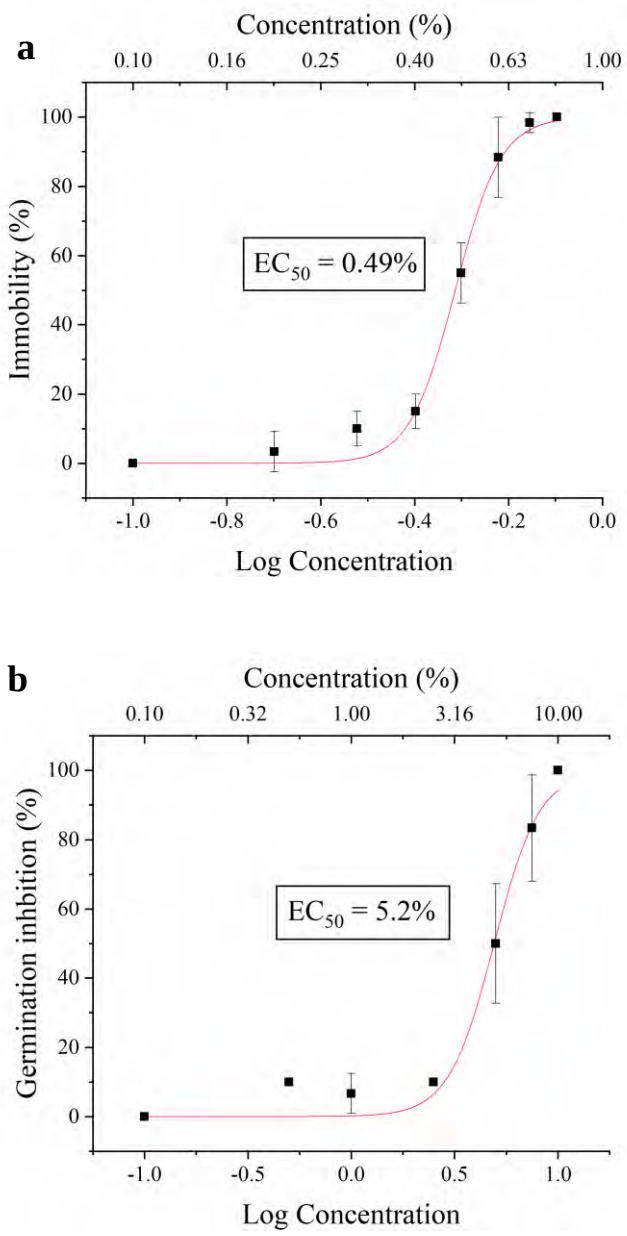

Source: Own authorship

4.2. Anaerobic treatment of PHWW in sequencing batch process

4.2.1. Monitoring

The reactors were operated for 253 days. Data obtained during the monitoring of each experimental condition tested are summarized in Table 10. An increase in effluent pH values was observed for all the conditions, 7.4 to 7.6 on average, which is likely related to the conversion of organic nitrogen into ammoniacal nitrogen during the anaerobic process. Nonetheless, the effluent pH remained within the pH range tolerated by methanogenic microorganisms (6 - 8) (CHERNICHARO, 2007).

Results of bicarbonate alkalinity indicate a considerable production of alkalinity in the effluent throughout the experiment, with values of 38 ± 3 %, showing the reactors' buffer capacity to neutralize the acids formed during the process. Another important aspect to consider is the ratio between intermediate alkalinity (alkalinity to volatile acids) and partial alkalinity (bicarbonate alkalinity) (IA/PA). Values lower than 0.3 indicate well-operated conditions avoiding system imbalance due to excessive VFA concentration (RIPLEY; BOYLE; CONVERSE, 1986). In this study, all IA/PA values were close to 0.3, this could have indicated balanced conditions, however, to verify this behavior it is necessary to also observe values of VFA generation, which are widely discussed in the next section.

Analyses of volatile suspended solids (VSS) were performed at the start and the end of the operation period, with an initial solids concentration of 5.6 ± 0.7 $gVSS.L^{-1}$, and final solids concentrations of 5.9 ± 0.2 $gVSS.L^{-1}$. These results indicate that the anaerobic biomass did not grow significantly during the system operation likely due to the presence of recalcitrant compounds in PHWW.

Table 10 - Monitoring values obtained during each experimental condition of the anaerobic treatment

Parameter	Experimental condition				
	I: 1.6g.L^{-1}	II: 2.4g.L^{-1}	III: 3.2g.L^{-1}	IV: 4g.L^{-1}	V: 4.8g.L^{-1}
pH_{IN}	7.52 ± 0.09	7.4 ± 0.07	7.3 ± 0.11	7.3 ± 0.1	7.4 ± 0.08
pH_{EF}	7.71 ± 0.16	7.6 ± 0.07	7.5 ± 0.18	7.5 ± 0.14	7.6 ± 0.09
BA_{IN} (mg.L^{-1})	646 ± 72	706 ± 96	849 ± 102	1003 ± 36	1025 ± 68
BA_{PROD} (%)	33%	41%	35%	38%	42%
IA/PA	0.27 ± 0.03	0.36 ± 0.02	0.31 ± 0.02	0.36 ± 0.05	0.34 ± 0.03
COD_{IN} (mg.L^{-1})	1619 ± 102	2254 ± 164	3221 ± 99	4221 ± 135	5104 ± 89
COD_{EF} (mg.L^{-1})	794 ± 52	1153 ± 101	1650 ± 77	2527 ± 130	3566 ± 129
COD removal (%)	51.1 ± 1.9^{a}	49.5 ± 2.1^{a}	48.8 ± 1.7^{a}	39.8 ± 3.2^{b}	30.1 ± 2.5^{c}
Y_{CH4} (NmL/gCODadd)	180 ± 12^{a}	171 ± 14^{ab}	158 ± 12^{b}	131 ± 8^{c}	99 ± 7^{d}
Y_{CH4} (NmL/gCODrem)	353 ± 26	320 ± 33	312 ± 28	314 ± 31	318 ± 27

Values are mean ± SD. Means followed by the same letter in columns do not differ statistically ($p > 0.05$).

BA: Bicarbonate alkalinity; BA_{PROD}: Produced alkalinity; IA/PA: Intermediate alkalinity/Partial alkalinity; COD: Chemical oxygen demand; Y_{CH4}: CH_4 yield

Source: Own authorship

According to Muñoz Sierra et al. (2018), the anaerobic treatment of industrial-chemical wastewaters generally results in low biomass yields. In previous studies with PHWW from microalgae, a diminution in VSS concentration was reported during its anaerobic treatment due to microbial intoxication (QUISPE-ARPASI et al., 2018), for instance, Bueno et al. (2021) observed this behavior even in a continuous experiment using a HAIB reactor. The configuration used in this study may have protected the biomass from these extreme effects and favored its retention in the system. The same findings were reported by Dias et al. (2021) while studying the anaerobic digestion of PHWW from spent coffee grounds under sequencing batch conditions, evidencing that under certain conditions is possible to protect the microbial community when using PHWW as a substrate.

4.2.2. COD removal

Figure 11 shows the influent and effluent COD concentrations and COD removal efficiencies observed throughout the operational period. The pre-exposition period lasted 28 days and served to determine the cycle time sufficient to consume biodegradable organic matter. In this phase, COD degradation was monitored along the cycle, observing that after three days removal efficiencies remained equal. Removal values of 56 ± 2% were obtained even when cycle time got shorter, from seven days to three days (Figure 12). Previous works studying the anaerobic biodegradability of PHWW in batch tests have reported that methane production stabilized after 10 or more days, with COD removal values close to the ones reported here (44-61%) (TOMMASO et al., 2015; ZHOU et al., 2015). However, COD degradation along the experimental assays was not reported in those researches. In this work, three days were enough to guarantee maximum values of organic matter degradation.

Figure 11 - Organic matter concentrations in the influent (■), effluent (●), and COD removal efficiencies (▲)

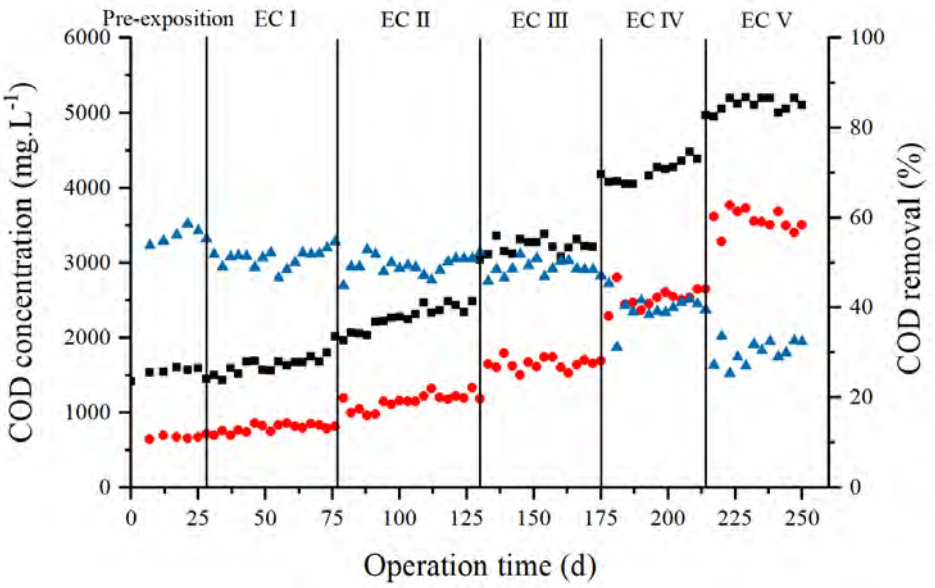

Source: Own authorship

Figure 12 - COD removal during the pre-exposition period along cycle time of 7 d (■), 5 d (●), 4 d (▲), and 3 d (▼)

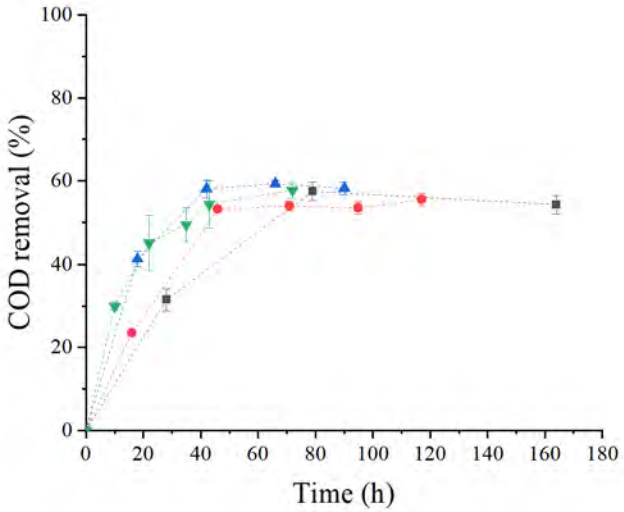

Source: Own authorship

Figure 13 shows the boxplot graphs of COD removal for every condition studied. Boxplot graphs depict the data through quartiles, medians, means, and outliers. In general, low variability was noted for each experimental condition, obtaining values of removal efficiencies within apparent steady-state conditions of 53 ± 1%, 51 ± 1%, 49 ± 1%, 41 ± 1%, and 31 ± 1%, for EC I, EC II, EC III, EC IV, and EC V, respectively. The low variability observed reflected a short period of biomass acclimation likely due to chosen operation mode and inoculum characteristics.

Figure 13 - Boxplot of COD removal for degradation for EC I: 1.6 $gCOD.L^{-1}$, EC II: 2.4 $gCOD.L^{-1}$, EC III: 3.2 $gCOD.L^{-1}$, EC IV: 4 $gCOD.L^{-1}$, and EC V: 4.8 $gCOD.L^{-1}$

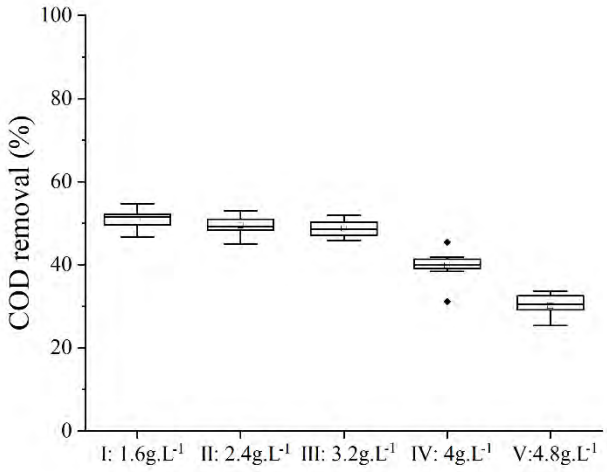

Source: Own authorship

Values of COD removal in EC I were lower than the ones observed in the pre-exposition period. This can be attributed to the adsorption of organic compounds onto the anaerobic sludge during the early stages of the operation, resulting in apparent higher degradation values. According to Hernandez and Edyvean (2008), a fraction of phenolic compounds is reduced by adsorption onto the sludge during anaerobic processes until reaching a saturation level. After

some time, adsorbed compounds can be released into the effluent and degraded (WIJETUNGA; LI; JIAN, 2010).

In EC II and EC III, the average values of COD removal efficiency were similar. The Tukey test does not show a significant difference between EC I, EC II, and EC III if the complete operational periods are taken into account. Thus, influent COD concentration did not influence COD removal efficiencies in these conditions. Moreover, such experimental conditions showed a significant consumption of organic matter (~50%). These results were higher than the ones reported for the anaerobic batch biodegradation of PHWW from *Spirulina* (42 - 45%) under similar influent COD concentrations (BUENO et al., 2020). In addition, Bueno et al. (2021) treated PHWW from *Spirulina* in horizontal-flow anaerobic biomass (HAIB) reactor obtaining COD removal efficiencies of 67%, 58%, and 37% for influent COD concentrations of 0.8, 1.6, and 3.2 $g.L^{-1}$. Although higher efficiencies were observed for concentrations of 0.8 and 1.6 $gCOD.L^{-1}$ in the HAIB reactor, our study presented greater efficiencies at a concentration of 3.2 $gCOD.L^{-1}$.

Higher values of COD removal during the continuous anaerobic treatment of PHWW were reported in other studies, as observed in Table 4. PHWW from cornstalk reached removal efficiencies up to 67% in a PBR (SI et al., 2018) and 62% in a UASB (CHEN et al., 2020). Another study treated PHWW from sewage sludge under anaerobic sequencing batch conditions and observed removal efficiencies up to 58%. This difference can be explained by the complex characterization of PHWW, which is strongly dependent on the feedstock (e.g. swine manure, cornstalk, and algae) and HTL operational conditions. For instance, when comparing PHWW from swine manure and *Spirulina*, the first one had a COD value of 40 $gCOD.L^{-1}$ and the largest group of compounds in the effluent was short-chain organic acids, representing 43% of the total compounds (YANG et al., 2018). Whereas PHWW from

Spirulina reached COD values of 89 $gCOD.L^{-1}$, and N&O heterocyclic compounds were the most abundant group of components identified in the effluent with values of 46% (ZHENG et al., 2017), making their anaerobic biodegradability harder to achieve. Despite this factor, the acclimated biomass was able to tolerate and metabolize organic loads up to 3.2 $gCOD.L^{-1}$ without decreasing its efficiency.

The remaining organic matter may be associated with refractory organics with high molecular size in PHWW resistant to biodegradation. According to Chen et al. (2017), PHWW from rice straw contains 21-34% of organic compounds with a higher molecular size than 1kDa. Razo-Flores et al. (1996) studied the biodegradability of various N-substituted aromatic and alkylphenol compounds, where despite using acclimate sludge, aniline and 2-cresol conversion was not achieved. Such compounds were previously reported in PHWW from *Spirulina*, reaching concentrations of 130 $mg.L^{-1}$ in the case of aniline (BUENO et al., 2021).

In EC IV and EC V, the increase in the organic load resulted in a drop in the removal efficiencies (40 and 30%). Tukey test confirmed these results, where a significant difference between the conditions was observed ($p \leq 0.05$). The same behavior was reported by Silva et al. (2013) while treating industrial biodiesel wastewater on an ASBR. After a gradual increase in the organic load (1.23 – 2.52 $gCOD.L^{-1}.d^{-1}$), the removal efficiencies dropped from 88% to 69% when submitted to the highest organic load tested.

4.2.3. Methane production

Figure 14 shows the boxplot graphs of CH_4 yield for each condition studied. CH_4 yields ranged from 180 ± 9 NmL/gCODadd (353 ± 26 NmL/gCODrem) to 99 ± 5 NmL/gCODadd (318 ± 27 NmL/gCODrem). According to the Tukey test, the highest methane yields were obtained for EC I, EC II, and EC III (Table 10). Chen et al. (2020a) and Dias et al. (2021) reported close values of CH_4 yields for the anaerobic degradation of PHWW from cornstalk

(194 NmL/gCODadd) and spent coffee grounds (187 NmL/gCODadd), in a UASB and ASBR, respectively. The CH_4 yields corresponded to an average value of 84% of the theoretical value.

Observed results indicate that the anaerobic consortium was capable of converting degradable organic matter into CH_4 and dealing with small amounts of toxicants up to influent concentrations of 3.2 $gCOD.L^{-1}$, whereas higher organic loads resulted in a negative effect on its methanogenic activity. Previously, Zheng et al. (2017) evaluated the potential toxicity of PHWW to methanogens through an anaerobic toxicity assay, observing inhibitory effects at concentrations higher than 4.5 $gCOD.L^{-1}$.

Figure 14 - Boxplot of CH_4 yields for EC I: 1.6 $gCOD.L^{-1}$, EC II: 2.4 $gCOD.L^{-1}$, EC III: 3.2 $gCOD.L^{-1}$, EC IV: 4 $gCOD.L^{-1}$, and EC V: 4.8 $gCOD.L^{-1}$

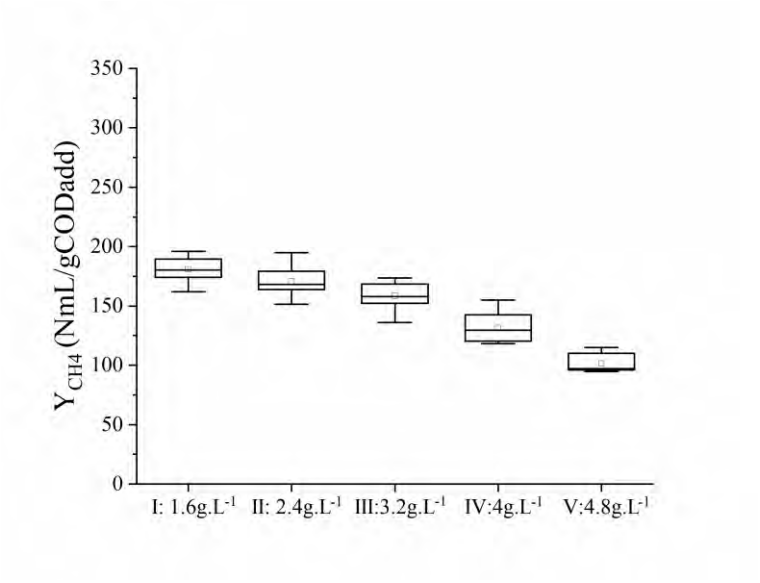

Source: Own authorship

Table 11 presents the COD balance obtained in each experimental condition after reaching operational stability, where an average value of 0.96 was obtained. Quotients smaller than 1 indicate that part of the removed COD was not converted into CH_4. These results could be

associated with cellular growth and maintenance functions (VAN LOOSDRECHT et al., 2016).

Table 11 - COD balance regarding the CH_4 production and COD removed achieved in each experimental condition after reaching operational stability

	Experimental conditions				
	I: 1.6g.L^{-1}	II: 2.4g.L^{-1}	III: 3.2g.L^{-1}	IV: 4g.L^{-1}	V: 4.8g.L^{-1}
COD_{IN} (g)	1036	1492	1928	2631	2988
COD_{EF} (g)	487	719	979	1638	2004
Experimental CH_4 (gCOD)	513	714	854	895	865
COD balance	0.97	0.96	0.95	0.96	0.96

COD: Chemical oxygen demand

Source: Own authorship

4.2.4. Temporal profiles

Profiles of organics degradation, intermediary metabolites, and CH_4 production were obtained after reaching apparent steady-state conditions, collecting samples from intermediate points along the cycle time of each experimental condition assessed. Figure 15 shows the profiles obtained for COD degradation. Table 12 presents the parameters obtained from the pseudo-first-order model, which was fitted satisfactorily to COD consumption in this study (Adj. $R^2 > 0.96$). The lowest values of *k* were 0.32 h^{-1} and 0.28 h^{-1}, obtained at influent COD concentrations of 4 and 4.8 gCOD.L^{-1}, where COD removal efficiencies were the most restricted.

Figure 15 - Temporal profiles of COD degradation for EC I: 1.6 gCOD.L^{-1} (a), EC II: 2.4 gCOD.L^{-1} (b), EC III: 3.2 gCOD.L^{-1} (c), EC IV: 4 gCOD.L^{-1} (c), and EC V: 4.8 gCOD.L^{-1} (e)

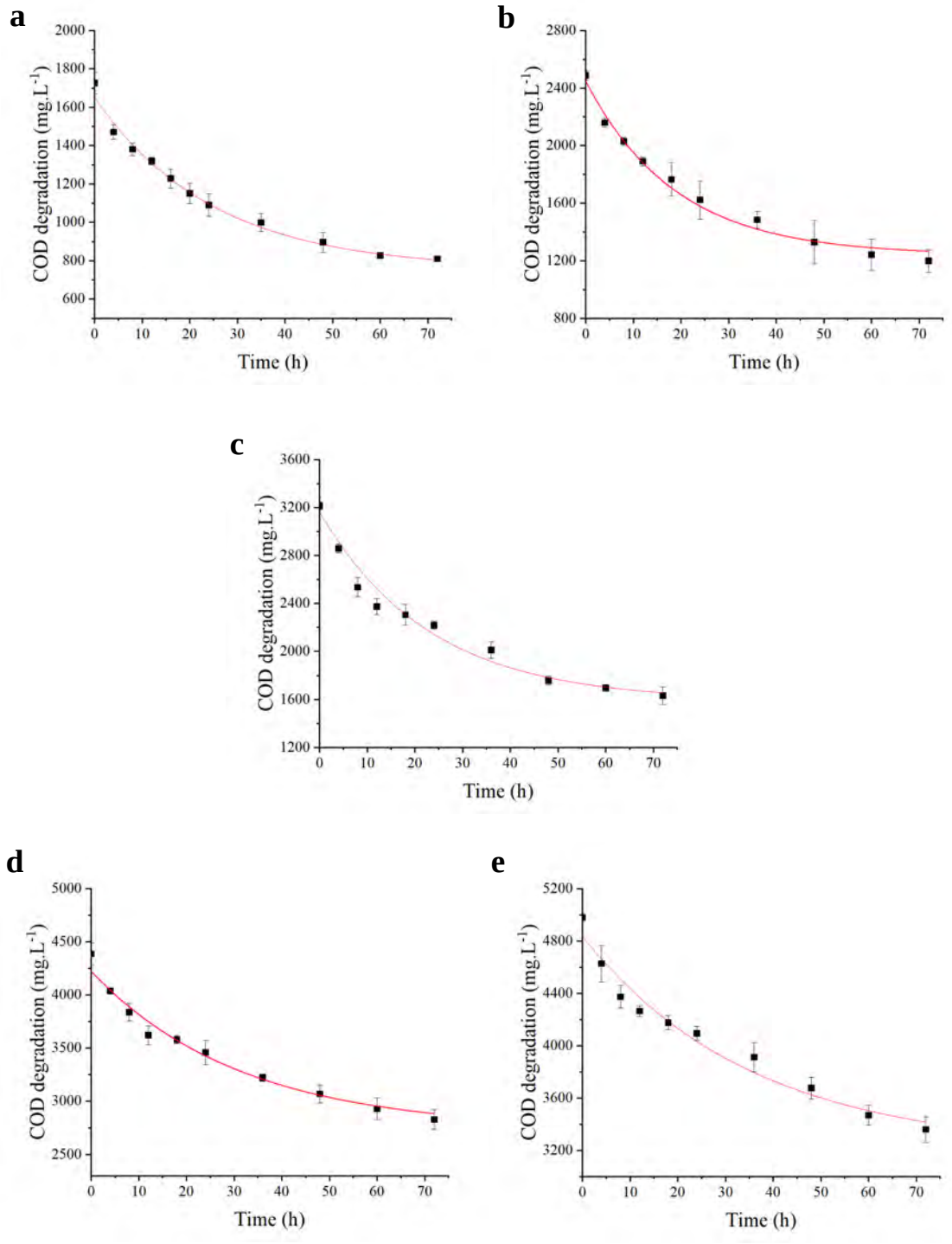

Source: Own authorship

Table 12 - Kinetic parameters obtained from the pseudo-first-order kinetic expression for COD degradation

Experimental condition	S_R (mgCOD.L^{-1})	S_I (mgCOD.L^{-1})	k (h^{-1})	Adj. R^2
I: 1.6g.L^{-1}	766	1675	0.044	0.99
II: 2.4g.L^{-1}	1156	2423	0.043	0.98
III: 3.2g.L^{-1}	1623	3123	0.047	0.98
IV: 4g.L^{-1}	2675	4274	0.033	0.99
V: 4.8g.L^{-1}	3182	4836	0.028	0.96

Source: Own authorship

Figure 16 presents the variation of VFA concentration along the cycle time for each experimental condition. EC I, ECII, and, EC III presented a similar behavior of generation and consumption of VFA, where the highest concentration of VFA was observed at 12 h of the cycle time. In general, only acetic acid was quantified in the influent, but together with propionic, butyric, and valeric acids were produced and consumed throughout the process.

In EC I, concentrations of acids below the detection limit were observed after just 24 h. Values of acetic and propionic acids reached 249 mgCOD.L^{-1} (12 h) and 205 mgCOD.L^{-1} (8 h), respectively. According to Chernicharo (2007), when the anaerobic consortium is balanced, methanogenic microorganisms utilize the intermediate metabolites as quickly as formed avoiding accumulation. In EC II, the highest concentrations of acetic and propionic acids were up to 461 and 496 mgCOD.L^{-1} (12 h), respectively. Although propionic, butyric, and valeric acids were degraded completely, a residual concentration of acetic acid was observed in the final effluent (30 mgCOD.L^{-1}) (Table 13), indicating the existence of some unfavorable conditions for acetoclastic methanogenic microorganisms (SPEECE, 1996).

Figure 16 - Temporal profiles of VFA concentration: acetic (■), propionic (■), butyric (■) and valeric (■) acids for EC I: 1.6 gCOD.L^{-1} (a), EC II: 2.4 gCOD.L^{-1} (b), EC III: 3.2 gCOD.L^{-1} (c), EC IV: 4 gCOD.L^{-1} (c), and EC V: 4.8 gCOD.L^{-1} (e)

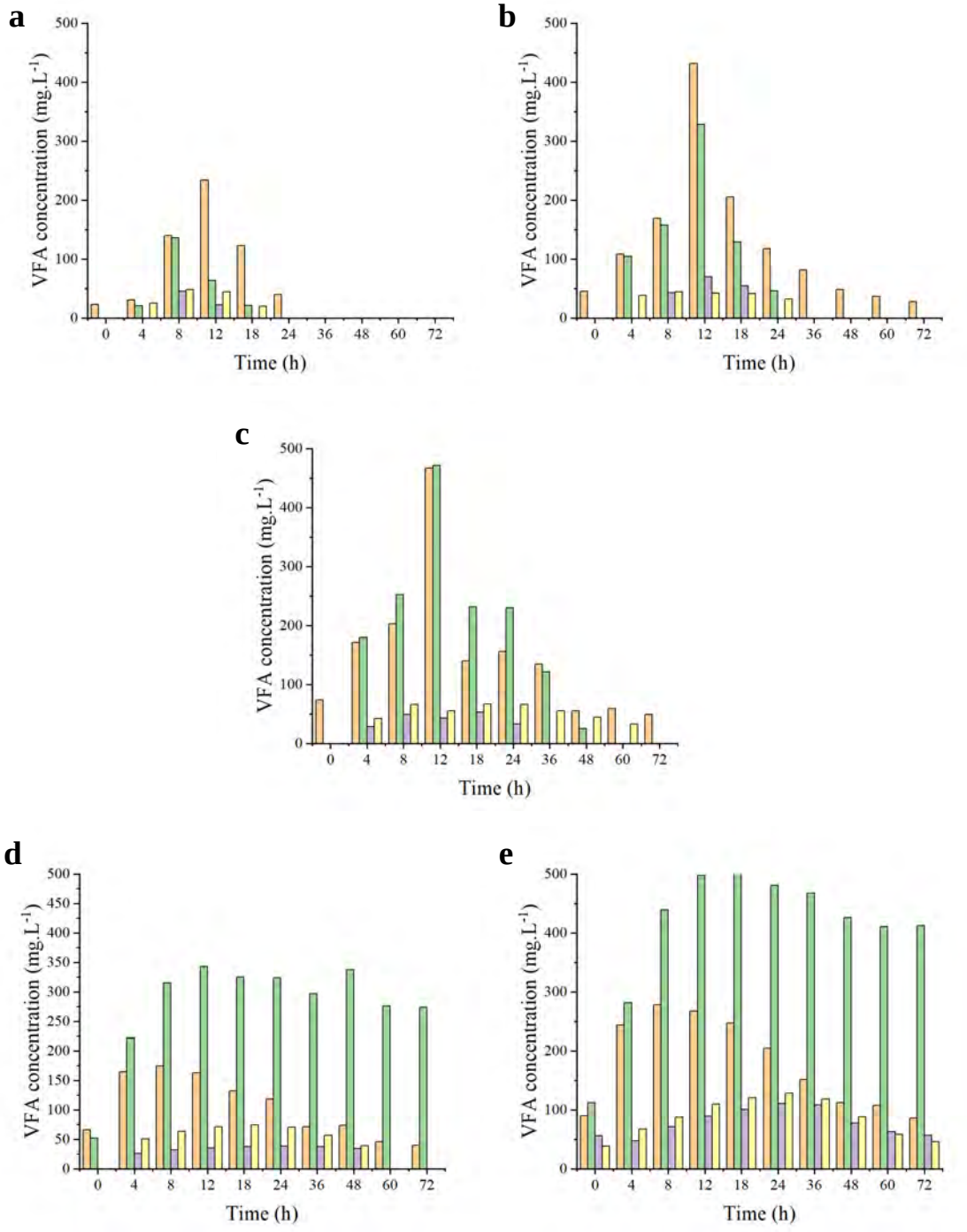

Source: Own authorship

In EC III, maximum values of acetic and propionic acids were similar, reaching ~500 $gCOD.L^{-1}$ each (12 h). Despite propionic acid generation and consumption showing balanced growth rates between acidogenic microorganisms and hydrogenotrophic methanogens, the higher accumulation of acetic acid (52 $mgCOD.L^{-1}$) indicates a stronger effect on acetoclastic methanogenic microorganisms.

Table 13 - Metabolites concentration at the end of the cycle time of the anaerobic test

Metabolites concentrations	Experimental condition				
	I	II	III	IV	V
Acetic acid ($mgCOD.L^{-1}$)	-	29.8	52.3	42.2	91.7
Propionic acid ($mgCOD.L^{-1}$)	-	-	-	413	622.7
Butyric acid ($mgCOD.L^{-1}$)	-	-	-	-	103.8
Valeric acid ($mgCOD.L^{-1}$)	-	-	-	-	94.1

Source: Own authorship

EC IV and EC V presented a high accumulation of propionic acid in the effluent (413 and 623 $gCOD.L^{-1}$, respectively) where only ~30% of the generated acid was consumed during the anaerobic treatment, implying that microorganism affinity was impaired. Propionate accumulation can likely occur in stress conditions such as nutritional limitation, load shocks, and toxic compounds presence due to hydrogen and acetate accumulation (AQUINO; CHERNICHARO, 2005). Since higher concentrations of PHWW were applied, the concentration of toxic compounds also increased and could cause such stress conditions in both operational periods. In EC V, butyric and valeric acids were also observed in the effluent, which indicates a major inhibition of the anaerobic consortium. Butyric acid accumulation indicates an acetogenesis limitation. Valeric acid is an intermediate in the degradation of proteins (FONSECA; DE OLIVEIRA; ZAIAT, 2020), and it is widely reported in the anaerobic

conversion of PHWW from microalgae (ZHENG et al., 2017; BUENO et al., 2021). Tommaso et al (2015) indicated the accumulation of butyric and valeric acids as a rate-limiting step during the anaerobic degradation of PHWW from algae. On the other hand, caproic acid was not produced in any experimental condition, indicating that it is not an intermediate of the anaerobic digestion of PHWW from *Spirulina*.

The increment in VFA concentration in the effluent as a result of the increase in organic load was also observed by Bueno et al. (2020), where also restricted values of propionic acid consumption were reported at the highest PHWW concentrations. In the present study, propionic acid was the main metabolite produced in the anaerobic degradation of PHWW, generated from nitrogenous compounds degradation by acetogenic and valerate-oxidizer microorganisms (PIND; ANGELIDAKI; AHRING, 2003). Despite VFA accumulation, the constant alkalinity production throughout the operational period showed favorable buffering conditions even at the highest PHWW concentration tested.

The degradation of total phenolic compounds was also reported for each experimental condition. The initial content of total phenolics was between 44 $mgGAE.L^{-1}$ for EC I and 169 $mgGAE.L^{-1}$ for EC V. Figure 17 presents the degradation profiles of total phenolic compounds. Restricted values were observed for phenolics removal (up to 28%). Although total phenol degradation was achieved previously in an ASBR when used as the sole carbon source (ROSENKRANZ et al., 2013), its simultaneous treatment in a mixture with other aromatic compounds can pose a challenge for the anaerobic consortium. For instance, Si et al. (2018) reported that although furfural and 5-HMF were completely converted in a UASB treating PHWW from cornstalk, organic aromatic nitrogen and phenolic compounds, such as 3-hydroxypyridine, phenol, and 4-ethyl-phenol, were only partially removed (54–75%).

Figure 17 - Temporal profiles of total phenolic compounds for EC I: 1.6 gCOD.L-1 (a), EC II: 2.4 gCOD.L-1 (b), EC III: 3.2 gCOD.L-1 (c), EC IV: 4 gCOD.L-1 (d), and EC V: 4.8 gCOD.L-1 (e)

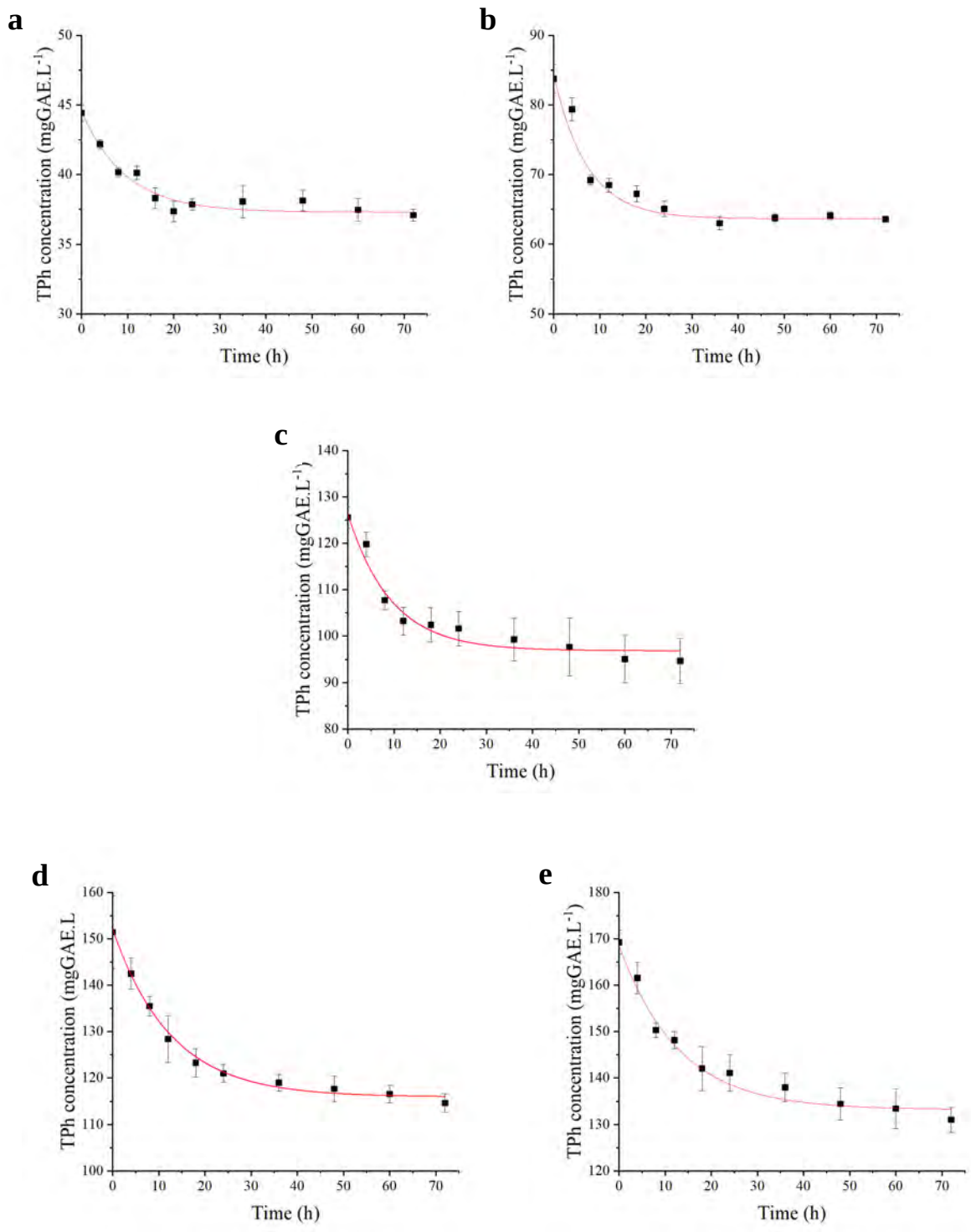

Source: Own authorship

A preferential metabolism of easily degradable substrates was indicated by Zheng et al. (2017) in the anaerobic batch experiments of PHWW from *Spirulina*. In the present study, VFA only accounted for 4% of the total organic matter quantified in PHWW, meaning that a significant amount of more complex compounds was also converted into CH_4, including phenolic compounds.

Table 14 presents the parameters obtained from the first-order model, which adjusted successfully to the TPh degradation values (Adj. $R^2 > 0.93$) The lowest values of *k* were 0.079 h^{-1} and 0.078 h^{-1}, obtained at the highest influent COD concentrations used (4 and 4.8 $gCOD.L^{-1}$, respectively). Moreover, *k* values obtained for TPh degradation were higher than those obtained for COD degradation, which indicates that other aromatic compounds were responsible for limiting the total organic matter degradation in these experiments.

Table 14 - Kinetic parameters obtained from the first-order kinetic expression

Experimental condition	S_R ($mgGAE.L^{-1}$)	S_I ($mgGAE.L^{-1}$)	k (h^{-1})	Adj. R^2
I: 1.6 $gCOD.L^{-1}$	37.3	44.5	0.105	0.96
II: 2.4 $gCOD.L^{-1}$	63.7	84.3	0.138	0.93
III: 3.2 $gCOD.L^{-1}$	96.8	126.4	0.101	0.95
IV: 4 $CODg.L^{-1}$	115.9	152.1	0.079	0.99
V: 4.8 $gCOD.L^{-1}$	133.2	168.6	0.078	0.97

Source: Own authorship

Figure 18 shows the cumulative CH_4 production per gram of VSS observed for each experimental condition, where the dotted lines represented the maximal theoretical value per gram of COD removed. NmL.gSSV-1

Figure 18 - Cumulative CH_4 production for EC I: 1.6 $gCOD.L^{-1}$ (a), EC II: 2.4 $gCOD.L^{-1}$ (b), EC III: 3.2 $gCOD.L^{-1}$ (c), EC IV: 4 $gCOD.L^{-1}$ (c), and EC V: 4.8 $gCOD.L^{-1}$ (e)

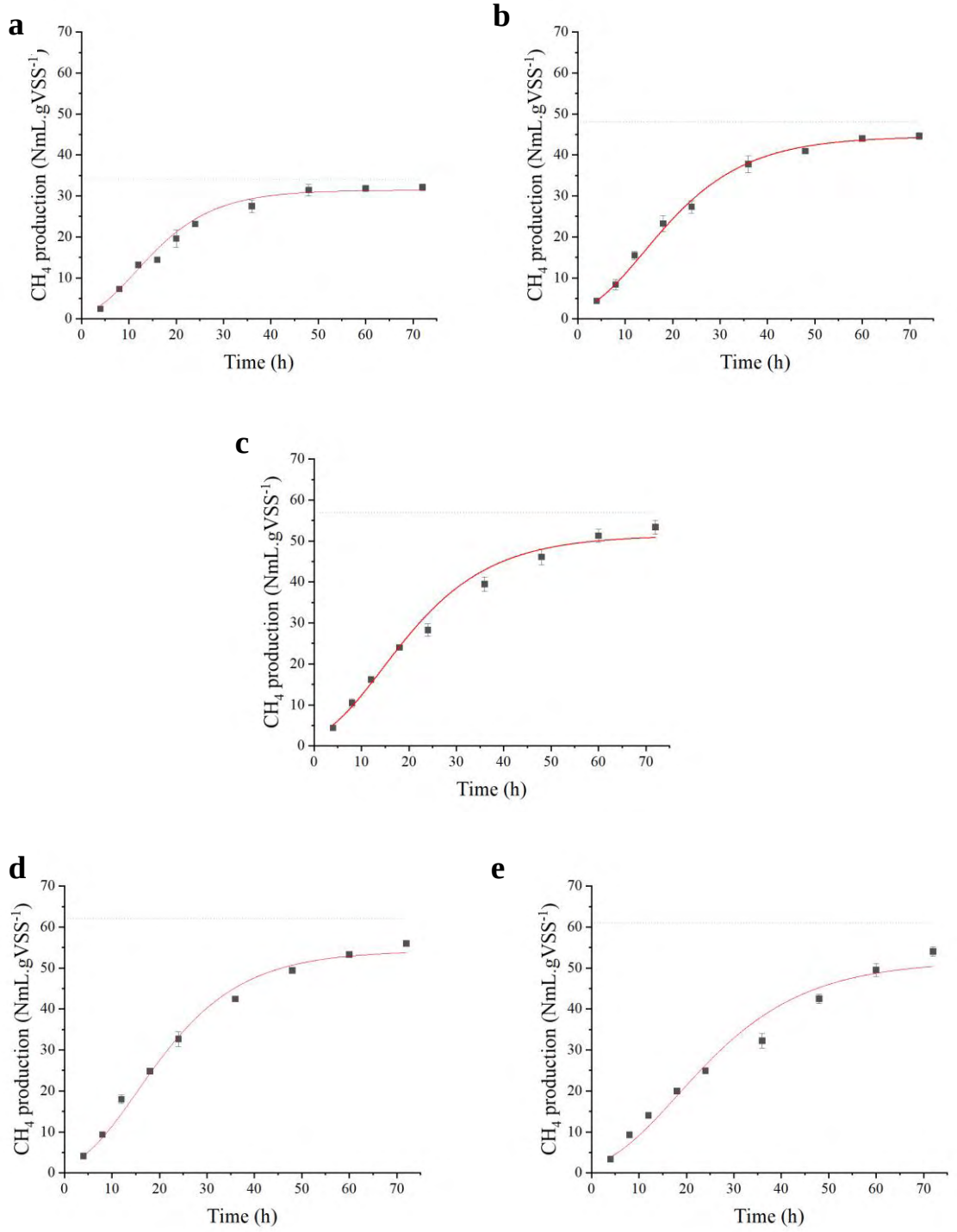

Source: Own authorship

The increase in the organic load led to a gradual increment in the volume of CH_4 generated where the highest methane production corresponded to the EC IV. These results can be explained by the higher availability of easily degradable substrate to be converted into CH_4. However, EC V (4.8 gCOD.L^{-1}) did not follow the same tendency as observed in Table 15, which presents the parameters estimated by the modified Gompertz model, methane production potential (P_{CH_4}), maximum specific methane production rate (k), and the duration of the lag phase (λ). The Gompertz model in this study (Adj. $R^2 > 0.97$) successfully fitted cumulative CH_4 production values.

Table 15 - Kinetic parameters obtained from the Gompertz equation

Experimental condition	P_{CH_4} (NmL.gVSS^{-1})	k (NmL.gVSS^{-1}.h^{-1})	λ (h)	Adj. R^2
I: 1.6gCOD.L^{-1}	31	1.26	2.33	0.979
II: 2.4gCOD.L^{-1}	45	1.38	2.1	0.999
III: 3.2gCOD.L^{-1}	51	1.51	1.93	0.988
IV: 4gCOD.L^{-1}	54	1.65	3.28	0.996
V: 4.8gCOD.L^{-1}	52	1.28	3.30	0.976

Source: Own authorship

In EC I, the temporal profiles of CH_4 production together with COD degradation showed that maximum values were reached in 48 h, which indicates that after that period no more biodegradable substrate was available to be converted into CH_4. Values of specific CH_4 production rates likely followed the tendency of the higher the organic load, the higher the production rate. EC V was the exception, a drop was observed (1.26 NmL.gVSS^{-1}.h^{-1}) with close values to the observed ones for EC I (1.3 NmL.gVSS^{-1}.h^{-1}).

No noticeable lag phases for CH_4 production were the result of the acclimation process applied. Previous studies reported lag phases between 15 h and 10 days for the anaerobic degradation of PHWW from algae in batch experiments (TOMMASO et al., 2015; QUISPE-ARPASI et al., 2018; BUENO et al., 2020). Razo-Flores et al. (1996) verified this effect while assessing the biodegradability of various N-substituted aromatic and alkylphenol compounds, where the use of biomass adapted to 2-nitrophenol reduced lag phases duration.

4.2.5. Kinetic analysis

The specific substrate utilization rates obtained from COD degradation profiles were plotted against initial concentrations of substrate (influent COD), and presented in Figure 19. Due to an evident decay in substrate utilization rates after reaching a maximum, an inhibition by substrate model was used to represent the data. Within them, the modified Haldane model, firstly proposed by Dwyer et al. (1986) for phenol biodegradation, provided an adequate fit and was able to predict the inhibitory effect of substrate concentration on a specific substrate utilization rate.

The kinetics parameters were determined using the Solver function in Microsoft Excel. The maximum substrate utilization rate obtained was (r'_{max}) 72 mgCOD.gVSS^{-1}.h^{-1}, whereas the half-saturation (K_s) and inhibition constant (K_i) were 14.5 gCOD.L^{-1} and 3.7 gCOD.L^{-1}, respectively, with an inhibition response coefficient (n) of 5.8. The modified Haldane model predicted that PHWW degradation rate was inhibited at concentrations above 3.7 gCOD.L^{-1}. For instance, the degradation rate was reduced by 38% at 5 gCOD.L^{-1}, indicating severe inhibition. These results verified the ones obtained for VFA generation and consumption, where higher concentrations than 3.2 gCOD.L^{-1} led to major process instability. Dias et al. (2021) reported the inhibition of the anaerobic degradation of PHWW from spent coffee grounds, at concentrations above 4.5 gCOD.L^{-1} due to its high content of phenolic compounds

(900 mgGAE.L^{-1}). In the present study, other recalcitrant compounds, besides phenolics, contributed to this effect.

Figure 19 - Specific substrate utilization rates vs substrate concentration

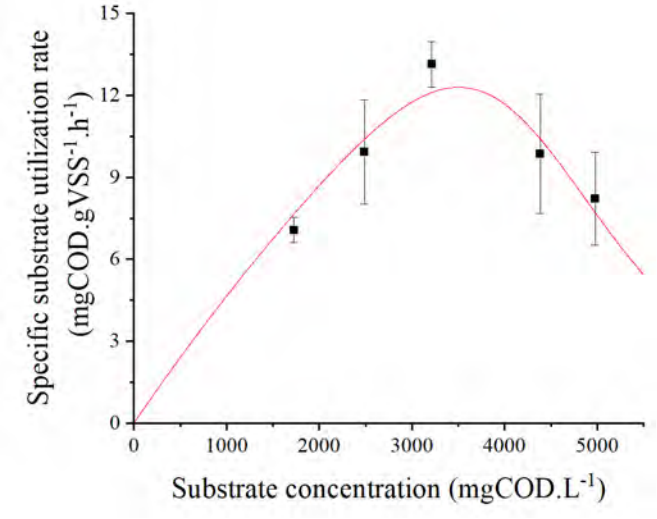

Source: Own authorship

The kinetic analysis presented here was able to describe the anaerobic degradation of PHWW from *Spirulina* after acclimation on a sequencing batch process and can contribute to a higher understanding of the fundamental aspects of PHWW degradation and its effect at stimulatory and inhibitory concentrations.

4.2.6. Microbial diversity

Changes in the microbial diversity were observed after the anaerobic treatment of PHWW in a sequencing batch process. Initially, 19% of the microbial community belonged to the Archaea kingdom and 81% to the Bacteria kingdom, whereas 31% of the microbial community in the reactors was constituted by Archaea, and 69% by Bacteria, which indicates enrichment of the Archaea during the operational period of the reactors. This effect can be observed in the

taxonomic results at the phylum level, where the *Euryachaeota* phylum, which comprehends the methanogenic archaea, became the most abundant phyla in the microbial community after the sequencing batch process (Figure 20). Within the seven major phyla detected in the reactors sample with relative abundances higher than 1%, *Synergistetes* was the most enriched (from <1% to 28%), which indicates this phylum was able to resist higher concentrations of PHWW and it could have include key microorganisms for PHWW degradation.

Figure 20 - Taxonomic classification of the reads at phylum level in the inoculum (a) and in the sludge after the anaerobic treatment of PHWW (b)

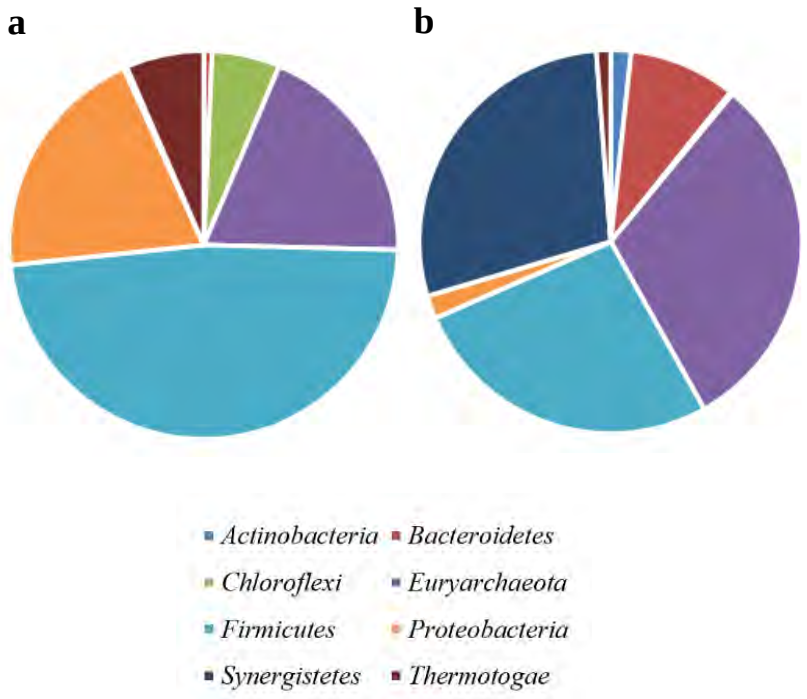

Source: Own authorship

Figure 21 shows a heatmap of the changes in the microbial community diversity after PHWW treatment. The most representative bacterial genera in the inoculum included *Trichococcus* (22%) and *Clostridium* (15.9%), followed by *Mesotoga* (6.5%), *Carnobacterium* (5.9%), *Jathinobacterium* (4.8%), *Longilinea* (4.3%), *Peptoclostridium* (4.1%), *Sulfuricurvum* (2.9%) and *Pseudomonas* (2.8%).

Figure 21 - Heatmap representing the microbial diversity at genus level in the inoculum and the sludge after the anaerobic treatment of PHWW

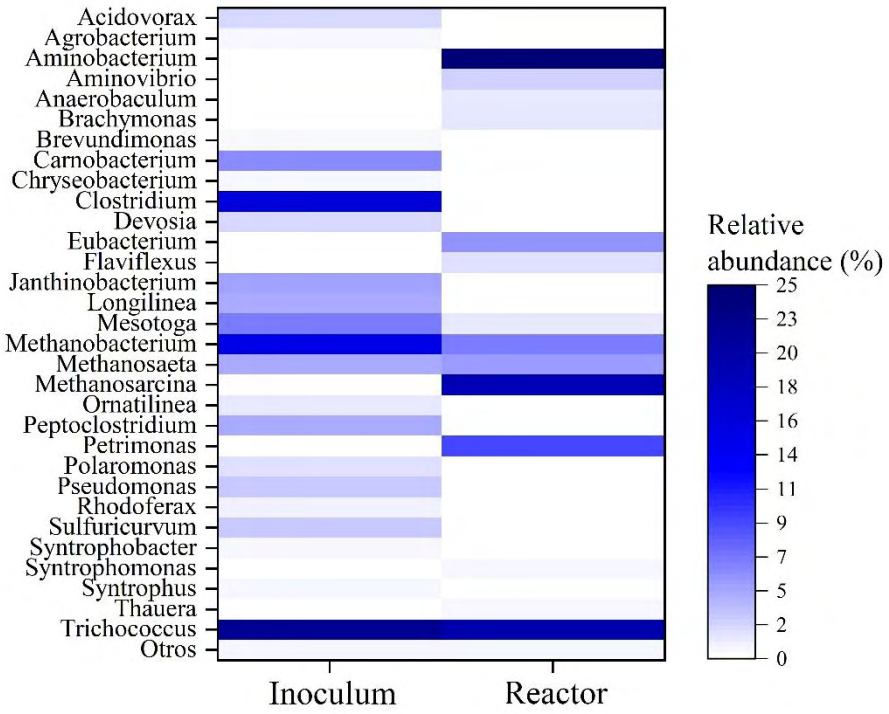

Source: Own authorship

After the acclimation to PHWW, the organic matter degradation was mainly supported by *Trichococcus* (19.7%), a fermentative bacteria that belong to phylum *Firmicutes* (STREPIS et al., 2020), and by amino-acid degraders: *Aminobacterium* (phylum *Synergistetes*) (24.7%), *Eubacterium* (phylum *Firmicutes*) (5.6%) and *Aminivibrio* (phylum *Synergistetes*) (2.4%) (ZINDEL et al., 1988; HAMDI et al., 2015). Such enrichment is related to the amount of protein-derived compounds typical of a PHWW from microalgae. According to Baena et al (1998), oxidation products from *Aminobacterium colombiense* growth, the main specie of *Aminobacterium* identified here, include acetate, propionate, valerate, and butyrate in mixed cultures, which explains the amount of these VFA generated along the anaerobic degradation of PHWW. On the other hand, *Eubacterium* and *Aminivibrio* have acetate, CO_2, and H_2 as their metabolism products.

Other representative genera with relative abundances higher than 1% include *Petrimonas* (9.1%), *Flaviflexus* (1.7%), *Anaerobaculum* (phylum *Synergistetes*) (1.3%), *Brachymonas* (phylum *Proteobacteria*) (1.3%) and *Mesotoga* (1.2%) (phylum *Thermotogae*). According to previous works, some species of *Petrimonas* (phylum *Bacteroidetes*) can cleavage the –N=N- double bond (GRABOWSKI et al., 2005; ZHU et al., 2020), and could have been responsible for the degradation of nitrogen aromatic compounds. Its enrichment was also reported by Usman et al. (2019) in ASBRs treating PHWW from sewage sludge. *Flaxiflexus* (phylum *Actinobacteria*) was reported to have the ability to hydrolyze macromolecules (CHENG et al., 2018) and which were probably responsible for breaking down the polymeric substrates in PHWW into soluble monomers before acidogenesis can proceed. Chen et al. (2017) reported microorganisms from the Phylum *Actinobacteria* in reactors treating PHWW from rice straw conversion with the highest amount of hard biodegradable organics.

Two species from the aromatic-degrader genera *Thauera* (0.4%) (phylum *Proteobacteria*) were also enriched during PHWW acclimation. *Thauera phenylacetica* is a phenol-degrader and *Thauera aromatica* can use phenol, toluene, and p-cresol as substrate. Both genera were isolated from a bioreactor treating coking wastewater (MAO et al., 2010), and were also used for the degradation of azo dyes in wastewater (ZHU et al., 2020). The increment in their abundance suggests specialization of the microbial community.

Although syntrophic microorganisms, such as *Syntrophomonas* (phylum *Proteobacteria*) and *Mesotoga* were also found in the reactors, their relative abundance was low (1.9%). These microorganisms are responsible for the production of acetate, carbon dioxide, and H_2 from intermediates such as propionic, butyric, valeric, and lactic acid (ROY et al., 1986; BEN HANIA et al., 2013), linking the fermentative and methanogenic microorganisms. The higher organic loads tested in EC IV and V incremented the amount of toxic compounds in the

reactors, causing unfavorable thermodynamic conditions, which especially inhibited the growth of *Syntrophobacter* (phylum *Proteobacteria*), a propionate-oxidizer bacteria that was found in the inoculum.

The most representative archaeal genera in the inoculum were *Methanobacterium* (14.9%) and *Methanosaeta* (4.1%), whereas, after PHWW acclimation, *Methanosarcina* became the most abundant genera in the microbial community (19%), followed by *Methanobacterium* (6.7%) and *Methanosaeta* (5.2%). The shift from *Methanobacterium*, hydrogenotrophic methanogens, to *Methanosarcina*, which produce methane through H_2/CO_2, methanol, methylamines, acetate, and CO (PASALARI et al., 2021), suggests that the methanogenesis pathway during PHWW anaerobic degradation in a sequencing batch process required the presence of metabolically-versatile methanogens such as *Methanosarcina*. Previous studies have reported *Methanosarcina* as the predominant methanogen in ASBRs treating PHWW from algae and sewage sludge (FERNANDEZ et al., 2018; USMAN et al., 2019). According to Karakashev et al. (2006), *Methanosarcina* is the most common methanogen in environments with high ammonia and organic acid content. Such conditions were observed in this study due to the conversion of amino acids and other organics, explaining the enrichment of these microorganisms after PHWW acclimation.

Although the results of this experiment showed some limitations for the treatment of PHWW from *Spirulina* in a sequencing batch process, where high dilution ratios were needed to avoid inhibition effects due to PHWW recalcitrant nature, kinetic aspects of reactors operation are still scarce in the literature and their correct application can lead to efficient reactor design. Moreover, the microbial diversity observed after PHWW acclimation proved that anaerobic communities have the potential to degrade a wide range of organic compounds

identified in PHWW including aromatics, while generating energy from their conversion, enhancing the energetic return of the hydrothermal liquefaction process.

4.3. Influence of intermittent aeration on PHWW anaerobic digestion

4.3.1. Monitoring

The two configurations were conducted for over 207 days divided into three experimental conditions each, previously detailed in Table 6. Table 16 presents the average values of the parameters monitored during the conditions studied. Higher pH values were reported for the R_2 effluent, likely due to CO_2 gas stripping from the system during the aerated phase (YUAN; GAO, 2010). Results of bicarbonate alkalinity show an average generation of 62% and 50% for each set-up, mainly attributed to NH_4 generated during both processes, which could act as buffer (ZHANG et al., 2014), influencing also IA/PA values. Such parameter did not present a significant difference between both configurations, for which VFA results were reported and discussed in Section 4.3.4,

As expected, both biological processes did not influence TKN removal, as the values for the influent and effluents remained similar. NH_4 content was also monitored since PHWW is rich in nitrogenous compounds and they can release ammonia during its conversion. On average, 56% of TKN in the influent was present in the form of ammonia and this percentage increased after the processes up to 81% on the R_1 effluent and 79% on the R_2 effluent. Additionally, the conversion of organic nitrogen into ammonia was lower in the R_2 effluent (EC III).

Analyses of volatile suspended solids were performed at the beginning of the experiments and the end of the operational period. Initial solids concentration in R_1 went from 5.8 ± 0.6 $gVSS.L^{-1}$ to 6 ± 0.5 $gVSS.L^{-1}$, where no significant growth was observed, attributed to the recalcitrant nature of PHWW.

Table 16 - Monitoring values obtained during each experimental condition in R_1 and R_2

Parameters	Influent	R_1 Effluent	R_2 Effluent
EC I: 1.6 $gCOD.L^{-1}$			
pH	7.43 ± 0.09	7.6 ± 0.15	8.17 ± 0.21
BA ($mg.L^{-1}$)	569 ± 76	870 ± 54	801 ± 112
BA_{PROD} (%)	-	52%	41%
IA/PA	-	0.29 ± 0.05	0.25 ± 0.06
TKN ($mg.L^{-1}$)	209 ± 21	211 ± 22	204 ± 20
NH_4 ($mg.L^{-1}$)	113 ± 11	176 ± 16	161 ± 12
EC II: 3.2 $gCOD.L^{-1}$			
pH	7.31 ± 0.19	7.51 ± 0.17	8 ± 0.12
BA ($mg.L^{-1}$)	671± 123	1180 ± 115	1077 ± 124
BA_{PROD} (%)	-	76%	61%
IA/PA	-	0.31 ± 0.06	0.28 ± 0.05
TKN ($mg.L^{-1}$)	405 ± 44	391 ± 31	370 ± 28
NH_4 ($mg.L^{-1}$)	228 ± 30	311 ± 12	294 ± 30
EC III: 4.8 $gCOD.L^{-1}$			
pH	7.48 ± 0.09	7.72 ± 0.18	8.27 ± 0.09
BA ($mg.L^{-1}$)	918 ± 58	1433 ± 71	1357 ± 96
BA_{PROD} (%)	-	56%	48%
IA/PA	-	0.31 ± 0.04	0.30 ± 0.03
TKN ($mg.L^{-1}$)	652 ± 36	637 ± 17	606 ± 25
NH_4 ($mg.L^{-1}$)	367 ± 28	516 ± 26	468 ± 18

COD: Chemical oxygen demand; BA: Bicarbonate alkalinity; BA_{PROD}: Produced alkalinity; IA/PA: Intermediate/Partial alkalinity; TKN: Total Kjeldahl Nitrogen

Source: Own authorship

Solids concentration in R_2 varied from 5.5 ± 0.6 $gVSS.L^{-1}$ to 5.2 ± 0.4 $gVSS.L^{-1}$. Although greater solid concentrations were expected in R_2 due to the high microbial synthesis by facultative microorganisms in aerobic conditions, such results were not observed in this study. A probable reason can be the indeed increase in cellular production resulting in poorer sludge settling and some washout occurrence. For instance, Arrojo et al. (2004) reported that an amount of small suspended biomass aggregates suffered this behavior when treating industrial wastewater in an SBR. Such aggregates were likely facultative and aerobic microorganisms growing on the anaerobic granule surface (BOTHEJU; BAKKE, 2011).

4.3.2. COD removal

COD removal efficiencies obtained for both configurations tested throughout all the experimental conditions are presented in Figure 22. Table 17 presents the performance indicators for all experimental conditions. In general, mean values of R_2 showed better efficiencies for COD removal than anaerobic conditions, according to Student's t-test ($p \leq 0.05$), except for EC III. EC I presented the best results, reaching 65 ± 1 % after reaching operational stability. In the work described by Menezes et al. (2019), the same behavior was observed for the removal of textile wastewater. Results indicated that the partially aerated SBR achieved higher COD removal efficiencies (81%) than the full ASBR (76%), using close COD influent concentrations (1.2 $CODg.L^{-1}$).

PHWW recalcitrance is associated with the high stability of its rich aromatic content. For instance, compounds widely reported in PHWW that are within the most stable aromatic compounds, are benzene and pyridine with aromaticity of 36-39 $kcal.mol^{-1}$ and 32 $kcal.mol^{-1}$, respectively. In contrast to furan, which aromaticity is 16 $kcal.mol^{-1}$ (BERRY; FRANCIS; BOLLAGL, 1987). Si et al. (2018) proposed a metabolic pathway for three dominant compounds (furfural, phenol, and pyridine) with these aromatic rings (furan, benzene, and

pyridine) during the anaerobic digestion of PHWW, and pyridine was proposed to be metabolized for aerobes or facultative microorganisms (Figure 4). In general, hydroxylation is considered a common mechanism for the degradation of aromatic compounds, such as benzene (Figure 3) and pyridine, and can occur much more favorably in the presence of oxygen than anaerobically, where oxygen is used by oxygenase enzymes and is inserted into the molecules as hydroxyl groups (KAISER; FENG; BOLLAG, 1996). For instance, Siqueira et al. (2018) studied the biodegradation of BTEX in UASB, where their removal efficiencies were between 55-82% under anaerobic conditions, and above 83% in microaerated conditions.

Figure 22 - Organic matter removal efficiency in the anaerobic reactors (■) and the partially aerated reactor (●)

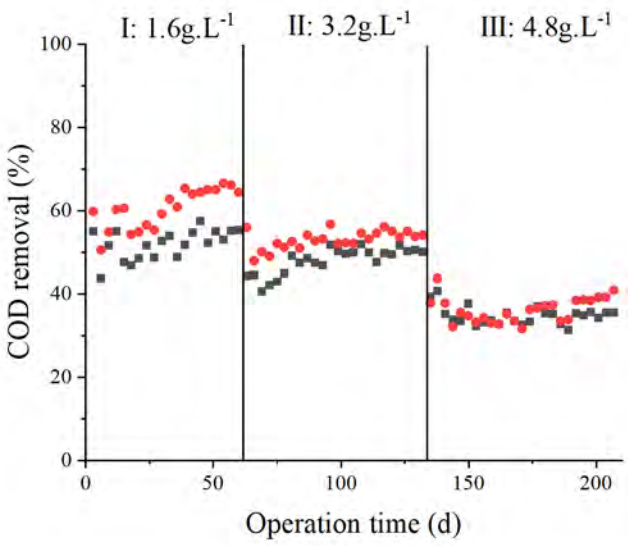

Source: Own authorship

In this study, the presence of oxygen may have stimulated various oxygenase enzymes in the facultative microorganisms with the capability to degrade aromatic compounds, which could have facilitated the following anaerobic biodegradation of by-products. For instance, benzene mineralization was studied under microaerophilic conditions by Yerushalmi et al.

(2001). They reported that after the activation of the aromatic ring by oxygenase enzymes, the resulting by-products can be degraded anaerobically. Therefore, it was evident that partially aerated conditions favored significantly PHWW biodegradability, resulting in higher COD removal efficiencies.

Table 17 - Performance indicators for all experimental conditions in R_1 and R_2

Parameters	R_1	R_2
EC I: 1.6 gCOD.L^{-1}		
COD removal (%)	51.9 ± 3.5	60 ± 4.7
Y_{CH4} (NmL/gCODadd)	173 ± 18	95 ± 9
Y_{CH4} (NmL/gCODrem)	341 ± 23	162 ± 21
EC II: 3.2 gCOD.L^{-1}		
COD removal (%)	48 ± 3.2	53 ± 2.2
Y_{CH4} (NmL/gCODadd)	166 ± 16	91 ± 7
Y_{CH4} (NmL/gCODrem)	323 ± 32	170 ± 15
EC III: 4.8 gCOD.L^{-1}		
COD removal (%)	34.8 ± 2.2	36 ± 3
Y_{CH4} (NmL/gCODadd)	111 ± 7	47 ± 4
Y_{CH4} (NmL/gCODrem)	316 ± 25	135 ± 14

COD: Chemical oxygen demand; Y_{CH4}: CH_4 yield

Source: Own authorship

4.3.3. Methane production

Figure 23 shows the boxplot graphs of CH_4 yields for both configurations studied. CH_4 yields ranged from 111 ± 7 NmL/gCODadd to 173 ± 18 NmL/gCODadd in R_1 and from 47 ± 4 NmL/gCODadd to 95 ± 9 NmL/gCODadd in R_2 (Table 17). An inhibition of CH_4 production was observed in R_2, where methanogenesis corresponded for 47%, 50%, and 40% of COD

removal in EC I, EC II, and EC III, respectively. Similar behavior was reported by Menezes et al. (2019) for the treatment of textile wastewater under partially microaerated conditions (42 - 50%). Oxygen presence could cause this effect by directly inhibiting methanogenic microorganisms (KATO; FIELD; LETTINGA, 1993), or by supporting the facultative anaerobes in their competition for substrate (HEDRICK; GUCKERT; WHITE, 1991).

Figure 23 - Boxplot of CH_4 yields for EC I: 1.6gCOD.L^{-1}, EC II: 3.2COD g.$L^{-1,}$ and 4.8 gCOD.L^{-1} in R_1 and R_2

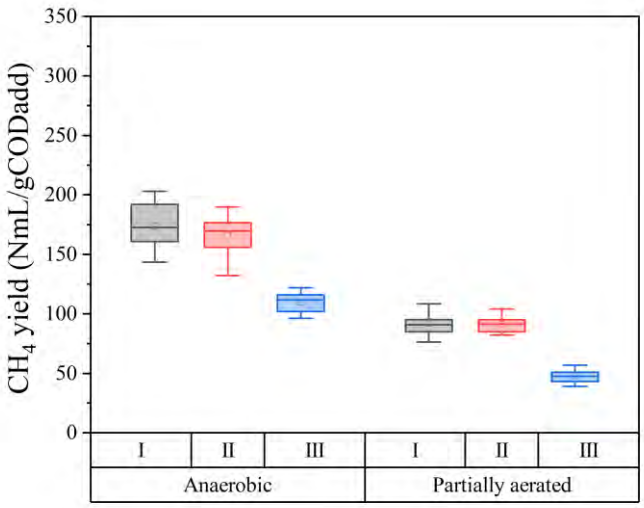

Source: Own authorship

Moreover, CH_4 produced per gram of COD added was maintained when COD influent concentrations were increased up to 3.2gCOD.L^{-1}, for both configurations. A drop in methane yield was observed for both conditions at concentrations of 4.8gCOD.L^{-1}, this effect likely occurred to higher concentrations of toxicants in PHWW that inhibited the microbial consortium. Additionally, no endogenous CH_4 production was observed in the anaerobic reactors, as observed in Table 18, which presents the COD balance regarding the influent COD, CH_4 production and effluent COD obtained in each experimental condition after reaching

operational stability. Average values of 0.92 and 0.71 were observed for R_1 and R_2, respectively.

Table 18 - COD balance regarding the CH_4 production and COD removed achieved in each experimental condition after reaching operational stability in R_1 and R_2

Experimental conditions	R_1	R_2
EC I: 1.6 $gCOD.L^{-1}$		
COD_{IN} (g)	820	828
COD_{EF} (g)	364	296
Experimental CH_4 (gCOD)	381	269
COD balance	0.91	0.68
EC II: 3.2 $gCOD.L^{-1}$		
COD_{IN} (g)	2120	2082
COD_{EF} (g)	1103	968
Experimental CH_4 (gCOD)	817	512
COD balance	0.91	0.71
EC III: 4.8 $gCOD.L^{-1}$		
COD_{IN} (g)	2876	2964
COD_{EF} (g)	1926	1802
Experimental CH_4 (gCOD)	809	424
COD balance	0.95	0.75

COD: Chemical oxygen demand

Source: Own authorship

Under oxygenation, part of energy (COD) destined for cell growth and maintenance can be inferred as larger in R_2 because aerobes and facultatives anaerobes are expected to grow faster

in these conditions due to their higher specific growth rate, substrate utilization rate and biomass yield when compared to fermentative, acidogenic, acetogenic and methanogenic microorganisms (BOTHEJU; BAKKE, 2011; NGUYEN; KHANAL, 2018), such organisms generally growth in suspension and are subjected to washout ocurrence, as verified by the results of VSS analysis at the end of the operation period of R_2.

4.3.4. Temporal profiles

After reaching steady-state conditions, temporal profiles of organics degradation, metabolites, CH_4 production, ORP, and DO were obtained. ORP and DO profiles are presented in Figure 24 and Figure 25, respectively. Such parameters were utilized to monitor the variation of oxygen levels along the cycle time.

On average, values of 342 ± 16 mV were observed in the anaerobic periods for both configurations. According to Hirasawa et al. (2008), the ORP values necessary for the growth of methanogenic archaea in mixture cultures, as found in the monitored reactors, are approximately lower than -330 mV. Thus, methanogens conditions were rapidly established and maintained along the first 48 h of the cycle time. A steeply rose was observed during intermittent aeration periods reaching maximum values of -66 mV (58 h), -125 mV (56.5 h), and -106 mV (52.3 h) in EC, EC II, and EC III, respectively. The same behavior was observed by Menezes al. (2019) during the intermittent aeration in an ASBR treating textile wastewater. Aeration supplied oxygen to the system reaching maximum values of DO of 4.9 $mg.L^{-1}$. Although similar values of DO were reported in reactors using activated biomass (YADAV; KHARDENAVIS; KAPLEY, 2014), DO concentrations were rapidly consumed and disappeared completely from the system, indicating that facultative microorganisms were consuming the available oxygen (KATO; FIELD; LETTINGA, 1997).

Figure 24 - Temporal profiles of ORP for anaerobic (■) and partially aerated (●) conditions: EC I: 1.6 gCOD.L^{-1} (a), EC II: 3.2 gCOD.L^{-1} (b), and EC III: 4.8 gCOD.L^{-1} (c)

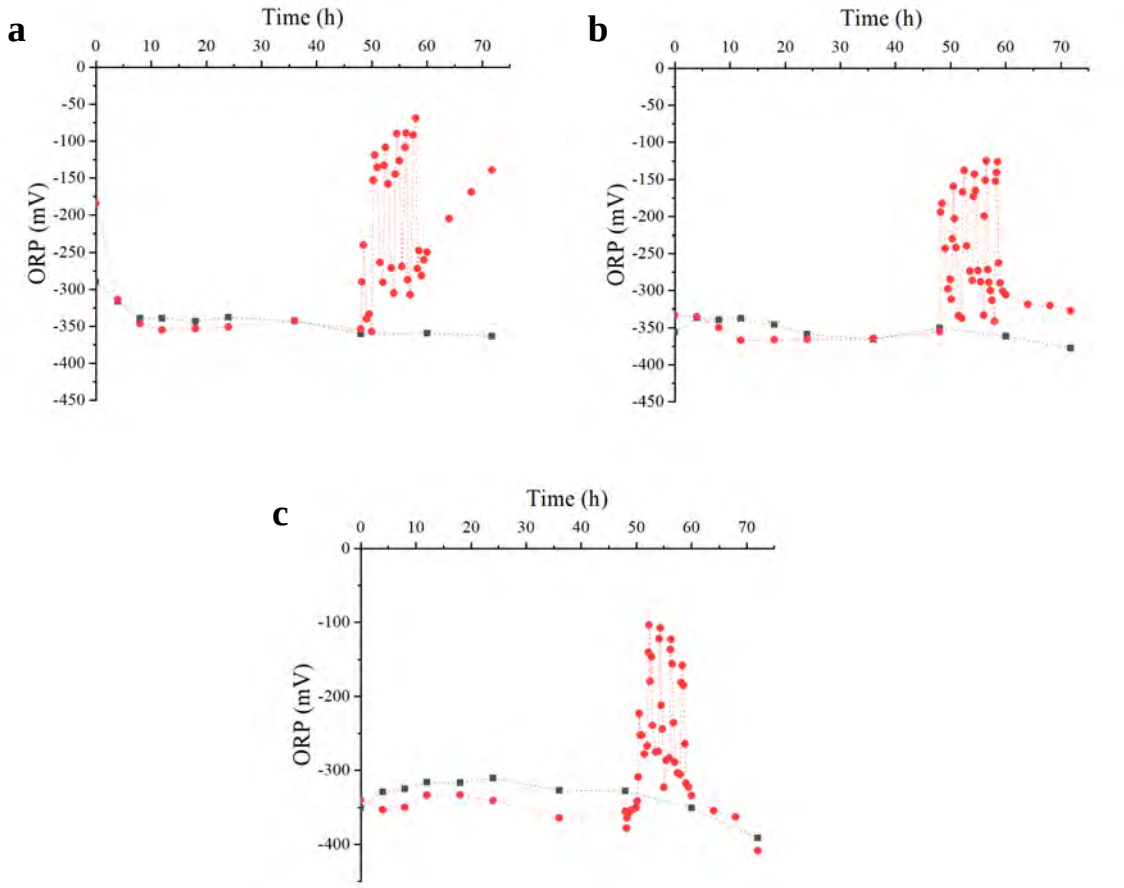

Source: Own authorship

In the last anaerobic stage, ORP profiles showed an increase in EC I (up to -151 mV), and much more reduced values in EC II and EC III (< -300 mV). The same tendency was observed in DO profiles, where a total consumption was observed in EC II and EC III, due to a great demand of DO for COD degradation in this period, maintaining DO values in low levels. On the other hand, DO values reached 1.5mg.L^{-1} in EC I, indicating some oxygen accumulation at the end of the cycle. In general, a correlation between values of ORP and DO was observed for both set-ups.

Figure 25 - Temporal profiles of DO for anaerobic (■) and partially aerated (●) conditions: EC I: 1.6 gCOD.L-1 (a), EC II: 3.2 gCOD.L-1 (b), and EC III: 4.8 gCOD.L-1 (c)

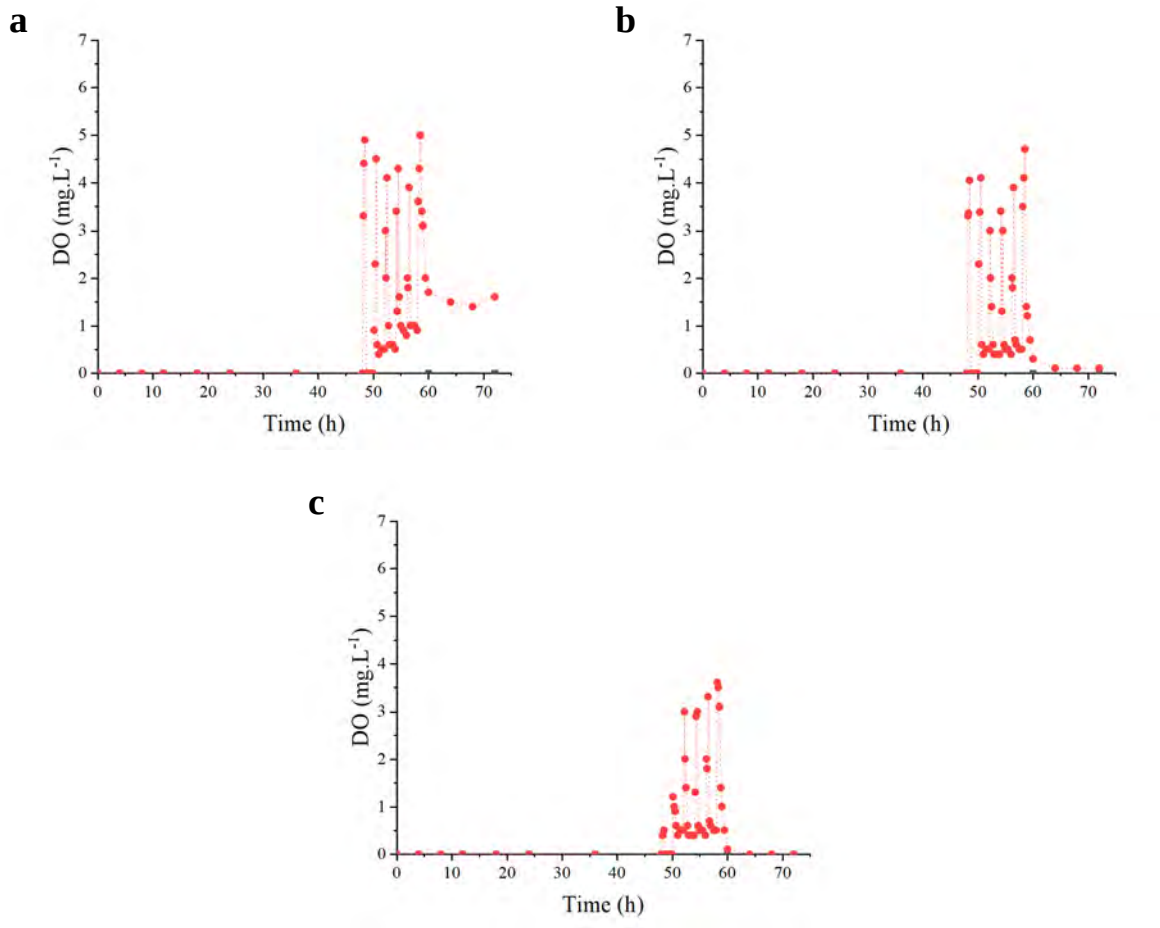

Source: Own authorship

Figure 26 shows the temporal profiles of COD degradation, where the pseudo-first-order model with residual concentration was adjusted successfully to COD consumption (Adj. R^2 > 0.97). In R_2, such model was adjusted only to the anaerobic stage. After 48 h of anaerobic stage, COD removal efficiencies reached 52% in EC I, accounting for 93% of the total COD degraded in R_1. In R_2, COD removal efficiencies were up to 48% after 48 h of treatment, representing 75% of the total COD degradation (Figure 27). From this comparison, it is clear that the anaerobic stage in R_2 was a key step for PHWW biodegradation. On the other hand, organic matter degradation in the intermittently aerated stage was on average 22 ± 1% of the total COD

consumed. At higher organic loads (3.2 and 4.8 gCOD.L^{-1}), COD degradation in the subsequent anaerobic step became more significant, accounting for at least 20% (Figure 27).

Figure 26 - Temporal profiles of COD degradation for R_1 (a) and R_2 (b): EC I: 1.6 gCOD.L-1 (■), EC II: 3.2 gCOD.L-1 (●), and EC III: 4.8 gCOD.L-1 (▲)

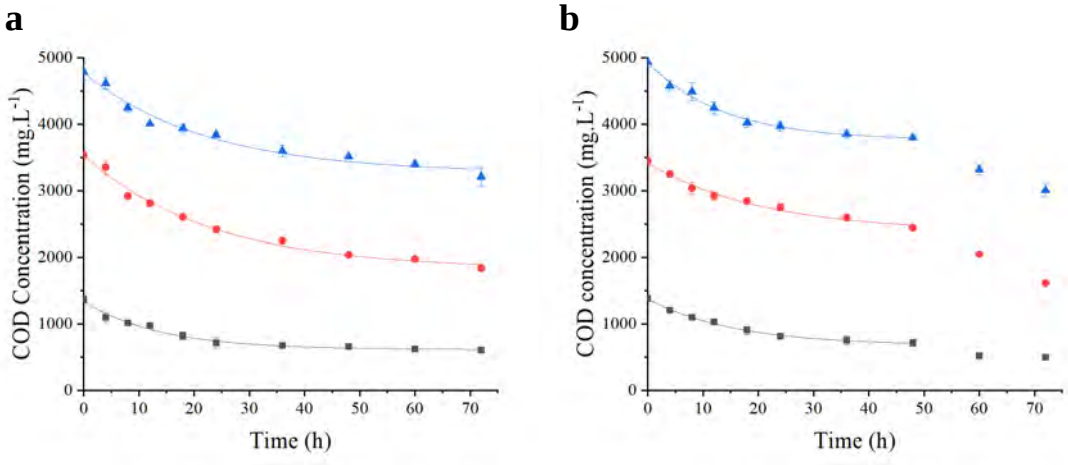

Source: Own authorship

Figure 27 - COD degradation distribution in R_2 during the anaerobic stage (■), microaerated (■) and anaerobic (■)

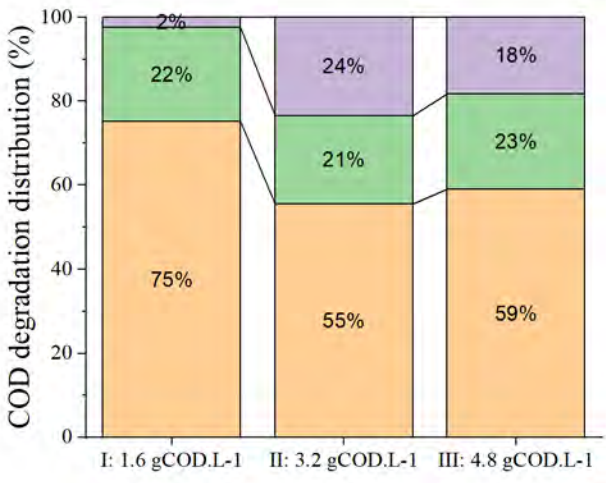

Source: Own authorship

Temporal profiles of VFA throughout the cycle are presented in Figure 28. In EC I, both profiles show that VFA generation was below the detection limit after 24 h of cycle time. Concentration of acetic acid reached 166 mgCOD.L^{-1} (12 h) and 112 mgCOD.L^{-1} (8 h) for R_1 and R_2, respectively. Besides acetic acid, propionic acid was observed in R_2, whereas butyric and valeric acids were also generated in R_1. Although no VFA accumulation indicates balanced anaerobic populations, lower generation of VFA was observed for R_2 (178 mgCOD.L^{-1}), which in the end resulted in lower CH_4 production when compared to R_1.

In EC II, the highest concentrations of volatile acids corresponded to propionic acid, reaching 341 mgCOD.L^{-1} (12 h) and 321 mgCOD.L^{-1} (18 h), for R_1 and R_2, respectively. Although a balanced generation/consumption was observed for propionic, butyric and valeric acids, a residual concentration of acetic acid was observed in R_1 (32 mgCOD.L^{-1}) (Table 19).

On the other hand, an accumulation was observed in R_2 at 48 h. Further VFA degradation was achieved in the following stages: intermittently aerated and anaerobic, where VFA removal efficiencies of 43% and 57% were achieved, respectively. Results were in accordance with Nguyen et al. (2019), where VFA concentration rapidly decreased after intermittent aeration started, during the degradation of lignocellulosic feedstock. They suggested that facultative bacteria switched from anaerobic fermentation to aerobic respiration in the presence of oxygen. Moreover, Wu et al. (2015) reported that DO values higher than 0.3 mg.L^{-1} decreased VFA concentrations while treating petrochemical wastewater in a full anaerobic bioreactor with limited aeration.

In EC III, a higher VFA accumulation was observed in R_1 (648 mgCOD.L_{-1}), likely due to a greater amount of toxicants, where acetic, propionic, butryric and valeric acids were found in the effluent (Table 19). Besides a methanogenic limitation, butyric and valeric acids accumulation indicated that acetogenesis was impaired (TOMMASO et al., 2015).

Figure 28 - Temporal profiles of VFA concentration: acetic (■), propionic (■), butyric (■) and valeric (■) acids in R_1 (a) R_2 (b)

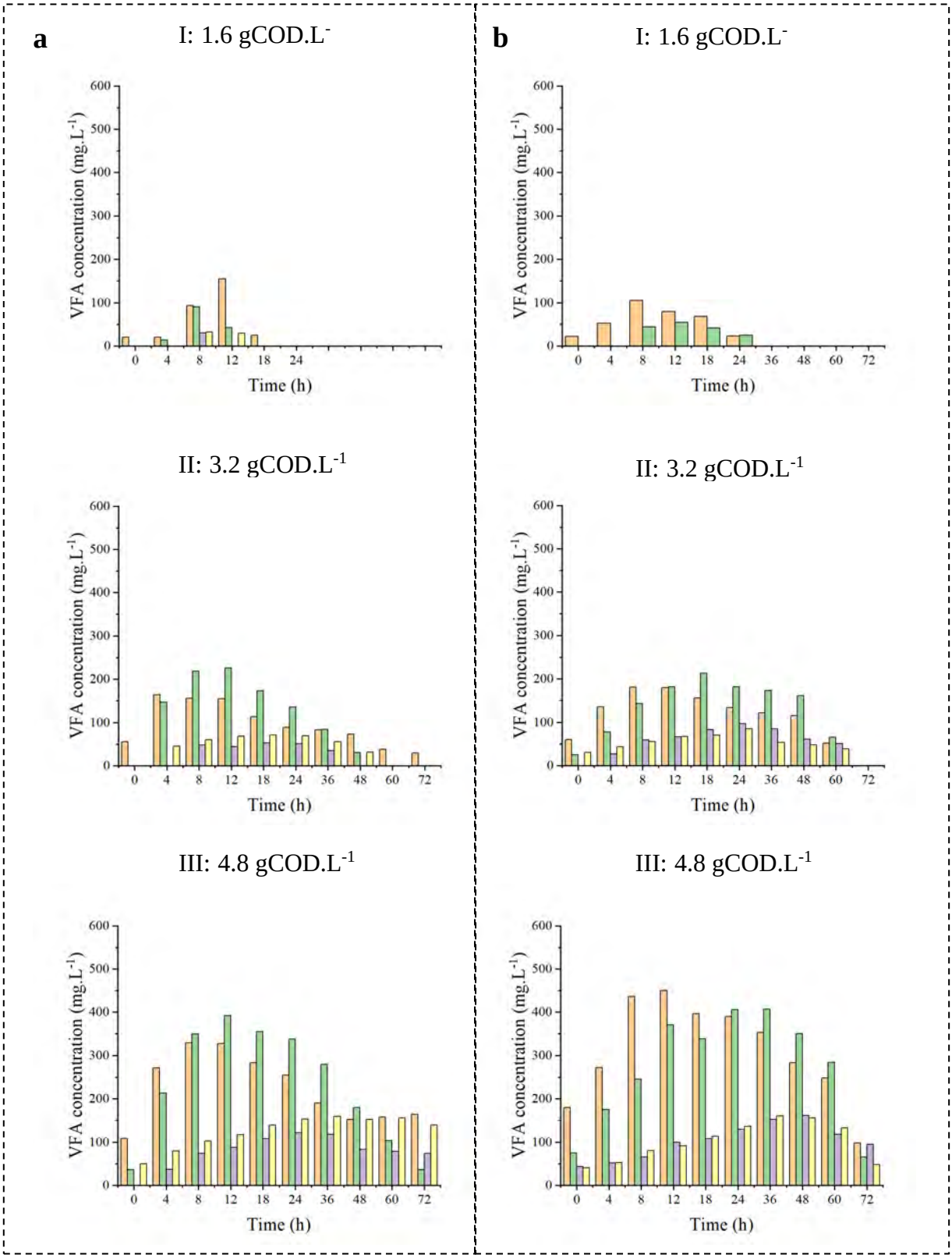

Source: Own authorship

Table 19 - Metabolites concentration at the end of the cycle time of R_1 and R_2

Metabolites concentrations	R_1			R_2		
	I	II	III	I	II	III
Acetic acid (mgCOD.L^{-1})	-	31.9	176.2	-	-	104
Propionic acid (mgCOD.L^{-1})	-	-	54	-	-	99
Butyric acid (mgCOD.L^{-1})	-	-	134	-	-	172
Valeric acid (mgCOD.L^{-1})	-	-	284	-	-	97

Source: Own authorship

Although propionic acid was also observed in the effluent (54 mgCOD.L^{-1}), its concentration was lower than the observed in the experiment in Section 4.2 under the same organic load (623 mgCOD.L^{-1}). A possible explanation could be the lower time of biomass acclimation to valeric acid in R_1, since this intermediate its typical from PHWW anaerobic digestion and it generates propionic and acetic acid during its degradation (PIND; ANGELIDAKI; AHRING, 2003). Such explanation was verified by the concentration of valeric acid in R_2 (284 mgCOD.L^{-1}) and the observed in the experiment in Section 4.2 (94 mgCOD.L^{-1}) where indeed a lower propionic acid concentration was found under the same organic load. Bueno et al, (2021) also observed lower propionic acid concentrations when valeric acid was accumulated during the continuous treatment of PHWW in a HAIB reactor.

High production of acetic acid was observed in R_2, reaching values of 482 mgCOD.L^{-1} (EC III). Although VFA were consumed in the intermittently aerated stage (27%) and the subsequent anaerobic stage (73%), an accumulation of acetic, propionic, butyric, and valeric acids was observed (472 mgCOD.L^{-1}). In general, VFA generation was promoted in R_2 likely due to an increase in fermentative/acidogenic bacteria abundance.

The degradation of total phenolic compounds in R_1 and R_2 is reported in Figure 29, where the initial content varied from 46 mgGAE.L^{-1} to 168 mgGAE.L^{-1}. Efficiencies up to 31% and 43% were observed in R_1 and R_2, respectively. Anaerobic degradation of phenolic compounds occurred mainly in the first 30 h. On the other hand, intermittently aerated stage enhanced phenolics degradations by 10%. Figure 30 shows the distribution of phenolics removal in R_2. In EC I, 70% of the degradation occurred in the first anaerobic stage, whereas at higher organic loads, the last anaerobic stage was responsible for 20% of the TPh conversion. Moreover, at least 21% of TPh removal occurred in the intermittently aerated stage.

Figure 29 - Temporal profiles of total phenolic compounds in R_1 (a) and R_2 (b): EC I: 1.6 gCOD.L-1 (■), EC II: 3.2 gCOD.L-1 (●), and EC III: 4.8 gCOD.L-1 (▲)

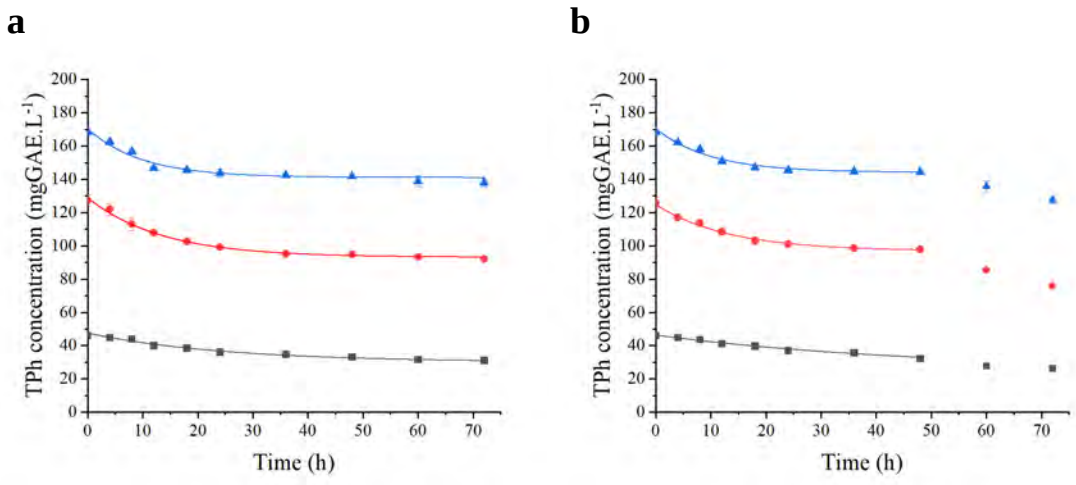

Source: Own authorship

Wu et al. (2015) reported that microaeration improved BTEX and phenol degradation from a petrochemical wastewater in an anaerobic reactor assisted with limited aeration, from 39% to 82%, for an initial concentration of 45 mg.L^{-1} (BTEX + phenol). According to Yerushlami et al. (2001), after the hydroxylation of the aromatic ring by oxygenase enzymes, catechol, identified as intermediate, can be metabolized anaerobically to benzoic acid in microaerated

conditions. Despite limited removal efficiencies observed, the long-term exposure to partially aerated conditions could have led to a gradual enrichment of the microbial consortium with facultative/aerobic species associated with the bioconversion of phenolic compounds, enhacing its degradation.

Figure 30 - TPh degradation distribution in R_2 during the anaerobic stage (■), microaerated (■) and anaerobic (■)

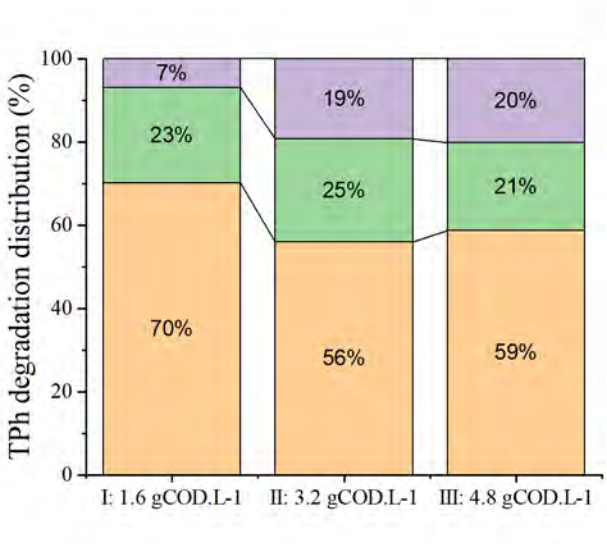

Source: Own authorship

Cumulative CH_4 production per gram of VSS in R_1 and R_2 is shown in Figure 31. As discussed before, CH_4 production was limited in R_2, due to a reduction in the methanogenic population abundance, as observed in the microbial diversity results (Section 4.3.5). In this experiment, methanogenesis and aerobic degradation contributed equally to COD removal, using the same microbial inoculum.

Figure 31 - Cumulative CH_4 production in R_1 (a) and R_2 (b): EC I: 1.6 gCOD.L-1 (■), EC II: 3.2 gCOD.L-1 (●), and EC III: 4.8 gCOD.L-1 (▲)

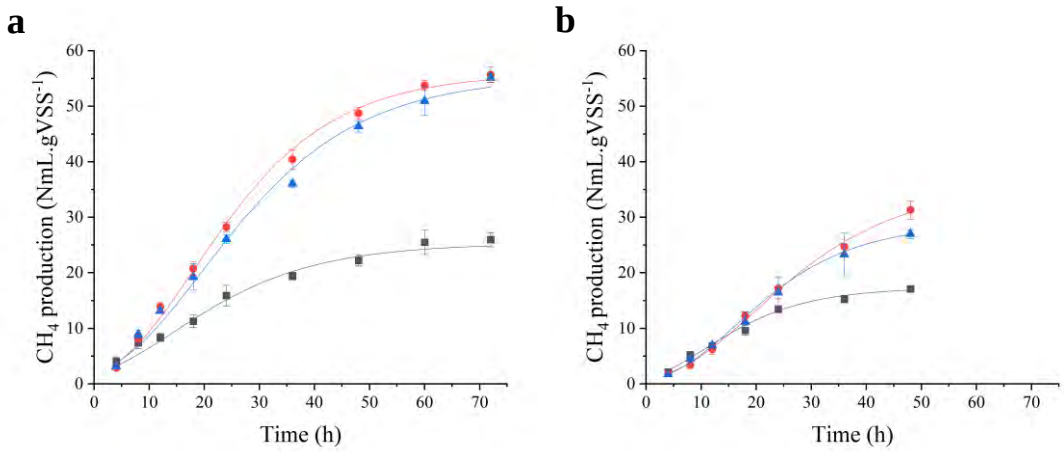

Source: Own authorship

4.3.5. Microbial diversity

The differences in the microbial communities in R_1 and R_2 are presented in Figure 32, which shows the results of the taxonomic analysis at phylum level. The six phyla, with relative abundances higher than 1%, identified in R_1 were distributed as follows: 38% belonged to the *Euryarchaeota* phylum, 35% to the *Firmicutes* phylum, 16% to the *Synergistete*s phylum, 6% to the Bacteriodetes phylum, 2% to the *Thermotogae* and 2% to the *Proteobacteria* phylum. In the case of R_2, the main five phyla identified included: *Proteobacteria* (28%), *Synergistete*s (25%), *Euryarchaeota* (20%), *Firmicutes* (18%), and *Bacteriodetes* (6%). Within these phyla, *Firmicutes* and *Proteobacteria*, generally recognized as hydrolytic fermentative microorganisms (PASALARI et al., 2021), constituted the most representative bacteria for R_1 and R_2, respectively. On the other hand, the most enriched phyla in both set-ups were *Euryarchaeota*, from 19% to 38%, and *Synergistetes*, from 0.3% to 25% respectively, when compared to the inoculum microbial abundance.

Figure 32 - Taxonomic classification of the reads in R_1 (a) and R_2 (b) at phylum level

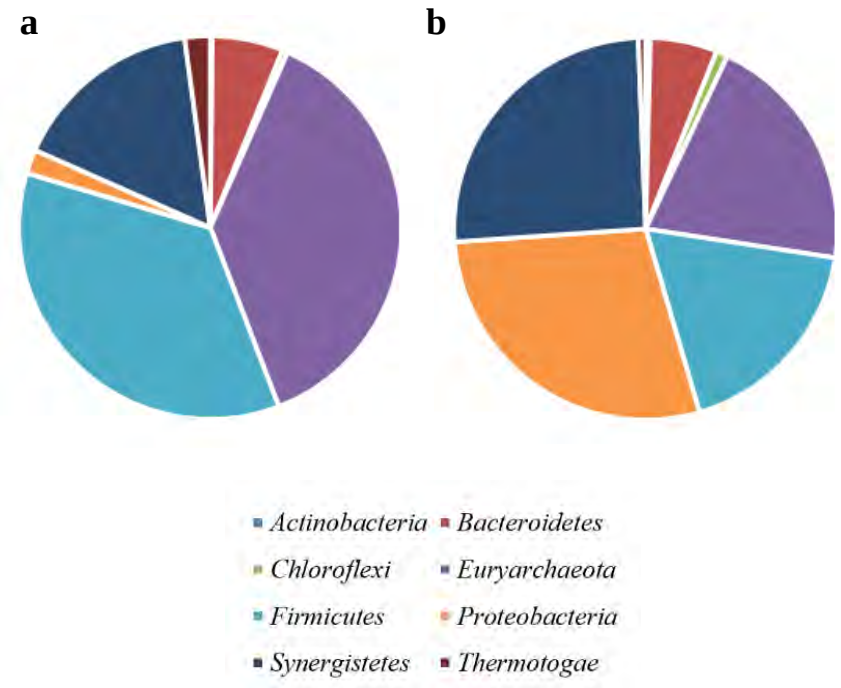

Source: Own authorship

Figure 33 shows a heatmap of the microbial diversity in R_1 and R_2, at genus level. *Trichococcus* (phylum *Firmicutes*) (19.9%), *Aminobacterium* (phylum *Synergistetes*) (14%), *Eubacterium* (phylum *Firmicutes*) (12.9%) were the dominant bacteria in R_1. These acidogenic microorganisms were the main ones responsible for organic degradation in PHWW. Other detoxifying microorganisms included *Petrimonas* (phylum Bacteriodetes) (6%), fermentative bacteria isolated from a biodegraded oil reservoir (GRABOWSKI et al., 2005). Their metabolites (lactate, formate, acetate, propionate, butyrate, valerate, ethanol, CO_2, and H_2) (ZINDEL et al., 1988; BAENA et al., 1998; STREPIS et al., 2020) were consumed by acetogenic microorganisms, such as *Mesotoga* (phylum *Thermotogae*) (2.2%), *Syntrophomas* (1.3%) (phylum *Firmicutes*) and *Acetoanaerobium* (phylum *Firmicutes*) (0.5%) (ROY et al., 1986; BEN HANIA et al., 2013). The latter genus catalyzes the formation of acetate from H_2 and CO_2 (KNAPP; BROMLEY-CHALLONER, 2003). The CH_4 production was supported

mainly by *Methanosarcina* (29%), a versatile methanogenic that can use acetate, methanol, and H_2/CO_2 as carbon source, and *Methanobacterium* (7.2%), which can convert H_2/CO_2, and formic acid into CH_4 (ANGELIDAKI et al., 2011).

Figure 33 - Heatmap representing the microbial diversity at genus level in R_1 and R_2

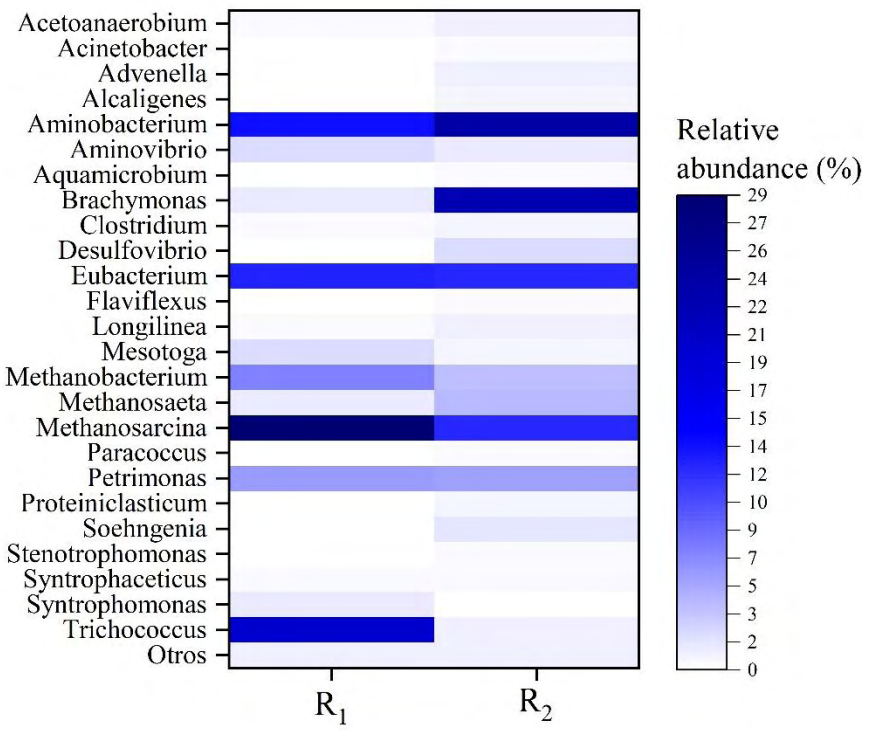

Source: Own authorship

Due to the use of the same inoculum, the most representative fermentative bacteria observed in R_1 were also reported in R_2, including *Aminobacterium* (23.9%), *Eubacterium* (12.4%), *Petrimonas* (5.7%), with close relative abundance except for *Aminobacterium*, which was more favored by oxygen availability. Regarding the syntrophic microorganisms, although a diminution in the relative abundance of *Mesotoga* (0.6%) and *Syntrophomonas* (0.1%) was found in R_2, a higher presence of *Acetoanaerobium* (1.1%) was observed. , which indicates that partially aerated conditions were better for their growth. *Desulfovibrio* (phylum *Proteobacteria*) (2.1%) are sulfate-reducing bacteria (SBR) that cannot oxidize acetate and

uses lactate and ethanol as electron donors to produce acetate (BRYANT et al., 1977). SBR capable of oxidizing acetate were not observed in this experiment indicating that the acetate generated was used for other metabolisms (HIRASAWA et al., 2008), acetoclastic methanogenesis, or aerobic respiration. Other anaerobic microorganisms favored by oxygen availability in comparison to full anaerobic conditions were *Soehngenia* (phylum *Firmicutes*) (1.6%), anaerobe genus that converts benzaldehyde into benzoate (PARSHINA et al., 2003). Both compounds are common intermediates of aromatic hydrocarbons degradation, previously identified in PHWW from cornstalk and *Spirulina* (SI et al., 2018; BUENO et al., 2021).

A coexistence with aerobic microorganisms (phylum *Proteobacteria*) was observed in R_2, where genera such as *Brachymonas* (22.7%), *Advenella* (1%), *Alcaligenes* (0.7%), *Stenotrophomonas* (0.4%), *Aquamicrobium* (0.3%) and *Paracoccus* (0.3%) were reported. *Brachymonas* are denitrifying bacteria that can degrade ethanol, benzoate, and some organic acids and aminoacids under aerobic conditions (HIRAISHI; SHIN; SUGIYAMA, 1995). This genus was the second most abundant in R_2, only after *Aminobacterium*, thus it was fundamental for PHWW organic degradation, especially during intermittently aerated periods. *Advenella* are also denitrifying bacteria that can degrade phenol under aerobic conditions Li et al. (2020) reported the degradation of up 1.2 $g.L^{-1}$ of phenol by the synergistic effect of *Advenella* and *Stenotrophomonas* co-culture. The latter is a strict aerobic genus that was also found in R_2 and was previously isolated from a UASB reactor treating petrochemical wastewater, it degrades sugars, amino acids, and benzoate. *Aquamicrobium* (phylum *Proteobacteria*) described as halotolerant bacteria, were reported to degrade petroleum hydrocarbons such as alkanes in saline conditions (WANG et al., 2015). *Alcaligenes* are heterotrophic microorganisms that can degrade isoquinoline, indole, and pyridine (FETZNER, 1998; CHANDRA et al., 2009). Both indole and pyridine have been identified in PHWW within the N-heterocyclic compounds (SHANMUGAM et al., 2017). Thus, although the individual removal of aromatic compounds

was not measured in this study, their degradation can be inferred by the presence of these bacteria.

Moreover, *Alcaligenes faecalis*, the specie identified in this study, is capable of performing aerobic ammonification, using organic substrates aerobically as source of carbon to convert ammonium into nitrogen gas (JOO; HIRAI; SHODA, 2005). This could explain the lower results of ammonia in R_2 effluent (Table 16), although it would be necessary to perform a nitrogen balance to verify this behavior.

The relative abundance of methanogenic microorganisms was lower in R_2 (20.4%) compared to R_1 (37.6%). Carvalho et al. (2020) observed the same behavior in two UASB reactors treating textile wastewater where the relative abundance of methanogens decreased under micro aerated conditions, meanwhile fermentative bacteria increased. At genus level, *Methanosarcina* (12.5%) was still the predominant methanogen in R_2 due to its flexibility; meanwhile, *Methanosaeta* (4.2%), exclusive acetoclastic, was the second most representative archaea in R_2. The maintenance of the methanogen microorganism's abundance in R_2 compared to the inoculum (19%) indicates that their methanogenic activity was mainly inhibited by the competition for substrate with facultative and aerobe bacteria due to oxygen availability (HEDRICK; GUCKERT; WHITE, 1991).

These results indicate that partially aerated conditions enhanced the organic matter removal of PHWW from *Spirulina* in a sequence batch process. The long-term exposure of an anaerobic consortium to partial oxygen availability led to a shift in the metabolic pathways, where aerobic microorganisms with key roles in the biodegradation of various aromatic compounds (including phenol and pyridine) coexisted with fermentative microorganisms. Although methanogens were not favored by these conditions, resulting in a decrease in CH_4 production, a partially aerated process presented a better performance than a full anaerobic process.

4.4. Photocatalysis as a post-treatment

4.4.1. UV photocatalysis experiments

It is clear from Table 7 that AD-PHWW obtained from HAIB reactor need a subsequent treatment to complete PHWW stabilization, reducing the compounds that were recalcitrant to the anaerobic process. In this sense, a photocatalytic post-treatment was tested using a CCD-FC approach to assess and optimize the effect of two parameters that may influence this process: initial pH and the use of H_2O_2 as an external oxidant. The responses for each photocatalytic treatment run are presented in Table 19.

Table 20 – Removal efficiencies of COD, TPh and color

Run	Initial pH $[x_1]$	Addition of H_2O_2 ($g.L^{-1}$) $[x_2]$	COD removal (%) $[y_1]$	TPh removal (%) $[y_2]$	Color removal (%) $[y_3]$
1	7	2	43.4	72.1	87.1
2	7	4	40.8	74.5	95.8
3	12	2	42.5	76.2	87.3
4	12	4	44.3	77.8	95.8
5	9.5	2	45.1	77.0	91.3
6	9.5	4	46.8	78.6	97.8
7	7	3	45.1	77.2	91.0
8	12	3	46.8	77.4	89.8
9	9.5	3	49.4	81.7	94.9
10	9.5	3	48.6	81.3	94.8
11	9.5	3	48.6	82.5	95.4

x: independent variables; y: response variables

Source: Own authorship

The models generated for COD, TPh, and color removal are shown in Eq. (18), (19), and (20), respectively. The adequacy of these models to represent the experimental data was verified by the results of the lack of fit test and the regression coefficient analysis (Adj. $R^2 \geq 0.85$), as observed in Table 20. The scatter in the data also confirmed these results when predicted values versus observed values were plotted at 95% confidence level (Figure 34).

Table 21 - ANOVA evaluation for the removal of COD, total phenolic compounds, and color

Factor	df	COD removal [y_1]		TPh removal [y_2]		Color removal [y_3]	
		SS	p	SS	p	SS	p
Linear							
x_1	1	3.105	0.045*	9.513	0.049*	0.182	0.638
x_2	1	0.124	0.617	5.448	0.107	92.905	0.000**
Quadratic							
x_1^2	1	23.826	0.001**	31.766	0.005**	36.789	0.001**
x_2^2	1	23.826	0.001**	23.267	0.01**	0.349	0.519
Interaction							
x_1x_2	1	4.657	0.022*	0.167	0.745	0.017	0.883
Lack of fit	3	1.696	0.320	6.285	0.161	3.439	0.077
Pure error	2	0.497	-	0.778	-	0.189	-
Total SS	10	75.06	-	29361.7	-	134.656	-
R^2		0.971	-	0.927	-	0.973	-
R^2 adj		0.942	-	0.854	-	0.946	-

**$p \leq 0.01$; * $p \leq 0.05$; df: Degree of freedom; SS: Sum of squares

Source: Own authorship

$$y_1 = -13.81 + 8.32x_1 - 0.49x_1^2 + 14.44x_2 - 3.07x_2^2 + 0.43x_1x_2 \quad (18)$$

$$y_2 = -7 + 11.51x_1 - 0.57x_1^2 + 19.91x_2 - 3.03x_2^2 - 0.082x_1x_2 \quad (19)$$

$$y_3 = 31.12 + 11.59x_1 - 0.61x_1^2 + 1.96x_2 + 0.37x_2^2 - 0.026x_1x_2 \quad (20)$$

Figure 34 - Predicted vs observed values of removal efficiencies of COD (a), TPh (b), and color (c) at 95% confidence level

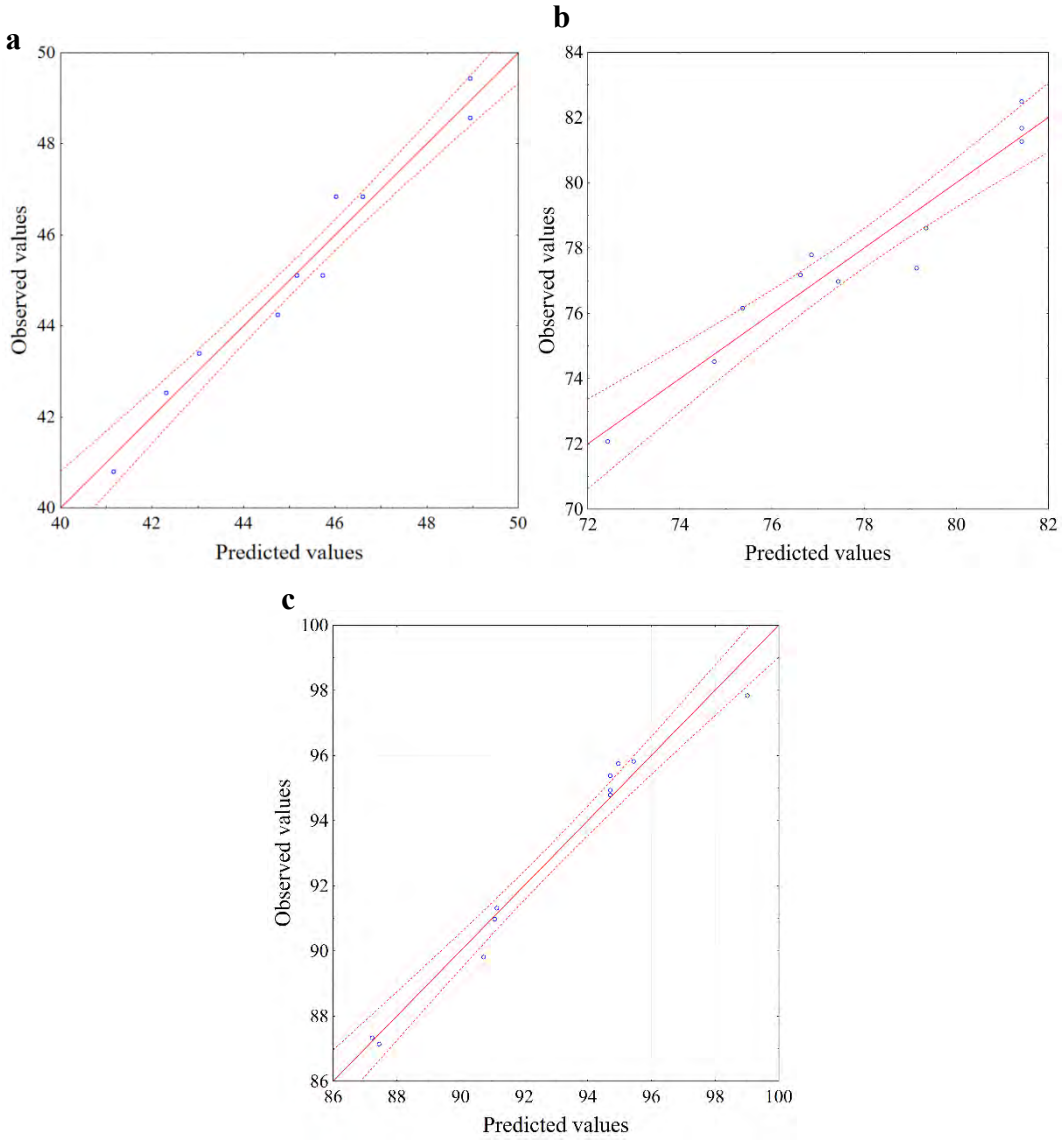

Source: Own authorship

4.4.2. Effect of initial pH

COD removal values varied from 41% to 50%, and were close to the ones reported by Costa and Alves (2013) for anaerobically pre-treated olive oil mill wastewater (≤ 59%). According to the ANOVA results and the model obtained for COD removal, both effects of initial pH were significant, however, the linear effect ($p = 0.045$) had positive influence on the removal efficiency and its quadratic effect ($p = 0.001$) had the opposite effect. This behavior means that pH values above 7 favored mineralization but values higher than optimal ones could be adverse to the process (Figure 35a). For instance, Yeber et al. (2000) reported a total organic carbon (TOC) removal of 55% at pH of 10.3 for cellulose bleaching effluent when initial COD and TOC values were 2255 $mg.L^{-1}$ and 980 $mg.L^{-1}$, respectively.

During the photocatalytic treatment, the irradiated catalyst can degrade organics directly, generating oxidizing sites (positive holes) and electrons on its surface (Eq. 1), or through the production of reactive radicals (Eq. 3) (BRAME et al., 2015). pH determines the surface charge (positive or negative) of the catalyst. For TiO_2, the point of zero charge (P_{ZC}) is at pH ~ 6.25, thus above this value, TiO_2 is negatively charged (TiO^-), generating more $HO^{\cdot}$ (AHMED et al., 2010). This aspect could have influenced the conversion of organic matter and aromatic compounds such as N-heterocyclic compounds and phenols, since the attack of the aromatic ring by $HO^{\cdot}$ radicals (hydroxylation) is the main mechanism of their conversion (KAUR; PAL, 2013). In this sense, the generation of $HO^{\cdot}$ radicals was crucial for AD-PHWW photodegradation. Moreover, the protonation/deprotonation of the organic compounds depends on their nature, and if pH favors its adsorption on the catalyst surface, faster photodegradation rates can be observed, however strong adsorption could prevent light to reach the catalyst surface (BIZANI et al., 2006).

Figure 35 - Response surface contour plots for COD (a), TPh (b), color (c) removal efficiencies, and the overlaying plot (d) as a function of pH and addition of H_2O_2

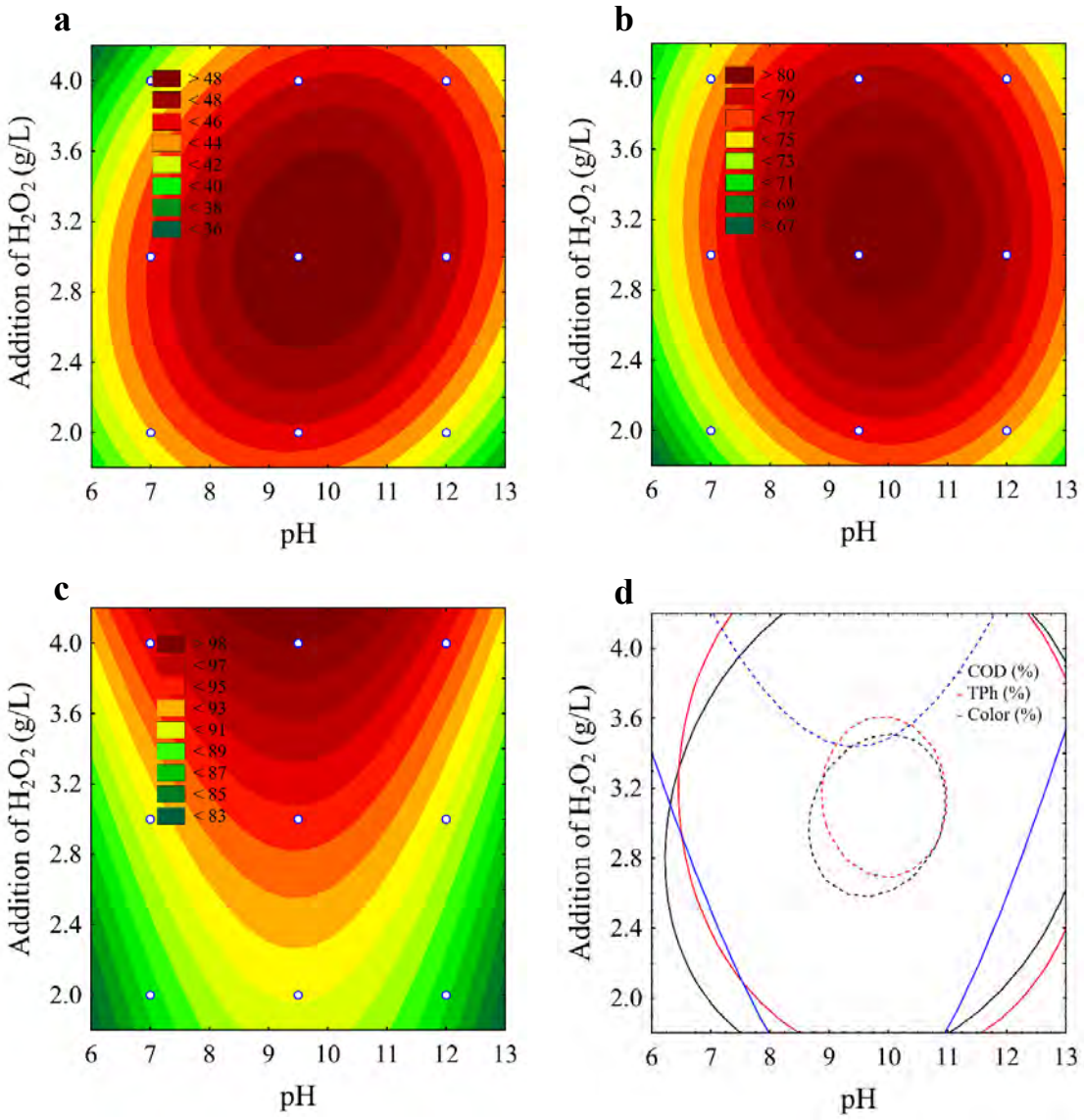

Source: Own authorship

The removal efficiencies of TPh compounds of the photocatalytic treatment were between 72.1% and 82.5% (Table 19), reaching final values of 5 mgGAE/L. The linear ($p = 0.049$) and quadratic ($p = 0.005$) effects of initial pH presented the same behavior as observed for COD degradation. Figure 35b shows that intermediate pH levels above 7 resulted in the highest TPh removal values, where similar pH was reported by Barakat et al. (2005) for the

photodegradation of 2-chlorophenol. Besides the importance of the generation of $HO^{\cdot}$ radicals to break down the phenyl ring (AHMED et al., 2010). TiO^{-} is the predominant species under alkaline conditions, and phenols are commonly present in their neutral forms in this pH (JING et al., 2011). This factor could have increased the adsorption of phenols on the catalyst due to the hydrogen bond, increasing the degradation rate.

Moreover, the quadratic effect of initial pH was significant for color removal ($p = 0.001$). As shown in the response surface contour plot (Figure 35c), intermediate alkaline pH values favored discoloration, which was also observed for COD and TPh removal, indicating a direct relationship between discoloration and organics removal. Costa and Alves (2013) reported similar relation between TPh and color removal, indicating that phenols were partly responsible for the effluent color.

4.4.3. Effect of the addition of H_2O_2

AD treatment converted a significant amount of organic matter contained in PHWW but did not have a significant effect on color removal, in contrast with the photocatalytic treatment, which reached almost a total discoloration (98%). Chatzisymeon, Xekoukolotakis, and Mantzavinos (2009) observed similar efficiencies (99%) treating olive oil mill wastewater, even when the effluent contained a higher initial COD value (1000 $mg.L^{-1}$). The use of H_2O_2 as an external oxidant generally enhances photodegradation processes by avoiding electron-hole recombination, acting as an electron acceptor, and by generating more $HO^{\cdot}$ radicals (AHMED et al., 2010). In this way, the linear effect of the addition of H_2O_2 was highly significant for color removal, where higher H_2O_2 concentrations resulted in greater discoloration efficiencies. Moreover, H_2O_2 can act as a bleaching agent for wastewaters (PEKAKIS; XEKOUKOULOTAKIS; MANTZAVINOS, 2006).

However, only the quadratic effect of H_2O_2 was significant for COD and TPh removal, and had a negative effect (Table 20 and Figure 35). These results could be attributed to the high

concentration of $HO^{\cdot}$ radicals due to the alkaline conditions and addition of H_2O_2. When in excess, H_2O_2 can act as $HO^{\cdot}$ scavenger (BIZANI et al., 2006). This could be the reason why the linear effect of H_2O_2 was not significant for COD and TPh removal ($p > 0.05$). Thus, optimum concentration must be reached to avoid decrease in the photodegradation efficiency. Additionally, the interaction between variables had a significant influence ($p = 0.022$) on COD removal (Table 21), and the response surface contour plot (Figure 35a) shows that removal efficiencies could be maximized at intermediate levels of initial pH and addition of H_2O_2.

4.4.4. UV photocatalysis evaluation

Figure 35(d) presents the overlay contour plot obtained for the three dependent variables, where the optimum region was identified. The thresholds of each response were established as removal efficiencies of COD > 44%, TPh > 81% and color > 97%. Thus, the best parameters values for the AD-PHWW photodegradation were in a range from 9.6 to 10.1 of pH and 3.4 to 3.55 $g.L^{-1}$ of H_2O_2. Experiments were conducted at optimal conditions to verify and validate the models obtained (pH of 9.6 and addition of H_2O_2 of 3.55 $g.L^{-1}$). Students' t test (95% confidence interval) indicates a good agreement between predictive and experimental results ($p > 0.05$) (Table 21).

Table 22 - Predicted and experimental values of the responses at optimum conditions

Response variables	Predicted values	Experimental values
COD removal (%)	48.14 ± 1.21	49.73 ± 2.64
Phenolics removal (%)	81.06 ± 2.18	83.08 ± 1.02
Color removal (%)	96.97 ± 1.56	94.99 ± 1.40

Values are mean ± SD

Source: Own authorship

Maximum removal efficiencies at optimal photocatalytic conditions were 50% for COD, 83% for TPh, and 95% for color (Table 22). Figure 36 shows AD-PHWW before and after the photocatalytic treatment. Although almost complete discoloration and high phenolic content conversion were observed, an important fraction of organics subjected to photocatalysis was not degraded (50%). This difference could have occurred due to the formation of colorless intermediates and compounds resistant to photocatalysis originally present in PHWW or generated during AD or photocatalytic treatment, as previously reported in the photocatalytic treatment of olive oil mill wastewater (COSTA; ALVES, 2013).

Table 23 - Removal efficiencies, rate constants (k), half-time ($t_{1/2}$), and regression coefficient of the photocatalytic AD-PHWW treatment

	Removal efficiency (%)	k ($min^{-1} \times 10^{-3}$)	$t_{1/2}$(min)	R^2
COD	50 ± 2.6	3.02 ± 0.035	230 ± 2.6	0.996
TPh	83 ± 1	7.63 ± 0.007	91 ± 0.1	0.981
VIS_{340}	95 ± 0.7	15.15 ± 1.061	46 ± 3.2	0.957
UV_{278}	82 ± 0.4	7.44 ± 0.311	93 ± 3.9	0.991
UV_{254}	80 ± 1.2	6.81 ± 0.262	102 ± 3.9	0.998

Values are mean ± SD (n = 3).

Source: Own authorship

Temporal profiles of degradation were obtained for COD, TPh and color, and expressed as removal efficiencies in Figure 37. The rate constants (k), half-time ($t_{1/2}$), and regression coefficients of the photocatalytic AD-PHWW treatment are presented in Table 20. Organics conversion rates were in the following order: VIS_{340} (color) > TPh > UV_{278} > UV_{254} > COD. Close values of rate constants were reported previously for the photodegradation of textile wastewater ($2.9 \times 10^{-3} - 6.6 \times 10^{-3} min^{-1}$) (SOUZA et al., 2016).

Figure 36 - Post-hydrothermal liquefaction wastewater values prior to (a) and after (b) the photocatalytic treatment

Source: Own authorship

Figure 37 - COD (■), TPh (●) and color removal (▲) efficiencies obtained in the photocatalytic treatment

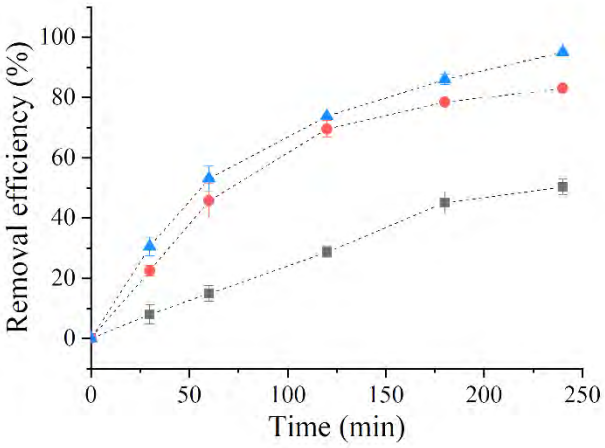

Source: Own authorship

Figure 38 shows changes in the UV-vis spectra of PHWW during the photocatalytic treatment. Additionally, mineralization reactions were monitored at UV_{254} and UV_{278}. In general, absorbance decreased with the same tendency, especially, the 260-300 nm region. In a previous study, Pinheiro, Touraud, and Thomas (2004) reported that this region is associated

with aromatic amines spectra. The reduction of this spectral zone could have occurred due to the breakage of aromatic rings into smaller compounds that were more difficult to degrade and contributed to the final COD (SOUZA et al., 2016).

Figure 38 - UV-vis spectral change of PHWW: HAIB in (■), HAIB out (●), 30 min (▲), 60 min (▼), 120 min (◆), 180 min (►), and 240 min (◄) of TiO2/UV treatment. (Dilution factor: 1:5)

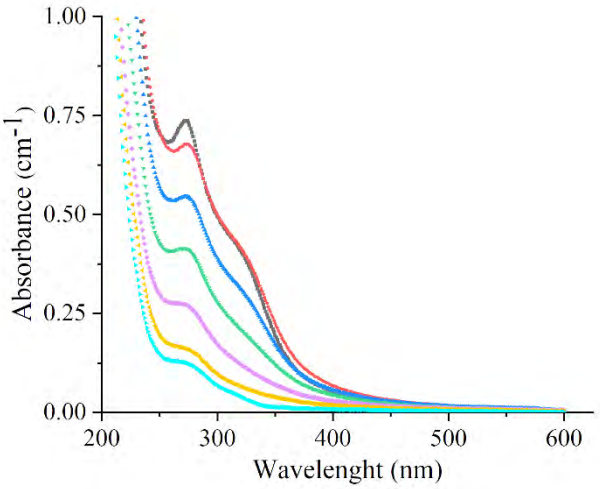

Source: Own authorship

4.4.5. Effects on Ecotoxicity

Figure 39 shows the concentration-response curves for PHWW before and after anaerobic and photocatalytic treatments. The increase in EC_{50} and reduction in TU_a values after the AD step show the reduction of PHWW toxicity (Table 23). Tukey's test showed a significant difference ($p = 0.000$) between the treatments. Chaparro and Pires (2015) evaluated the acute effect of pulp mill wastewater on *D. similis* before and after treatment in a HAIB reactor, obtaining lower TU_a after AD treatment, due to the conversion of some recalcitrant compounds.

Figure 39 - Concentration vs immobility curves for PHWW: HAIB in (■), HAIB out (●), TiO_2/UV out (▲)

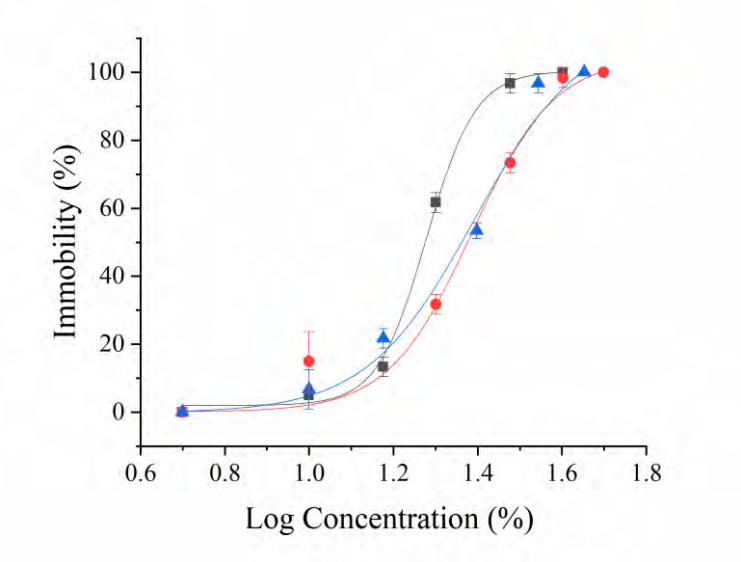

Source: Own authorship

Table 24 - Changes in EC_{50} and TUa values along with the treatments

Condition	EC_{50}	TU_a
HAIB in	18.9 ± 0.3^b	5.3 ± 0.1^a
HAIB out	23.3 ± 0.4^a	4.3 ± 0.1^b
UV/TiO_2 out	22.8 ± 0.8^a	4.4 ± 0.2^b

Values are mean ± SD. Means followed by the same letter in rows do not differ statistically ($p > 0.05$)

Source: Own authorship

On the other hand, the assessment of the wastewater toxicity level after advanced oxidation processes is necessary, because, these processes often generate intermediate compounds or by-products that could be more toxic to biological systems than the original wastewater (RIZZO, 2011). Tukey's test results show that the acute toxicity did not increase or decrease significantly

after photocatalytic treatment (Table 23). These results indicate that, despite the high concentration of aromatics and organic compounds that were photodegraded, some toxic by-products could have been produced during treatment, matching the acute AD-PHWW toxicity before its treatment. Similar results were reported for the photocatalytic treatment of olive oil mill wastewater, where the EC_{50} for *V. fischeri* remained the same even after the photocatalytic treatment (CHATZISYMEON; XEKOUKOULOTAKIS; MANTZAVINOS, 2009).

Phytotoxic data of wastewaters have become relevant for the possibility of reusing effluents for plant irrigation avoiding the use of fresh water and recycling the remaining nutrients of biological treatments. Thus, the phytotoxicological effects of the different treatments on *Eruca sativa* Mill seeds were evaluated and presented in Table 24 and Figure 40. Although acute toxicity was not observed for *E. sativa* Mill, germination and root elongation were reported for each condition.

Table 25 - Changes in values of germination ratio and germination index along with the treatments

Condition	Germination rate (%)	Germination index (%)
HAIB in	83.3 ± 4.7	47.4 ± 11.6[b]
HAIB out	90 ± 8.2	84.9 ± 12.2[a]
UV/TiO_2 out	96.7 ± 4.7	96.6 ± 5.4[a]

Values are mean ± SD. Means followed by the same letter in rows do not differ statistically ($p > 0.05$)

Source: Own authorship

According to Tukey's test, germination rate values did not show a significant difference between treatments. On the other hand, germination index values showed a decrease in the

PHWW phytotoxicity after the anaerobic process, which remained similar after the photocatalytic treatment, thus, verifying the acute toxicity results for *D. similis*. Root and shoot elongation values did not present a significant difference between control and samples before and after photocatalysis, indicating that samples were not negatively affected by the treatment because presented values similar to control.

Figure 40 - Roth elongation (□) and shoot length (◪) differences for control and PHWW

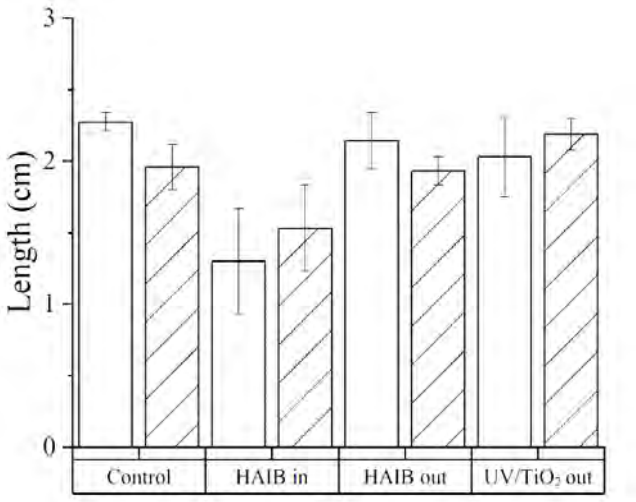

Source: Own autorship

5. Conclusions

The sequential anaerobic treatment of PHWW from *Spirulina* was investigated in a sequencing batch process, assessing increasing organic matter concentrations (1.6, 2.4, 3.2, 4, and 4.8 $gCOD.L^{-1}$). COD removal efficiencies between 53% and 49%, for influent COD concentrations of 1.6 $g.L^{-1}$, 2.4 g.L-1, 3.2 $g.L^{-1}$, with CH_4 yield in a range of 180 and 158 $NmL.gCODadd^{-1}$ were observed. Higher organic loads presented lower values of COD removal and CH_4 yields, besides VFA accumulation (especially propionic acid). The kinetic analysis showed that the modified Haldane model adjusted to experimental data, indicating a strong inhibition at COD concentrations higher than 3.7 $gCOD.L^{-1}$. Microbial diversity analysis revealed that *Trichococcus*, *Aminobacteria,* and *Methanosarcina* were the most representative microorganisms after biomass acclimation to PHWW.

The effect of intermitted micro-aeration on PHWW biodegradation was tested in two sequencing batch processes, comparing a full anaerobic set-up (R_1) to an anaerobic-partially aerated set-up (R_2) and evaluating three organic matter concentrations (1.6, 3.2, and 4.8 $gCOD.L^{-1}$). Higher removal efficiencies of COD and phenolic compounds were obtained for R_2, besides a diminution in VFA accumulation. On the other hand, CH_4 production was reduced by 45% due to oxygen availability. An enrichment of aerobic microorganisms capable of degrading aromatic compounds was observed in R_2.

Photocatalysis was studied as a post-treatment of AD-PHWW to further stabilize the effluent. Removal efficiencies reached 50% for COD, 83% for phenolic compounds, and 95% for color after 240 min of irradiation under optimum conditions of pH (9.6) and H_2O_2 addition ($3.55g.L^{-1}$). Both variables had a significant effect on removal efficiencies of COD, phenolic compounds, and color ($p < 0.05$). Results of ecotoxicity bioassays with *D. similis* and *E. sativa* Mill showed that treated PHWW was not negatively influenced by UV-photodegradation.

6. Recommendations for future research

Topics in which further research would be beneficial are presented below:

- Anaerobic reactor with recirculation. The use of effluent recirculation could help reduce recalcitrant compounds concentration, avoiding the application of high dilution ratios and providing a more efficient mass transfer between the microbial consortium and the substrate.
- Microaerated continuous reactor. The application of optimum micro aerated conditions to a continuous anaerobic reactor could improve PHWW aromatic degradation without harming the methanogenic population. Some parameters to optimize could be aeration flow rate, dosing point, and recirculation use.

References

ADORNO, M.; HIRASAWA, J.; VARESCHE, M. B. Development and Validation of Two Methods to Quantify Volatile Acids (C2-C6) by GC/FID : Headspace (Automatic and Manual) and Liquid-Liquid Extraction (LLE). **Americal Journal of Analytical Chemistry**, v. 5, p. 406–414, 2014.

AHMED, S. et al. Heterogeneous photocatalytic degradation of phenols in wastewater: A review on current status and developments. **Desalination**, v. 261, p. 3–18, 2010.

AHMED, S. et al. Influence of parameters on the heterogeneous photocatalytic degradation of pesticides and phenolic contaminants in wastewater: A short review. **Journal of Environmental Management**, v. 92, n. 3, p. 311–330, 2011.

ALBA, L. G. et al. Hydrothermal Treatment (HTT) of Microalgae: Evaluation of the Process As Conversion Method in an Algae Biorefinery Concept. **Energy Fuels**, v. 26, p. 642–657, 2012.

ALIMORADI, S. et al. Effect of temperature on toxicity and biodegradability of dissolved organic nitrogen formed during hydrothermal liquefaction of biomass. **Chemosphere**, v. 238, p. 124573, 2020.

ALMEIDA, W. et al. AnSBBR applied to biomethane production for vinasse treatment: Effects of organic loading, feed strategy and temperature. **Brazilian Journal of Chemical Engineering**, v. 34, n. 3, p. 759–773, 1 jul. 2017.

AMARAL, F. et al. Hydraulic retention time influence on azo dye and sulfate removal during the sequential anaerobic–aerobic treatment of real textile wastewater. **Water Science and Technology**, v. 76, n. 12, p. 3319–3327, 2017.

ANGELIDAKI, I. et al. Defining the biomethane potential (BMP) of solid organic wastes and energy crops: A proposed protocol for batch assays. **Water Science & Technology**, v. 59, n. 5, p. 927–934, 2009.

ANGELIDAKI, I. et al. Biomethanation and Its Potential. **Methods in Enzymology**, v. 494, p. 327–351, 2011.

APHA. **Standard Methods for the Examination of Water and Wastewater**Washington DCAmerican Public Health Association, , 1998. .

APOLLO, S.; ONYANGO, M. S.; OCHIENG, A. Integrated UV photodegradation and

anaerobic digestion of textile dye for efficient biogas production using zeolite. **Chemical Engineering Journal**, v. 245, p. 241–247, 2014.

AQUINO, S.; CHERNICHARO, C. Acúmulo de ácidos graxos voláteis em reatores anaeróbios sob estresse: causas e estratégias de controle. **Engenharia Sanitária e Ambiental**, v. 10, n. 2, p. 152–161, 2005.

ARROJO, B. et al. Aerobic granulation with industrial wastewater in sequencing batch reactors. **Water Research**, v. 38, n. 14–15, p. 3389–3399, 1 ago. 2004.

BAENA, S. et al. Aminobacterium colombiense gen. nov. sp. nov., an amino acid-degrading anaerobe isolated from anaerobic sludge. **Anaerobe**, v. 4, n. 5, p. 241–250, 1998.

BARAKAT, M. et al. Photocatalytic degradation of 2-chlorophenol by Co-doped TiO2 nanoparticles. **Applied Catalysis B: Environmental**, v. 57, n. 1, p. 23–30, 2005.

BEN HANIA, W. et al. Mesotoga infera sp. nov., a mesophilic member of the order Thermotogales, isolated from an underground gas storage aquifer. **International Journal of Systematic and Evolutionary Microbiology**, v. 63, n. PART8, p. 3003–3008, 1 ago. 2013.

BERRY, D.; FRANCIS, A.; BOLLAGL, J. Microbial Metabolism of Homocyclic and Heterocyclic Aromatic Compounds under Anaerobic Conditions. **MICROBIOLOGICAL REVIEWS**, v. 51, p. 43–59, 1987.

BILLER, P. et al. Nutrient recycling of aqueous phase for microalgae cultivation from the hydrothermal liquefaction process. **Algal Research**, v. 1, n. 1, p. 70–76, 2012.

BILLER, P. et al. Effect of hydrothermal liquefaction aqueous phase recycling on bio-crude yields and composition. **Bioresource Technology**, v. 220, p. 190–199, 2016.

BILLER, P.; ROSS, A. Potential yields and properties of oil from the hydrothermal liquefaction of microalgae with different biochemical content. **Bioresource Technology**, v. 102, n. 1, p. 215–225, 2011.

BIZANI, E. et al. Photocatalytic decolorization and degradation of dye solutions and wastewaters in the presence of titanium dioxide. **Journal of Hazardous Materials**, v. 136, p. 85–94, 2006.

BOTHEJU, D.; BAKKE, R. **Oxygen Effects in Anaerobic Digestion-A ReviewThe Open Waste Management Journal**. [s.l: s.n.].

BRAME, J. et al. Inhibitory effect of natural organic matter or other background constituents on photocatalytic advanced oxidation processes: Mechanistic model development and

validation. **Water Research**, v. 84, p. 362–71, 1 nov. 2015.

BRYANT, M. P. et al. Growth of Desulfovibrio in Lactate or Ethanol Media Low in Sulfate in Association with H2-Utilizing Methanogenic Bacteria. **Applied and Environmental Microbiology**, v. 33, n. 5, p. 1162–1169, 1977.

BUENO, B. et al. Anaerobic digestion of aqueous phase from hydrothermal liquefaction of Spirulina using biostimulated sludge. **Bioresource Technology**, v. 312, p. 123552, 2020.

BUENO, B. et al. Continuous Anaerobic Treatment of the Aqueous Phase of Hydrothermal Liquefaction from Spirulina Using a Horizontal-Flow Anaerobic Immobilized Biomass (HAIB) Reactor. **Water, Air, and Soil Pollution**, v. 232, n. 97, p. 1–16, 2021.

CAPORASO, J. G. et al. Ultra-high-throughput microbial community analysis on the Illumina HiSeq and MiSeq platforms. **The ISME Journal 2012 6:8**, v. 6, n. 8, p. 1621–1624, 8 mar. 2012.

CARVALHO, J. et al. Microaerated UASB reactor treating textile wastewater: The core microbiome and removal of azo dye Direct Black 22. **Chemosphere**, v. 242, p. 125157, 2020.

CHANDRA, R. et al. Isolation and characterization of potential aerobic bacteria capable for pyridine degradation in presence of picoline, phenol and formaldehyde as co-pollutants. **World Journal of Microbiology and Biotechnology**, v. 25, n. 12, p. 2113–2119, 16 nov. 2009.

CHAPARRO, T. R.; PIRES, E. C. Post-treatment of anaerobic effluent by ozone and ozone/UV of a kraft cellulose pulp mill. **Water Science and Technology**, v. 71, n. 3, p. 382–389, 2015.

CHATZISYMEON, E.; XEKOUKOULOTAKIS, N.; MANTZAVINOS, D. Determination of key operating conditions for the photocatalytic treatment of olive mill wastewaters. **Catalysis Today**, v. 144, n. 1–2, p. 143–148, 2009.

CHEN, H. et al. Biogas production from hydrothermal liquefaction wastewater (HTLWW): Focusing on the microbial communities as revealed by high-throughput sequencing of full-length 16S rRNA genes. **Water Research**, v. 106, p. 98–107, 2016.

CHEN, H. et al. Methane potentials of wastewater generated from hydrothermal liquefaction of rice straw: Focusing on the wastewater characteristics and microbial community compositions. **Biotechnology for Biofuels**, v. 10, n. 1, p. 140, 2017.

CHEN, H. et al. Mesophilic and thermophilic anaerobic digestion of aqueous phase generated from hydrothermal liquefaction of cornstalk: Molecular and metabolic insights. **Water Research**, v. 168, p. 115199, 1 jan. 2020.

CHEN, W.-T. et al. Hydrothermal liquefaction of mixed-culture algal biomass from wastewater treatment system into bio-crude oil. **Bioresource Technology**, v. 152, p. 130–139, 2014.

CHEN, Y. et al. Thermochemical conversion of low-lipid microalgae for the production of liquid fuels: challenges and opportunities. **RSC Adv.**, v. 5, p. 18673–18701, 2015.

CHEN, Y.; CHENG, J.; CREAMER, K. Inhibition of anaerobic digestion process: A review. **Bioresource Technology**, v. 99, n. 10, p. 4044–4064, 2008.

CHENG, Z. et al. Enhancement of surfactant biodegradation with an anaerobic membrane bioreactor by introducing microaeration. **Chemosphere**, v. 208, p. 343–351, 1 out. 2018.

CHERNICHARO, C. Anaerobic Reactors. In: **Biological Wastewater Treatment**. [s.l: s.n.]p. 175.

CHOU, W. L. et al. The effect of petrochemical structure on methane fermentation toxicity. **Progress in Water Technology**, v. 10, n. 5, p. 545–558, 1979.

ÇINAR, Ö. et al. Effect of cycle time on biodegradation of azo dye in sequencing batch reactor. **Process Safety and Environmental Protection**, v. 86, n. 6, p. 455–460, 1 nov. 2008.

COSTA, J.; ALVES, M. Posttreatment of olive mill wastewater by immobilized TiO 2 photocatalysis. **Photochemistry and Photobiology**, v. 89, n. 3, p. 545–551, 2013.

DEMIRBAS, A. Political , economic and environmental impacts of biofuels : A review. **Applied Energy**, v. 86, p. S108–S117, 2009.

DIAS, M. et al. Anaerobic digestion of hydrothermal liquefaction wastewater from spent coffee grounds. **Biomass and Bioenergy**, v. 148, p. 106030, 2021.

DICKEL, O.; HAUG, W.; KNACKMUSS, H.-J. Biodegradation of nitrobenzene by a sequential anaerobic-aerobic process. **Biodegradation 1993 4:3**, v. 4, n. 3, p. 187–194, set. 1993.

DOBLE, M.; KUMAR, A. **Biotreatment of Industrial Effluents**. Massachusetts: Elsevier Inc., 2005.

DWYER, D. F. et al. Kinetics of phenol biodegradation by an immobilized methanogenic consortium. **Applied and Environmental Microbiology**, v. 52, n. 2, p. 345–351, 1986.

EBOIBI, B. et al. Effect of operating conditions on yield and quality of biocrude during hydrothermal liquefaction of halophytic microalga Tetraselmis sp. **Bioresource Technology**, v. 170, p. 20–29, 2014.

ELLIOTT, D. et al. Hydrothermal liquefaction of biomass: Developments from batch to continuous process. **Bioresource Technology**, v. 178, p. 147–156, 2014.

FERNANDEZ, S. et al. Anaerobic digestion of organic fraction from hydrothermal liquefied algae wastewater byproduct. **Bioresource Technology**, v. 247, p. 250–258, 1 jan. 2018.

FERREIRA, L. F. et al. Evaluation of sugar-cane vinasse treated with Pleurotus sajor-caju utilizing aquatic organisms as toxicological indicators. **Ecotoxicology and Environmental Safety**, v. 74, n. 1, p. 132–137, 1 jan. 2011.

FETZNER, S. **Bacterial degradation of pyridine, indole, quinoline, and their derivatives under different redox conditionsAppl Microbiol Biotechnol**. [s.l.] 237±250 Ó Springer-Verlag, 1998. .

FONSECA, R. F.; DE OLIVEIRA, G. H. D.; ZAIAT, M. Modeling anaerobic digestion metabolic pathways for antibiotic-contaminated wastewater treatment. **Biodegradation**, v. 31, n. 4–6, p. 341–368, 1 dez. 2020.

FRANCHI, O. et al. Correlations between microbial population dynamics, bamA gene abundance and performance of anaerobic sequencing batch reactor (ASBR) treating increasing concentrations of phenol. **Journal of Biotechnology**, v. 310, p. 40–48, 2020.

FRANK, E. D. et al. Life cycle comparison of hydrothermal liquefaction and lipid extraction pathways to renewable diesel from algae. **Mitigation and Adaptation Strategies for Global Change**, v. 18, n. 1, p. 137–158, 2013.

GAI, C. et al. Energy and nutrient recovery efficiencies in biocrude oil produced via hydrothermal liquefaction of Chlorella pyrenoidosa. **RSC Advances**, v. 4, n. 33, p. 16958, 2014.

GAI, C. et al. An investigation of reaction pathways of hydrothermal liquefaction using Chlorella pyrenoidosa and Spirulina platensis. **Energy Conversion and Management**, v. 96, p. 330–339, 2015a.

GAI, C. et al. Characterization of aqueous phase from the hydrothermal liquefaction of

Chlorella pyrenoidosa. **Bioresource Technology**, v. 184, p. 328–35, 2015b.

GARCIA ALBA, L. et al. Microalgae growth on the aqueous phase from Hydrothermal Liquefaction of the same microalgae. **Chemical Engineering Journal**, v. 228, p. 214–223, 2013.

GARCIA, V. S. et al. Degradation of p-cresol, resorcinol, and phenol in anaerobic membrane bioreactors under saline conditions. **Chemical Engineering Journal**, v. 430, p. 132672, 2022.

GHATTAS, A.-K. et al. Anaerobic biodegradation of (emerging) organic contaminants in the aquatic environment. **Water Research**, v. 116, p. 268–295, 2017.

GRABOWSKI, A. et al. Petrimonas sulfuriphila gen. nov., sp. nov., a mesophilic fermentative bacterium isolated from a biodegraded oil reservoir. **International Journal of Systematic and Evolutionary Microbiology**, v. 55, n. 3, p. 1113–1121, 1 maio 2005.

GUPTA, V. K. et al. Photo-catalytic degradation of toxic dye amaranth on TiO2/UV in aqueous suspensions. **Materials Science and Engineering C**, v. 32, n. 1, p. 12–17, 2012.

HAMDI, O. et al. Aminobacterium thunnarium sp. Nov., a mesophilic, amino acid-degrading bacterium isolated from an anaerobic sludge digester, pertaining to the phylum Synergistetes. **International Journal of Systematic and Evolutionary Microbiology**, v. 65, n. 2, p. 609–614, 1 fev. 2015.

HEDRICK, D. B.; GUCKERT, J. B.; WHITE, D. C. The effects of oxygen and chloroform on microbial activities in a high-solids, high-productivity anaerobic biomass reactor. **Biomass and Bioenergy**, v. 1, n. 4, p. 207–212, 1 jan. 1991.

HERNANDEZ, J. E.; EDYVEAN, R. G. J. Inhibition of biogas production and biodegradability by substituted phenolic compounds in anaerobic sludge. **Journal of Hazardous Materials**, v. 160, p. 20–28, 2008.

HIRAISHI, A.; SHIN, Y. K.; SUGIYAMA, J. Brachymonas denitrificans gen. nov., sp. nov., and aerobic chemoorganotrophic bacterium which contains rhodoquinones, and evolutionary relationaships of rhodoquinone producers to bacterial species with various quinone classes. **The Journal of General and Applied Microbiology**, v. 41, n. 2, p. 99–117, 1995.

HIRASAWA, J. et al. Application of molecular techniques to evaluate the methanogenic archaea and anaerobic bacteria in the presence of oxygen with different COD:Sulfate ratios in a UASB reactor. **Anaerobe**, v. 14, n. 4, p. 209–218, 2008.

IOANNOU, L. A.; PUMA, G. L.; FATTA-KASSINOS, D. Treatment of winery wastewater by physicochemical, biological and advanced processes: A review. **Journal of Hazardous Materials**, v. 286, p. 343–368, 2015.

JENA, U. et al. Evaluation of microalgae cultivation using recovered aqueous co-product from thermochemical liquefaction of algal biomass. **Bioresource Technology**, v. 102, p. 3380–7, 2011.

JENA, U.; DAS, K. Comparative Evaluation of Thermochemical Liquefaction and Pyrolysis for Bio-Oil Production from Microalgae. **Energy & Fuels**, v. 25, p. 5472–5482, 2011.

JENA, U.; DAS, K.; KASTNER, J. R. Effect of operating conditions of thermochemical liquefaction on biocrude production from Spirulina platensis. **Bioresource Technology**, v. 102, n. 10, p. 6221–9, 2011.

JING, J. et al. Photocatalytic degradation of nitrogen-containing organic compounds over TiO2. **Journal of Molecular Catalysis A: Chemical**, v. 351, p. 17–28, 2011.

JOO, H. S.; HIRAI, M.; SHODA, M. Characteristics of ammonium removal by heterotrophic nitrification-aerobic denitrification by Alcaligenes faecalis No. 4. **Journal of Bioscience and Bioengineering**, v. 100, n. 2, p. 184–191, 1 ago. 2005.

KAISER, J.-P.; FENG, Y.; BOLLAG, J.-M. **Microbial Metabolism of Pyridine, Quinoline, Acridine, and Their Derivatives under Aerobic and Anaerobic ConditionsMICROBIOLOGICAL REVIEWS**. [s.l: s.n.].

KAMIŃSKI, M. et al. Determination of carbon monoxide, methane and carbon dioxide in refinery hydrogen gases and air by gas chromatography. **Journal of Chromatography A**, v. 989, n. 2, p. 277–283, 2003.

KARAKASHEV, D. et al. Acetate oxidation is the dominant methanogenic pathway from acetate in the absence of Methanosaetaceae. **Applied and Environmental Microbiology**, v. 72, n. 7, p. 5138–5141, jul. 2006.

KATO, M.; FIELD, J.; LETTINGA, G. Methanogenesis in granular sludge exposed to oxygen. **FEMS Microbiology Letters**, v. 114, p. 317–324, 1993.

KATO, M.; FIELD, J.; LETTINGA, G. Anaerobe Tolerance to Oxygen and the Potentials of Anaerobic and Aerobic Cocultures for Wastewater Treatment. **Brazilian Journal of Chemical Engineering**, v. 14, n. 4, p. 395–407, 1997.

KAUR, J.; PAL, B. Photocatalytic degradation of N-heterocyclic aromatics — effects of

number and position of nitrogen atoms in the ring. **Environ Sci Pollut Res**, v. 20, p. 3956–3964, 2013.

KHANAL, S. K. et al. Anaerobic Bioreactors/Digesters: Design and Development. **Current Developments in Biotechnology and Bioengineering: Biological Treatment of Industrial Effluents**, p. 261–279, 1 jan. 2017.

KLEMMER, M. et al. Effect of Aqueous Phase Recycling in Continuous Hydrothermal Liquefaction. **Industrial & Engineering Chemistry Research**, v. 55, p. 12317–12325, 2016.

KNAPP, J. S.; BROMLEY-CHALLONER, K. C. A. Recalcitrant organic compounds. In: **Handbook of Water and Wastewater Microbiology**. London: Academic Press, 2003. p. 559–595.

KUMAR, K. et al. Recent developments on biofuels production from microalgae and macroalgae. **Renewable and Sustainable Energy Reviews**, v. 65, p. 235–249, 2016.

KUMAR, K.; PORKODI, K.; ROCHA, F. Langmuir–Hinshelwood kinetics – A theoretical study. **Catalysis Communications**, v. 9, n. 1, p. 82–84, 2008.

LEOW, S. et al. Prediction of microalgae hydrothermal liquefaction products from feedstock biochemical composition. **Green Chem.**, v. 17, n. 6, p. 3584–3599, 2015.

LI, C. M. et al. Enhancement of phenol biodegradation: Metabolic division of labor in co-culture of Stenotrophomonas sp. N5 and Advenella sp. B9. **Journal of Hazardous Materials**, v. 400, 5 dez. 2020.

LÓPEZ BARREIRO, D. et al. Cultivation of microalgae with recovered nutrients after hydrothermal liquefaction. **Algal Research**, v. 9, p. 99–106, 2015.

MABUZA, J. et al. Investigating the synergy of integrated anaerobic digestion and photodegradation using hybrid photocatalyst for molasses wastewater treatment. **Euro-Mediterranean Journal for Environmental Integration**, v. 2, n. 1, p. 17, 2017.

MADDI, B. et al. Quantitative characterization of the aqueous fraction from hydrothermal liquefaction of algae. **Biomass and Bioenergy**, v. 93, p. 122–130, 2016.

MADIGOU, C. et al. Acclimation strategy to increase phenol tolerance of an anaerobic microbiota. **Bioresource Technology**, v. 216, p. 77–86, 2016.

MADSEN, R. et al. Hydrothermal co-liquefaction of biomasses – quantitative analysis of bio-crude and aqueous phase composition. **Sustainable Energy Fuels**, v. 1, n. 4, p. 789–805,

2017.

MAO, Y. et al. Versatile aromatic compound-degrading capacity and microdiversity of Thauera strains isolated from a coking wastewater treatment bioreactor. **Journal of Industrial Microbiology and Biotechnology**, v. 37, n. 9, p. 927–934, 1 set. 2010.

MENEZES, O. et al. Coupling intermittent micro-aeration to anaerobic digestion improves tetra-azo dye Direct Black 22 treatment in sequencing batch reactors. **Chemical Engineering Research and Design**, v. 146, p. 369–378, 2019.

MONTGOMERY, D. C. **Design and analysis of experiments**. 8th ed. ed. New York: John Wiley & Sons., 2013.

MORAES, B. S.; ZAIAT, M.; BONOMI, A. Anaerobic digestion of vinasse from sugarcane ethanol production in Brazil: Challenges and perspectives. **Renewable and Sustainable Energy Reviews**, v. 44, p. 888–903, 1 abr. 2015.

MUÑOZ SIERRA, J. D. et al. Impact of long-term salinity exposure in anaerobic membrane bioreactors treating phenolic wastewater: Performance robustness and endured microbial community. **Water Research**, v. 141, p. 172–184, 15 set. 2018.

NGUYEN, D. et al. Intermittent micro-aeration: New strategy to control volatile fatty acid accumulation in high organic loading anaerobic digestion. **Water Research**, v. 166, p. 115080, 1 dez. 2019.

NGUYEN, D.; KHANAL, S. K. A little breath of fresh air into an anaerobic system: How microaeration facilitates anaerobic digestion process. **Biotechnology Advances**, v. 36, n. 7, p. 1971–1983, 2018.

NOGUEIRA, V. et al. Photocatalytic Treatment of Olive Oil Mill Wastewater Using TiO2 and Fe2 O3 Nanomaterials. **Water Air & Soil Pollution**, v. 227, p. 88, 2016.

PARKIN, G. F.; OWEN, W. F. Fundamentals of Anaerobic Digestion of Wastewater Sludges. **Journal of Environmental Engineering**, v. 112, p. 867–920, 1986.

PARSHINA, S. N. et al. Soehngenia saccharolytica gen. nov., sp. nov. and Clostridium amygdalinum sp. nov., two novel anaerobic, benzaldehyde-converting bacteria. **International Journal of Systematic and Evolutionary Microbiology**, v. 53, n. 6, p. 1791–1799, 1 nov. 2003.

PASALARI, H. et al. Perspectives on microbial community in anaerobic digestion with emphasis on environmental parameters: A systematic review. **Chemosphere**, v. 270, p.

128618, 1 maio 2021.

PEKAKIS, P.; XEKOUKOULOTAKIS, N.; MANTZAVINOS, D. Treatment of textile dyehouse wastewater by TiO2 photocatalysis. **Water Research**, v. 40, n. 6, p. 1276–86, 2006.

PELEGRINI, N.; PELEGRINI, R.; PATERNIANI, J. Ecotoxicological evaluation of leachate from the Limeira sanitary landfill with a view to identifying acute toxicity. **Ambiente e Agua - An Interdisciplinary Journal of Applied Science**, v. 2, n. 3, p. 34–43, 2006.

PETERNEL, I. et al. Comparative study of UV/TiO2, UV/ZnO and photo-Fenton processes for the organic reactive dye degradation in aqueous solution. **Journal of Hazardous Materials**, v. 148, n. 1–2, p. 477–484, 2007.

PHAM, M. et al. Chemical and Biological Characterization of Wastewater generated from Hydrothermal Liquefaction of Spirulina. **Environmental Science & Technology**, v. 47, p. 2131–2138, 2013.

PIND, P. F.; ANGELIDAKI, I.; AHRING, B. K. Dynamics of the anaerobic process: Effects of volatile fatty acids. **Biotechnology and Bioengineering**, v. 82, n. 7, p. 791–801, 30 jun. 2003.

PINHEIRO, H.; TOURAUD, E.; THOMAS, O. Aromatic amines from azo dye reduction: status review with emphasis on direct UV spectrophotometric detection in textile industry wastewaters. **Dyes and Pigments**, v. 61, n. 2, p. 121–139, 2004.

PITTMAN, J. K.; DEAN, A. P.; OSUNDEKO, O. The potential of sustainable algal biofuel production using wastewater resources. **Bioresource Technology**, v. 102, n. 1, p. 17–25, 2011.

POSMANIK, R. et al. Coupling hydrothermal liquefaction and anaerobic digestion for energy valorization from model biomass feedstocks. **Bioresource Technology**, v. 233, p. 134–143, 2017.

PRIAC, A.; BADOT, P.-M.; CRINI, G. Treated wastewater phytotoxicity assessment using Lactuca sativa: Focus on germination and root elongation test parameters. **Comptes Rendus Biologies**, v. 340, n. 3, p. 188–194, 2017.

QUISPE-ARPASI, D. et al. Anaerobic and photocatalytic treatments of post-hydrothermal liquefaction wastewater using H2O2. **Bioresource Technology Reports**, v. 3, p. 247–255, 2018.

RAMOS-TERCERO, E. A.; BERTUCCO, A.; BRILMAN, D. W. F. Process water recycle in hydrothermal liquefaction of microalgae to enhance bio-oil yield. **Energy and Fuels**, v. 29, p. 2422–2430, 2015.

RAZO-FLORES, E. et al. Biodegradability of N-substitued aromatics and alkylphenols under methanogenic conditions using granular sludge. **Water Science and Technology**, v. 33, n. 3, p. 47–57, 1996.

RAZO-FLORES, E. et al. Biodegradation of Mixtures of Phenolic Compounds in an Upward-Flow Anaerobic Sludge Blanket Reactor. **Journal of Environmental Engineering**, v. 129, n. 11, p. 999–1006, 1 nov. 2003.

RIPLEY, L.; BOYLE, W.; CONVERSE, J. Improved alkalimetric monitoring for anaerobic digestion of high-strenght wastes. **Journal (Water Pollution Control Federation)**, v. 58, n. 5, p. 406–411, 1986.

RITTMAN, B.; MCCARTY, P. **Environmental biotechnology: Principles and Applications**. [s.l: s.n.]

RIZZO, L. Bioassays as a tool for evaluating advanced oxidation processes in water and wastewater treatment. **Water Research**, v. 45, n. 15, p. 4311–4340, 2011.

ROBERTS, G. et al. Promising pathway for algal biofuels through wastewater cultivation and hydrothermal conversion. **Energy and Fuels**, v. 27, p. 857–867, 2013.

ROSENKRANZ, F. et al. Relationship between phenol degradation efficiency and microbial community structure in an anaerobic SBR. **Water Research**, v. 47, n. 17, p. 6739–6749, 1 nov. 2013.

ROY, F. et al. Synthrophomonas sapovorans sp. nov., a new obligately proton reducing anaerobe oxidizing saturated and unsaturated long chain fatty acids. **Archives of Microbiology 1986 145:2**, v. 145, n. 2, p. 142–147, jul. 1986.

RUIRUI, L. et al. Application of zeolite adsorption and biological anaerobic digestion technology on hydrothermal liquefaction wastewater. **Int J Agric & Biol Eng Open Access at Int J Agric & Biol Eng**, v. 10, n. 101, p. 163–168, 2017.

SCHENK, P. M. et al. Second Generation Biofuels: High-Efficiency Microalgae for Biodiesel Production. **BioEnergy Research**, v. 1, n. 1, p. 20–43, mar. 2008.

SHANMUGAM, S. et al. Treatment of aqueous phase of bio-oil by granular activated carbon and evaluation of biogas production. **Bioresource Technology**, v. 223, p. 115–120, 2017.

SI, B. et al. Inhibitors degradation and microbial response during continuous anaerobic conversion of hydrothermal liquefaction wastewater. **Science of The Total Environment**, v. 630, p. 1124–1132, 2018.

SI, B. et al. Anaerobic conversion of the hydrothermal liquefaction aqueous phase: fate of organics and intensification with granule activated carbon/ozone pretreatment. **Green Chemistry**, v. 21, n. 6, p. 1305–1318, 2019.

SILVA, R. et al. Anaerobic treatment of industrial biodiesel wastewater by an ASBR for methane production. **Applied Biochemistry and Biotechnology**, v. 170, n. 1, p. 105–118, 12 maio 2013.

SINGLETON, V.; ORTHOFER, R.; LAMUELA-RAVENTÓS, R. Analysis of total phenols and other oxidation substrates and antioxidants by means of Folin-Ciocalteu Reagent. **Methods in Enzymology**, v. 299, p. 152–178, 1999.

SIQUEIRA, J. P. S. et al. Process bioengineering applied to BTEX degradation in microaerobic treatment systems. **Journal of Environmental Management**, v. 223, p. 426–432, 1 out. 2018.

SOUZA, R. P. et al. Photocatalytic activity of TiO2, ZnO and Nb2O5 applied to degradation of textile wastewater. **Journal of Photochemistry and Photobiology A: Chemistry**, v. 329, p. 9–17, 2016.

SPEECE, R. E. **Anaerobic Biotechnology for Industrial Wastewater**. Nashville: Archae Press, 1996.

STREPIS, N. et al. Genome-guided analysis allows the identification of novel physiological traits in Trichococcus species. **BMC Genomics**, v. 21, n. 1, p. 1–13, 8 jan. 2020.

TIAN, W. et al. Effect of operating conditions on hydrothermal liquefaction of Spirulina over Ni/TiO2 catalyst. **Bioresource Technology**, v. 263, p. 569–575, 2018.

TOMMASO, G. et al. Chemical characterization and anaerobic biodegradability of hydrothermal liquefaction aqueous products from mixed-culture wastewater algae. **Bioresource Technology**, v. 178, p. 139–46, 2015.

TOOR, S.; ROSENDAHL, L.; RUDOLF, A. Hydrothermal liquefaction of biomass: A review of subcritical water technologies. **Energy**, v. 36, p. 2328–2342, 2011.

USMAN, M. et al. Molecular and microbial insights towards understanding the anaerobic digestion of the wastewater from hydrothermal liquefaction of sewage sludge facilitated by

granular activated carbon (GAC). **Environment International**, v. 133, p. 105257, 2019.

VAN LOOSDRECHT, M. et al. **Experimental Methods in Wastewater Treatment**. London: IWA Publishing, 2016.

VEERESH, G. S.; KUMAR, P.; MEHROTRA, I. Treatment of phenol and cresols in upflow anaerobic sludge blanket (UASB) process: a review. **Water Research**, v. 39, n. 1, p. 154–170, 1 jan. 2005.

WANG, X. et al. Draft Genome Sequence of Aquamicrobium defluvii Strain W13Z1, a Psychrotolerant Halotolerant Hydrocarbon-Degrading Bacterium. **Genome Announcements**, v. 3, n. 4, 2015.

WANG, Y.; QIAN, P. Y. Conservative Fragments in Bacterial 16S rRNA Genes and Primer Design for 16S Ribosomal DNA Amplicons in Metagenomic Studies. **PLOS ONE**, v. 4, n. 10, p. e7401, 9 out. 2009.

WIJETUNGA, S.; LI, X. F.; JIAN, C. Effect of organic load on decolourization of textile wastewater containing acid dyes in upflow anaerobic sludge blanket reactor. **Journal of Hazardous Materials**, v. 177, n. 1–3, p. 792–798, 15 maio 2010.

WU, C. et al. Improving hydrolysis acidification by limited aeration in the pretreatment of petrochemical wastewater. **Bioresource Technology**, v. 194, p. 256–262, 1 out. 2015.

YADAV, T. C.; KHARDENAVIS, A. A.; KAPLEY, A. Shifts in microbial community in response to dissolved oxygen levels in activated sludge. **Bioresource Technology**, v. 165, n. C, p. 257–264, 1 ago. 2014.

YANG, L. et al. Improve the biodegradability of post-hydrothermal liquefaction wastewater with ozone: conversion of phenols and N-heterocyclic compounds. **Water Science and Technology**, v. 2017, n. 1, p. 248–255, 2018.

YEBER, M. C. et al. Photocatalytic degradation of cellulose bleaching effluent by supported TiO2 and ZnO. **Chemosphere**, v. 41, n. 8, p. 1193–1197, 2000.

YERUSHALMI, L. et al. Detection of intermediate metabolites of benzene biodegradation under microaerophilic conditions. **Biodegradation 2001 12:6**, v. 12, n. 6, p. 379–391, 2001.

YU, G. et al. Distributions of carbon and nitrogen in the products from hydrothermal liquefaction of low-lipid microalgae. **Energy & Environmental Science**, v. 4, p. 4587–4595, 2011.

YUAN, X.; GAO, D. Effect of dissolved oxygen on nitrogen removal and process control in

aerobic granular sludge reactor. **Journal of Hazardous Materials**, v. 178, n. 1–3, p. 1041–1045, 15 jun. 2010.

ZAIAT, M. et al. MINI-REVIEW Anaerobic sequencing batch reactors for wastewater treatment: a developing technology. **Appl Microbiol Biotechnol**, v. 55, p. 29–35, 2001.

ZHANG, C. et al. Reviewing the anaerobic digestion of food waste for biogas production. **Renewable and Sustainable Energy Reviews**, v. 38, p. 383–392, 2014.

ZHENG, M. et al. Anaerobic digestion of wastewater generated from the hydrothermal liquefaction of Spirulina: Toxicity assessment and minimization. **Energy Conversion and Management**, v. 141, p. 420–428, 2017.

ZHOU, Y. et al. Anaerobic digestion of post-hydrothermal liquefaction wastewater for improved energy efficiency of hydrothermal bioenergy processes. **Water Science and Technology**, v. 72, n. 12, p. 2139–2147, 2015.

ZHU, Y. et al. Cultivation of granules containing anaerobic decolorization and aerobic degradation cultures for the complete mineralization of azo dyes in wastewater. **Chemosphere**, v. 246, p. 125753, 1 maio 2020.

ZINDEL, U. et al. Eubacterium acidaminophilum sp. nov., a versatile amino acid-degrading anaerobe producing or utilizing H2 or formate. **Archives of Microbiology 1988 150:3**, v. 150, n. 3, p. 254–266, jul. 1988.